UNIVERSITETET I AGDER

ENE500 Master's Thesis 2018

Modelling and simulation of BIPV installations in Norway

By
Rune Birkeland

Supervisor:
Anne Gerd Imenes

This master's thesis is carried out as a part of the education at the University of Agder and is therefore approved as a part of this education. However, this does not imply that the University answers for the methods that are used or the conclusions that are drawn.

University of Agder, 2018
Faculty of Engineering and Science

Preface

First of all I want to thank my supervisor Dr. Anne Gerd Imenes for guidance throughout this semester. Who has taken her time to answer my questions and advise regarding the structure of this thesis.

I would like to thank Morten Gregertsen in UNION eiendmsutvikling and Magnhild Kallhovd for answering my questions related to the systems evaluated in this thesis. I would also like to thank Shaun Falconer for the help and encouragement.

Lastly I would like to thank Cecilie Syvertsen Drange for all the support and dinners this semester

Rune Birkeland
University of Agder,
Grimstad,
Thursday 31st May, 2018

Individual declaration

The individual student or group of students is responsible for the use of legal tools, guidelines for using these and rules on source usage. The statement will make the students aware of their responsibilities and the consequences of cheating. Missing statement does not release students from their responsibility.

1.	I hereby declare that my thesis is my own work and that I have not used any other sources or have received any other help than mentioned in the thesis.	☑
2.	I further declare that this thesis: - not been used for another exam at another department/university/university college in Norway or abroad; - does not refer to the work of others without it being stated; - does not refer to own previous work without it being stated; - have all the references given in the literature list; - is not a copy, duplicate or copy of another's work or manuscript.	☑
3.	I am aware that violation of the above is regarded as cheating and may result in cancellation of exams and exclusion from universities and colleges in Norway, see Universitets- og høgskoleloven §§4-7 og 4-8 og Forskrift om eksamen §§ 31.	☑
4.	I am aware that all submitted theses may be checked for plagiarism.	☑
5.	I am aware that the University of Agder will deal with all cases where there is suspicion of cheating according to the university's guidelines for dealing with cases of cheating.	☑
6.	I have incorporated the rules and guidelines in the use of sources and references on the library's web pages.	☑

Publishing Agreement

Authorization for electronic publishing of the thesis. Author(s) have copyrights of the thesis. This means, among other things, the exclusive right to make the work available to the general public (Åndsverkloven. §2). All theses that fulfill the criteria will be registered and published in Brage Aura and on UiA's web pages with author's approval. Theses that are not public or are confidential will not be published.	
I hereby give the University of Agder a free right to make the task available for electronic publishing:	Yes ☑
Is the thesis confidential? (confidential agreement must be completed)	No ☑
- If yes: Can the thesis be published when the confidentiality period is over?	
Is the task except for public disclosure? (contains confidential information. see Offl. §13/Fvl. §13)	No ☑

Abstract

In this thesis, three BIPV-installations has been simulated, the simulated results of each system have been compared to actual production for the real system. The parameters which are assessed in this thesis are production, performance ratio and different system losses. The BIPV-installations which are simulated, are Skarpnes, Solsmaragden and Brynseng located in Arendal, Drammen and Oslo respectively. The simulations are done by obtaining weather data, such as global horizontal irradiance and temperature. The weather data was retrieved in different ways. PVsyst was used to generate synthetic data, real measured data on site was used and weather stations located in close proximity was also used. A hypothesis has been carried out in this thesis, regarding facade installations are more beneficial for northern latitudes, compared to southern latitudes. This thesis simulated the same photovoltaic system mounted on the rooftop and on the facade. Installation located in northern latitudes had more similar production for facade compared to rooftop installations than installations for southern latitudes. South oriented facade installations are more productive compared to other orientations. The results of this thesis are in compliance with the literature for this professional area.

The simulations estimated a production deviation within a range of 0.24% - 10.69%. Performance results showed values within the range of 65.2% - 81.5%. Losses with regard to these deviations were examined and irregularities in irradiation on-site measuring and shading showed most critical for the installations. Due to huge losses with regards to shading, a partial shading model was used to illustrate the losses for the Brynseng installation. The thesis found the performance of the systems as expected, however the Brynseng system being an installation with improvement potential.

The simulations display deviation in production and discovers issues regarding losses for the chosen systems. This information may be used to achieve more accurate evaluation and understanding of BIPV systems located in Norway.

Nomenclature

Symbols

α_c	Albedo component
β	Plane tilt
η	Efficiency
γ	Diode quality factor
ϕ_z	Solar zenith angle
Θ_T	Tilt angle of array
ε	Inclination of the earth's axis
G_{sc}	Solar constant
I_{mp}	Maximum power point current
P_{mp}	Maximum power point
V_{mp}	Maximum power point voltage
W_p	Watt peak
a_c	Albedo coefficient
AAE	Annual average efficiency
AAE_s	Annual average efficiency of the system
B_c	Beam component
d	number of days
D_c	Diffuse component
E	Energy output
E_{array}	Energy output of the array
E_{Grid}	Energy injected into grid
G	Effective irradiance
G_{Eff}	Global irradiance considering soiling- and shading losses

G_{ref}	Reference irradiance
GII	Global incident irradiance
H	Solar insolation
H_p	Sun height on PV plane
H_p	Sun height on horizontal PV plane
I	Current
I_d	Diode current
k	Boltzmann's constant
K_b	Clearness index of beam
Lc	Collection losses
Ls	System losses
mu_{ISC}	Temperature coefficient to the short circuit current
N_{es}	Number of cells in series
P_0	Installed PV capacity
q	Charge of electron
R_L	Load
R_s	Series resistance
R_{sh}	Shunt resistance
S_{pr}	Specific production
T	Temperature
T_c	Cell temperature
T_{amb}	Ambient temperature
T_{coe}	Temperature coefficient
T_{cref}	Reference temperature
V	Voltage
Y_r	reference yield

Y_t	Specific yield

Abbreviations

CO_2	Carbon dioxide
H_2O	Water
O_2	Oxygen
$sc - Si$	Single crystal silicon
AC	Alternating current
AM	Air Mass
BAPV	Building applied photovoltaic
BIPV	Building integrated photovoltaic
CdTe	Cadium telluride
CIGS	Copper-indium-gallium-diselenide
CIS	Copper-indium-diselenide
CPV	Concentrator photovoltaic
DC	Direct current
DHI	Diffuse horizontal irradiance
DNI	Direct normal irradiance
GHI	Global horizontal irradiance
IAM	Incident angle modifier
MPP	Maximum Power Point
MPPT	Maximum Power Point Tracker
NREL	National renewable energy laboratory
PI	Performance index
POA	Plane of array
PR	Performance ratio
PV	Photovoltaic

PVPS	Photovoltaic power system program
PVSS	Photovoltaic system simulation program
RMSE	Root mean square error
SAM	System advisor model
SAPM	Sandia array performance model
SAPV	Stand-Alone Photovoltaic
SAPV	Stand-alone photovoltaic
Si-Poly	Silicon poly crystalline

Contents

List of Figures

List of Tables

1 Introduction

With the shift towards green energy, different renewable energy sources are under development. The electricity produced in Norway is based on hydro-power[2], with solar energy being a growing competitor for renewable energy. As a result of existing electricity contribution from renewable energy sources, PV systems are usually installed on residential and commercial buildings. The Norwegian climate makes solar energy, a source worth expanding and investing in, as substantiated by the growing photovoltaic (PV) sector in Norway. Due to the cold climate and northern latitudes, with low sun angles, facade installations make a suitable option.

There is an ongoing survey of building Integrated photovoltaics (BIPV) in Norway, which is a nationwide project for BIPV and building applied photovoltaic (BAPV) installations [3]. This thesis will conduct a simulation of BIPV systems constructed in Norway, evaluate the results in comparison with actual production results for these installations and evaluate rooftop mounted PV system productions in comparison with facade mounted PV systems. The systems included in this thesis are the zero-emission houses at Skarpnes south of Arendal, the office building Solsmaragden located in Drammen and Brynseng school in Oslo.

There are several software packages for simulating and modeling a Photovoltaic system. A model used for PV performance aims to calculate the power output of a PV system. This system usually contains PV panels, inverters, charge controllers and other components. A simulation of a PV system is based on models. During the development of the renewable branch, lots of models and simulation tools have been developed. In order to evaluate a simulated PV system, loss parameters are important to address.

Sandia National Laboratories has been a contributor to these modeling and simulation software packages [1]. This thesis will use the PV software PVsyst, which will be used to simulate three different BIPV systems, evaluate production and loss results for the systems and cover a hypothesis for PV performance. Simulated losses can be an indicator of which improvements are required for PV systems. Facades experience more losses due to incident in collector plane in comparison to roof installations. Where rooftop installations may experience soiling losses due to snow, in Northern latitudes, facade installations experience shading due to objects nearby. To address shading losses, the software Simulink has been used to create a partial shading model. This model is based on a string installed at the Brynseng system, in order to inspect power loss due to shading.

For the hypothesis, a literature review has been conducted for facades being an advantage for northern latitude compared to southern latitudes. For this hypothesis, simulation in PVsyst is done to compare facade and roof installation in order to validate the hypothesis. The thesis will inspect if there are considerable differences for PV on roofs and facades for the same location.

2 Theory

In this chapter, some theoretical background will be given on solar radiation, PV- module, system performance characteristics and PV software used for PV performance modeling and simulation. Section 2.1 until 2.3 contains information gathered from [4], and other sources will be listed. This thesis focuses on BIPV system performance, and for this task, it is essential to know how a PV system works and what factors that have an impact on the system.

2.1 Solar radiation

The radiation from the sun's surface is equivalent to that of a 6000K blackbody[1]. As the radiation enters the earth's atmosphere, parts of the radiation are scattered in the atmosphere, illustrated in Figure 2. Sunlight is typically reduced by 30% before it reaches the Earth's surface due to Rayleigh scattering by molecules, dispersed by dust particles and aerosols and absorption by atmospheric gases like CO_2, H_2O, ozone and O_2. This scattering gives diffuse radiation, sunlight which has been dispersed in the atmosphere but reaches the Earth's surface. As the atmosphere reflects, absorbs and scatters the radiation, the earth surface absorbs and reflects it. Direct radiation is the sunlight coming directly from the sun. The sum of direct and diffuse radiation equals the global radiation. The path length this radiation must pass through to get to earth's surface is known as the Air-mass (AM), which calculated approximately as:

$$AM = \frac{1}{cos\phi_z} \tag{1}$$

Where ϕ_z is the Solar zenith angle, the angle between the sun and the point directly overhead. The path length, for the radiation, increases with increased zenith angle.

Before entering earth atmosphere, the spectral distribution of sunlight is defined as Air mass zero (AM0). The spectrum of the solar radiation is close to the blackbody at 6000K. At different wavelength and temperature, the energy distribution varies as illustrated in figure 1.

[1] An ideal absorber, and emitter, of radiation

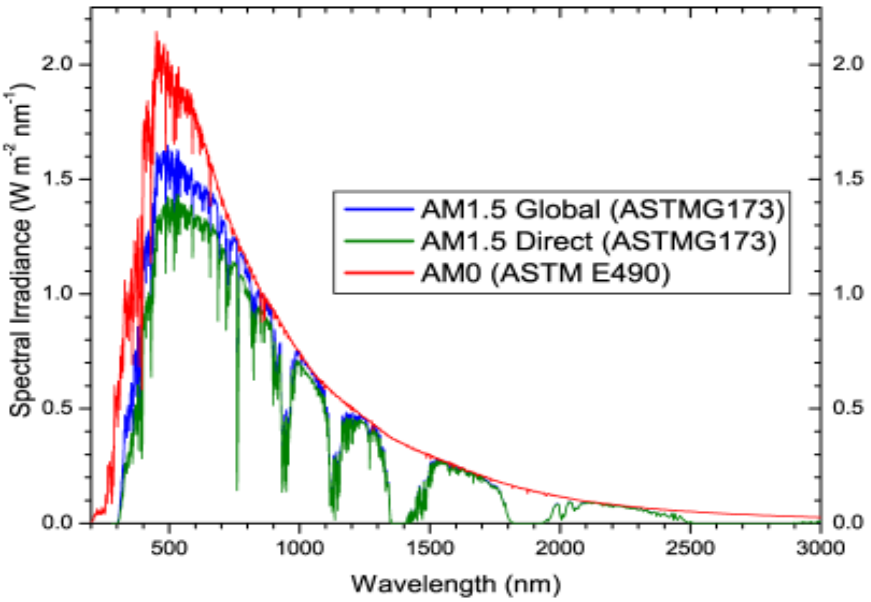

Figure 1: Spectral distribution [5].

Figure 1 shows a typical energy distribution for AM of 1.5 spectrum, which is the one under standard solar cell testing [4].

The power density at earth orbit is known as the solar constant. This value can vary slightly because of the elliptic shape, but is accepted to be:

$$G_{sc} = 1366 \frac{W}{m^2}$$

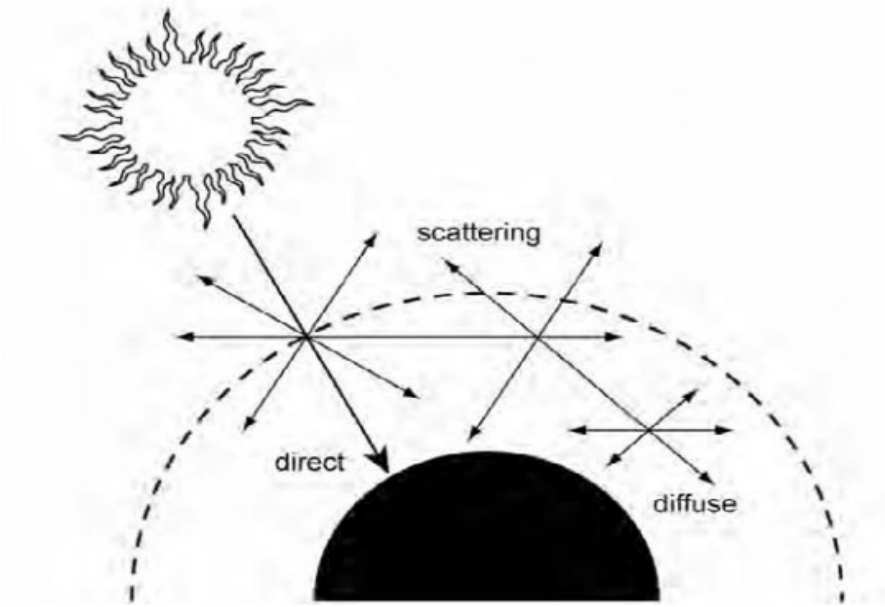

Figure 2: Radiation scattered in the atmosphere [4].

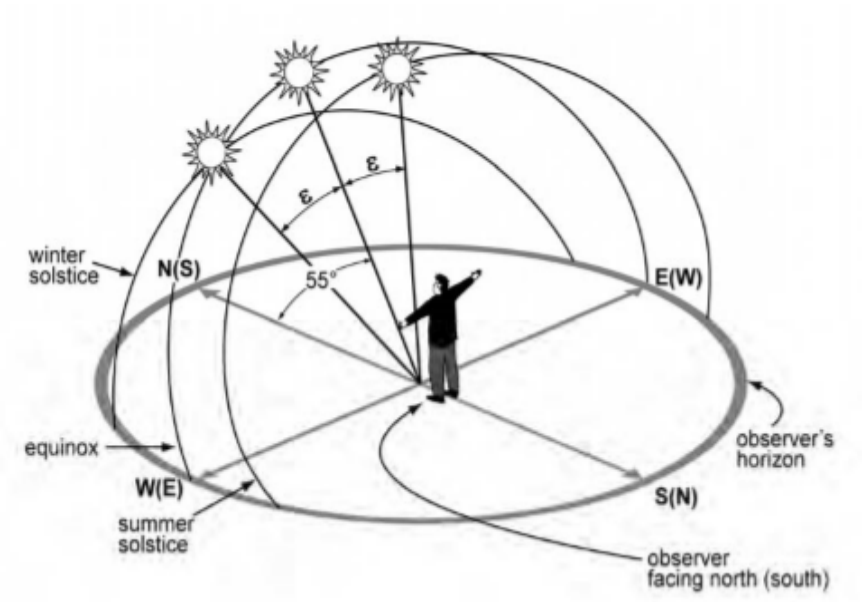

Figure 3: Motion of the sun for an observer [4].

Figure 3 gives an illustration of the motion of the sun for an observer at latitude $35°N$, and ε is the inclination of the earth's axis of rotation relative to its plane of revolution about the sun (= 23.45°) [4]. The variation of ε causes the Earth's seasons and can be found [4]:

$$\varepsilon = 23.45° sin \frac{360}{365} \cdot (d - 81) \tag{2}$$

Here d is the day number, which means d=1 is January 1st.

2.1.1 Albedo coefficient

The content in Section 2.1.1 is retrieved from the software PVsyst and [6]. Albedo coefficient is the part of global incident irradiation which is reflected by the ground in front of the tilted plane. As the horizontal irradiation is computed onto the tilted plane, the albedo effect takes place. Due to the horizontal irradiation component, the albedo component seen by the plane is zero for a horizontal plane but will increase with tilt. The albedo component is part of the Hay transposition model, which applies differently to various components of the irradiance. The Albedo component can be described as:

$$\alpha_c = a_c \cdot GHI \cdot (1 - cos(\beta)/2) \tag{3}$$

Where α_c is the albedo component, a_c is the albedo coefficient, GHI is the global horizontal irradiance and β is the plane tilt. The $(1 - cos(\beta)/2)$ part of the equation is a result of constant irradiance coming from all directions, seen by the plane. This means larger contribution for the albedo component with increased tilt up until 180(∘).

As seen in Table 1 different albedo coefficient values are given according to PVsyst and the National Laboratory collaborative [1].

Urbane situation	0.14 - 0.22
Grass	0.15 - 0.25
Fresh grass	0.26
Fresh snow	0.82
Wet snow	0.55 - 0.75
Dry asphalt	0.09 - 0.15
Wet asphalt	0.18
Concrete	0.25 - 0.35
Red tiles	0.33
Aluminium	0.85
New galvanised steel	0.35
Very dirty galvanised steel	0.08

Table 1: Albedo coefficient values

For obtaining the most accurate albedo value, direct measurement on the site is required. The measurement is a ratio of irradiance measured by a pyranometer oriented towards the ground, and another pyranometer measuring the global horizontal irradiance.

2.2 PV module performance characteristics

Usually, cells with similar characteristics are connected to form modules. Several modules can be connected to form solar arrays. The module's output is decided by the cell with the lowest output, due to every single cell has its unique characteristics. If there are cells which are not operating properly, either in series or parallel, it is called a mismatched cell. This mismatch can lead to some of the cells generating and others dissipating power. The difference between actual output power and the maximum achievable output for component cells is called the mismatch loss.

2.2.1 Efficiency of PV materials

Section 2.2.1 is based on the annual trend report from IEA-pvps [7]. The report divides solar cells into these categories: wafer-based crystalline[2], compound semiconductor (thin-film), or organic. With more than 94% of cell production in IEA-pvps countries to be crystalline silicon. The single crystal silicon cells(sc-Si) has a commercial efficiency between 16% and 25%. The mulitcrystalline silicon cells(mc-Si) have an average conversion efficiency around 14-18%. The compound semiconductor PV cell is used in concentrator PV (CPV) systems with tracking systems, with a

[2]Single crystal and multicrystalline silicon

conversion efficiency of 40% and higher. Thin-film uses materials such as cadmium telluride (CdTe), and copper-indium-(gallium)-diselenide (CIGS and CIS). The CdTe material has reached efficiency up to 22% in labs. The organic thin-film PV cells, based on dye or organic semiconductors are new technology and still in the development and research phase.

The report also inspects PV module efficiency. The wafer-based crystalline modules have an efficiency between 14 and 22,8%. Encapsulated PV cells in thin-film modules, either fixed or flexible module, can reach an efficiency within a range of 7% to 16.8%. CPV modules can reach an efficiency of 38%. PV modules are usually rated in the range of 50 W up to 350 W, products for building integrated photovoltaic are rated even higher.

2.2.2 Photovoltaic cell and operation

Solar cells are produced from a semiconductor material, usually silicon-based. When a cell is exposed to light, it produces an electric current; this is called the photovoltaic effect. For characteristic of solar cells/module output, maximum power point can be used, which is the maximum value of the product $V_{mp} \cdot I_{mp}$. As seen in Figure 4, the maximum power is the largest fitting rectangle under the IV curve, and illustrates the cell/module characteristic IV curve:

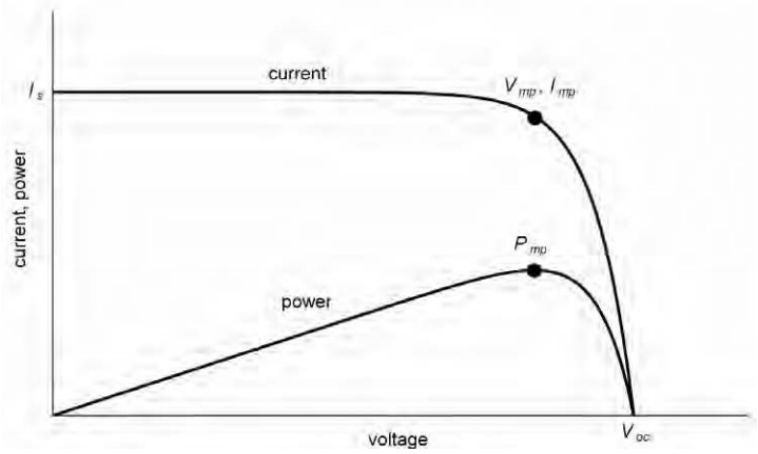

Figure 4: IV Curve [4].

When illuminated with sunlight, a single solar cell can generate approximately 600 mV. To get the desired voltage, the cells are connected in series, usually 36 cells in series. The desired current is obtained by paralleling the cells, as the single cell only can generate approximately 30 mA/cm^2. The PV module is a construction of solar cells connected to a string, in series and parallel. Modules can then be connected in series to create a string. Connecting strings in parallel will result in an array. Figure 5 illustrates the difference between cell, module, string and array.

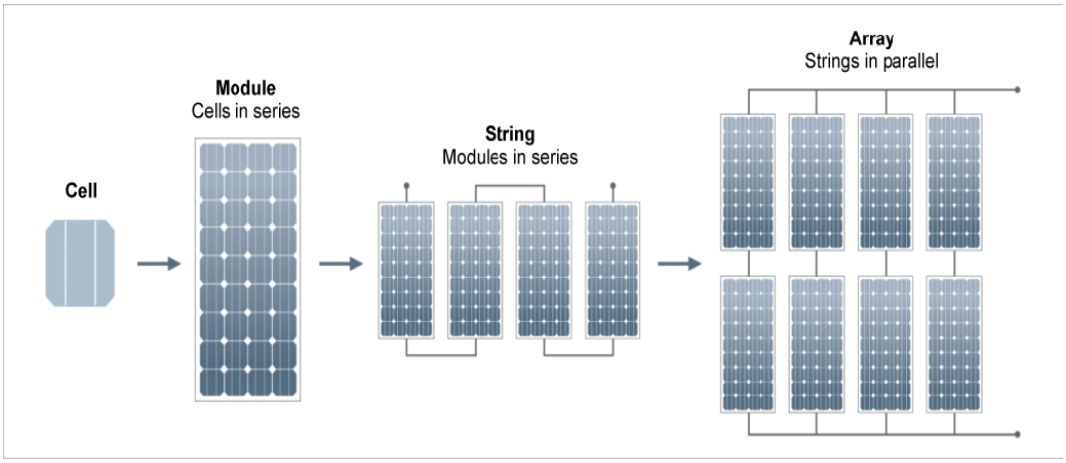

Figure 5: Illustration of cell, module, string and array.[8]

2.2.3 Effect of temperature

The temperature is significant when talking about the performance of a PV system. The total effect is a minor increase in current and a significant reduction in voltage, fill factor and cell output.

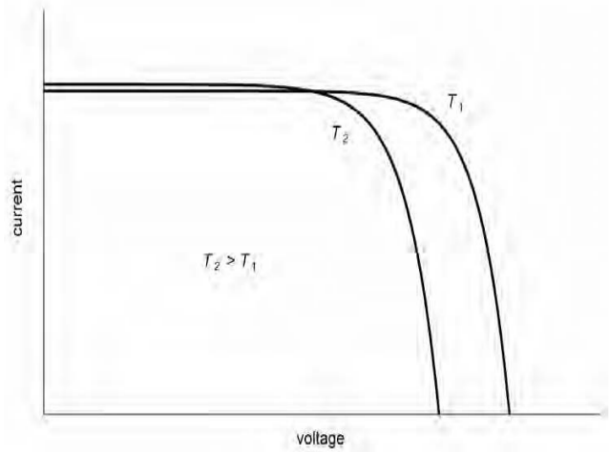

Figure 6: Effect of temperature on solar cell [4]

In Figure 6, one can see that an increase from T1 to T2 shifts the IV curve to a lower voltage output. Operating temperature of cells is affected by ambient air temperature, wind velocity, the intensity of sunlight on the module. $-0.45\%/K$ is a typical change in power output for a silicon solar cell based on temperature.

2.2.4 Standard test condition and efficiency of PV module

Under sunlight of 1 kW/m^2, the power output at maximum power point (MPP) is called the "peak power" of the cell. In photovoltaic terms, this is rated, as the panels "peak" watts, W_p. The watt peak (W_p) is used when rating the PV, in terms of output power (P_{mpp}) under standard test conditions (STC) [9]:

- 1000 W/m^2 (1 sun)
- $T_c = 25°$ cell temperature
- Spectral distribution AM1.5

The parameters used to calculate the efficiency of the PV module [10]:

$$\eta_{STC} = \frac{P_{mpp}}{1000 \cdot A} \tag{4}$$

Here A is the area of the PV module.

2.3 PV system

A PV system consists of one or more PV modules, and all components required for the cells to be able to deliver electricity to load or grid. The system is either connected to a series of loads (off-grid) or an electricity network (grid-connected PV)

2.3.1 Grid connected PV system

Grid-connected systems contain an inverter converting direct current (DC) into alternating current (AC), which is supplied into an electrical network. The conversion efficiency is usually in the range of 95 % up to 99 %. Most inverters contain a Maximum Power Point Tracker (MPPT), which constantly changes the load impedance to gain maximum power from the PV array.

The grid-connected system can be divided into two main alternatives, PV arrays installed at the end user site or as the utility for generation stations. The first alternative is the type of system installed on rooftops and integrated into buildings.
There is one case that can cause several damages to the utility grid. This problem is known as Islanding, that is if the grid-connected system continues to operate when the grid shuts down. Mostly this is handled by the inverter or at the distribution network.

2.3.2 Fixed and tracking

It is possible to install a PV system fixed or with different tracking orientation. The fixed PV arrays are mounted on location in a specific orientation and angle. A Fixed installed PV system is the most common type. The tilt angle is chosen based on seasonal power requirement, and the orientation is based on the installation being located in the northern or southern hemisphere. The

tilt angle should be low at summer and high at winter or the tilt could be annually optimized. It is possible to change the array angle for example seasonally or monthly manually.
Contrary to the fixed system, a tracking system is a system orientates itself towards the sunlight. This type of systems can be either 1-axis or 2-axis, see Figure 7.
A 1-axis tracking system typically follows the sun from east to west, and the output can increase up to 20% compared to a fixed array. A 2-axis system has the same function as 1 axis system but can as well follow the sun from east to west. The 2-axis provide a power output increase as high as 40 % higher than the fixed array.

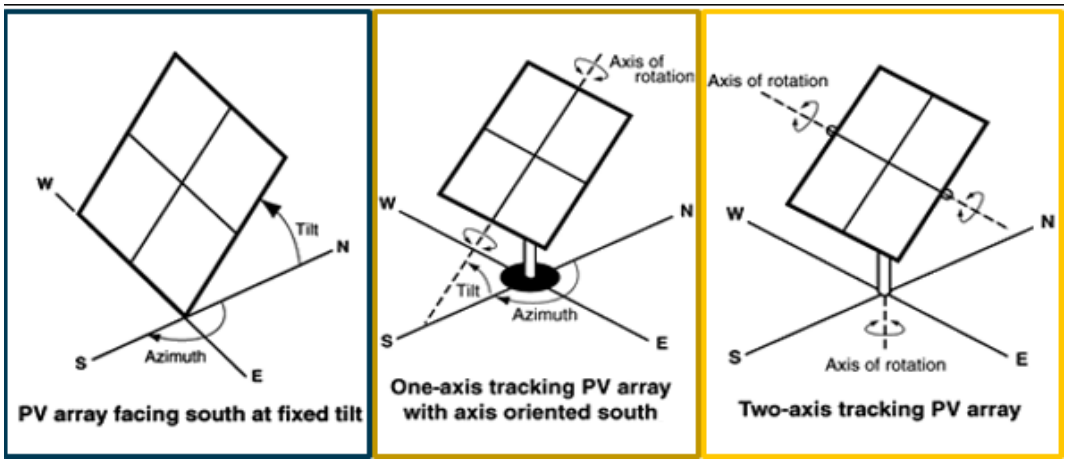

Figure 7: Illustration fixed and tracking PV array [11].

2.4 PV performance assessment method

Several methods and metrics have been proposed for evaluating a PV system, and they are essential for analyzing the performance of the system. These methods and metrics are means to verify the system performance under a range of conditions [12]. Yield is one of the most common metrics which is used to analyze PV systems [13, 14, 15]. For system comparison, it is also necessary to have some information regarding the installation site, the kind of system, building integrated photovoltaic or building attached photovoltaic, PV area, type, installation angle and year of the commission. James et al. [16] stated that BIPV systems experience reduced performance (i.e., electricity generation) compared to BAPV PV systems due to it being mounted directly on building surfaces. Which co-relates to high temperature in some cases due to the little air gap, and can cause overheating [17].

According to the international energy agency (IEA) [18], system performance is usually analyzed by specific yield (kWh/kW_p) installed and performance ratio. An article published by Imenes [13], states that yield is strongly dependent on efficiency. Efficiency depends on factors like spectrum and intensity as well as temperature.
There are several metric calculations for analyzing PV systems, and this paper will elaborate on:

- Specific yield

- Performance ratio
- Temperature corrected performance ratio
- Performance index

As well as methods/models used in PV system analysis:

- PVsyst
- PVSOL
- Solar advisor model

2.4.1 Specific Yield

Specific yield is proposed for analyzing PV system of different sizes [14]. The main reason for monitoring a system is to evaluate the yield, which can be used to analyze the system performance and to identify design flaws and malfunctions. Specific yield Y_t is the net electrical energy output (E) divided by the installed PV capacity (P_0). Specific yield is represented by the equation:

$$Y_t = \frac{E}{P_0} = \frac{Energy\ production\ [kWh]}{Installed\ PV\ capacity\ [kW_p]} \tag{5}$$

According to Jardine et al. [15], energy production and peak power output are related. However, due different technologies, the different response to temperature, insolation, and spectral quality, specific yield show variation.

For further evaluating an installation, reference yield (Y_r) is introduced. The reference yield is the total in-plane solar insolation (H) divided by the array reference irradiance (G_{ref}); therefore, the reference yield is the number of peak sun-hours. Reference yield is used when calculating PR.

$$Y_r = \frac{H}{G_{ref}} = \frac{Solar\ insolation\ [kWh/m^2]}{1\ [kW/m^2]} \tag{6}$$

As yield is commonly used, it leads to lots of research regarding system performance based on yield, and this report will give some examples. An example of yield being used to analyze the performance of PV system is given in a paper by Ayompe et al. [19]. The paper evaluated a grid-connected PV system in Dublin, Ireland. The data was collected between November 2008 and October 2009. It was compared to systems installed in Germany, Poland and Northern Ireland. The installation in Dublin had higher performance compared to the other installations, due to high wind speed and low ambient temperature. Another study was done by Jahn and Nasse [20], for evaluating installation with low yield and performance. The paper concluded with shading from trees and structures had a major impact, 34%, on the reduction in the yield.

Another example is the paper written by Jardine et al. [15], where specific yield is used to evaluate installations located in UK and Spain, based on the PV material used. Both installations

had lower performance than predicted, due to lower insolation during the test period. However, the result also gave an indication of crystalline silicon technologies performed better under colder operating temperature.

2.4.2 Performance ratio and temperature corrected performance ratio

Evaluating systems performance after a PR model is by far the most widely used today [21]. Leloux et al. argued that PR is used because of the thorough energy production assessment that is crucial for economic analysis.
The difference between 1 and PR are all types of energy losses. These losses are for example mismatch, shading, wiring, dust, thermal, DC/AC conversion, failures and PV module power lower than nominal rating.

The performance ratio PR is the actual yield divided by the reference yield. By normalizing with respect to irradiance, it quantifies the overall effect of losses on the rated output due to inverter inefficiency, wiring, mismatch, and other losses when converting from DC to AC power [22]. The effect of losses is also affected by PV module temperature, incomplete use of irradiance by reflection, soiling or snow. System downtime and component failures also make an impact. PR is represented by the following equation:

$$PR = \frac{Y_t}{Y_r} = \frac{Production\ energy}{Expected\ energy} = \frac{Production\ energy[kWh]}{\sum[I[\frac{W}{m^2}] * \frac{Peak\ Power[W]}{1000[\frac{W}{m^2}]}]} \tag{7}$$

Here production energy is the measurement of the site output in kWh, and the expected energy is found by multiplying the sensor readings by the rated peak power of the PV system. This metric is highly sensitive to temperature variation. Systems do not always operate at STC therefore thermal losses may be taken into account. Calculating a temperature corrected PR, referring to STC conditions is represented by the following equation:

$$PR_{STC} = \frac{Production\ energy}{[Expected\ energy] * [1 + (T[^\circ C] - 25^\circ C) * T_{coe}[\frac{\%}{^\circ C}]]} \tag{8}$$

Here production energy is divided by the expected energy, measured temperature and temperature coefficient. Where T is the measured module temperature in $[^\circ C]$.
T_{coe} is the temperature coefficient, given in percent, per degree difference. The temperature coefficient is the module's M_{mpp} temperature coefficient.

Thermal losses occur when PV cell temperature differs from STC.
If the temperature of the PV cell is lower than $25[^\circ C]$, the output increases. Using temperature corrected PR will neglect thermal losses but it requires measuring or estimating the solar cells operation temperature.
Leloux et al.[21], stated that thermal losses are site-dependent, which means a climatic impact on the system. This makes it inconvenient for qualifying the systems technical quality. According to Kurtz et al.[12], sensors can become loose which leads to reflect the true module temperature

poorly. Instead of sensor measuring module temperature, it is possible to measure the module temperature directly. When using direct measurement, there is no need to define a model for module temperature. Direct measurement is more accurate for use in small systems. Temperature changes related to passing clouds and gusts of wind are better quantified when using this direct measurement.

2.4.3 Performance index

Even a high-quality system, which is properly maintained, endures losses due to inverter DC/AC conversion. Performance Index (PI) is a method that gives the possibility of comparing PV system under different climatic and installation conditions, same as PR. The difference is when using PI, DC/AC losses can be subtracted, which gives a more accurate performance evaluation of the PV system itself. According to Leloux et al. [21] PI value equal to 1 corresponds a system free of shading, dust, wiring losses and free of failures for its inverter and PV generator.
When using PI, the actual PI value is compared to the desired PI value of 1. The difference between these two values can be explained as preventable energy losses.

PI can therefore be used as an performance indicator, and can be defined as [21]:

$$PI = \frac{Y_t}{\frac{H_{STC}}{G_{STC}} \int G(1 - \Delta H_{STC})(1 - \Delta H_{DC/AC})dt} \tag{9}$$

From the equation, the term $(1 - \Delta H_{DC/AC})$ perform the task of subtracting DC/AC conversion losses.

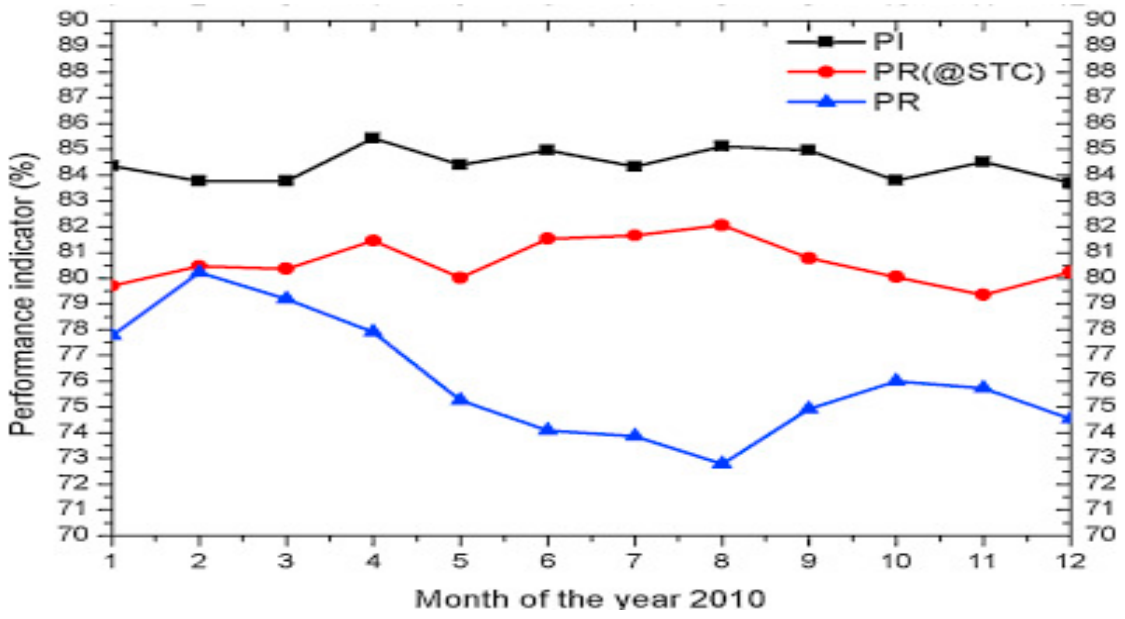

Figure 8: Comparison between PR, PR at STC and PI for a typical system in France, 2010 [21]

An example of PI is given, in Figure 8 [21]. A PI value of 0.85 means the system operates 15

percent inferior to the reference system, which has the PI value of 1. The Figure gives an overview of what can be expected when comparing the performance of a system regarding PR, PR_{STC} and PI. PR gives lowest system performance(%), due to losses. Temperature corrected PR neglects thermal losses and gives better system performance. Due to a more comprehensive analysis, PI gives higher performance values than PR. These values are indicating that the systems operate on an acceptable level.

2.5 PV software

This section will mainly present theory regarding PVsyst and models which are used for the software in order to evaluate PV systems. PVSOL and system advisor model will also be presented.

2.5.1 PVsyst

PVsyst is a software used to simulate, study, sizing and analyze [6, 23, 24, 25], as well as predicting energy yield photovoltaic systems [26]. PVsyst simulates grid-connected- stand alone-, pumping- and DC Grid PV systems [23]. PVSOL is also a software which provides dynamic simulations for design and optimization of PV systems, with storage systems [27, 28]. PVSOL also provides wiring design, shading analyses and full component selection [25]

For simulating a PV site, in PVsyst, data have to be imported. These meteorological data are: global irradiation and temperature [29, 30], these inputs play the main role in the simulation. In addition, horizontal diffuse irradiation and wind velocity are optional data inputs. PVsyst is also able to work with measured ambient temperature and compute the module temperature, which is done using a thermal model [29]. Directly measured module temperature can also be used. Simulations are often performed in hourly steps [29, 31]. The software can be used to optimize a PV installation, based on parameters like tilt-, pitch- and azimuth angle [31]. PVsyst is often used to optimize PV installations related to yield [31], and detection of failure on module, string and inverter level [29]. Using models in simulation software, $(I_{sc}, V_{oc}, W_{mp}, I_{mp})$ parameters are determined by the manufacturer's specification [32]. This may lead to errors related to parameter's uncertainty due to the simulated module will not be an exact representation of actual module. In order to obtain reliable energy yield simulations, it is important to have an accurate module model [26].

2.5.2 models and parameterization

Important models on irradiance level are Hay and Perez is applied for irradiance determined on the module. In PVsyst incidence angle modifier (IAM) is a loss parameter due to the reflection of beam component on cover glass [32].
Global incident in collector plane is the irradiance viewed from the collector plane, and plays a major role in evaluating system losses in PVsyst[33]. PVsyst uses 2 transposition models:

1. Hay's model which is a robust model, and can handle diffuse irradiation when the knowledge is not perfect.

2. Perez model which is a more sophisticated model, but requires well-measured data.

2.5.3 Hay's model

Hay transposition model can be applied to different components of the irradiance.
1. Beam component on the tilted plane as a function of tilt angle and the incidence angle, which makes this a pure geometrical transformation.

$$B_c = DNI \cdot \frac{H_p}{H_{hp}} \tag{10}$$

Where B_c is the beam component $[W/m^2]$, DNI is the direct normal irradiance $[W/m^2]$, H_p is the sun height on the plane and H_{hp} is the sun height on the horizontal plane.

2. Diffuse component is an isotropic distribution.

$$D_c = DHI \cdot [(1 - Kb) \cdot (1 + cos(\theta_T)/2) + Kb \cdot \frac{H_p}{H_{hp}}] \tag{11}$$

Where D_c is the diffuse component, DHI is diffuse horizontal irradiance, θ_T is the tilt angle of the array and Kb clearness index of the beam.

3. Albedo component as described in Section 2.1.1

2.5.4 Perez's model

This model is an advancement of diffuse sky models and used in PVsyst. Information regarding this model is obtained from [33, 34] and is described in Appendix E.

2.5.5 PVSOL

PVSOL also requires global irradiation, temperature and may also require wind velocity [35]. All data used in PVSOL requires being in an hourly format. PVSOL is able to simulate storage systems, which gives the possibility of calculating self-consumption of a PV system more precisely [27]. PVSOL evaluates system parameters such as: total energy produced, PV array surplus, energy not converted by the system, system efficiency, solar fraction, optimum tilt angle of solar panel etc [28] PVSOL may work with a maximum of 100 000 modules, simulating systems by the minute with any module arrays in various orientations. This software also gives the possibility of combining multiple inverters, even when they are equipped with different MPP trackers [27]. PVSOL has the complexity to model partial system shading and bypass diode effects unlike other commercial PV software [36, 37].

2.5.6 System Advisor Model

System Advisor Model (SAM) is a financial and performance model designed to assist in the decision making process for people working in the renewable energy industry [38, 39]. SAM is also an electric power generation model and estimates power delivery to a grid-connected building and an electric grid [40]. SAM also compare energy production between multiple renewable energy technologies [25]. SAM also provides sophisticated and tightly integrated analysis tools for solar energy. PV performance models are used to make an assumption or predict how much energy a chosen system is able to produce, being subject to weather conditions at a given location [41, 40]. SAM is developed by the National Renewable Energy Laboratory in collaboration with Sandi National Laboratory through the DOE Solar Energy Technologies Program [42, 1]. SAM has a useful feature that it provides access to different array performance models [39]. SAM takes lots of input, enabling SAM to do an in-depth performance modeling [25]. Algorithms used in the models are described in table 2.

Solar Radiation	Array Performance	Inverter
Isotropic sky	Sandia PV array performance model (empirical)	Sandia inverter performance model
Hay and Davies	5-parameter performance model (semi-empirical)	Single point efficiency
Reindl	PVWatts	
Perez et al.	Simple efficiency model	

Table 2: Algorithms which can be used in SAM for solar radiation, array and inverter performance [1]

SAM has the ability to download data from online databases such as: NREL National Solar Radiation Database, NREL WIND Toolkit and METEONORM [38, 1]. All PV performance models rely on ambient air temperature and solar radiation [41]. SAM's performance model can be applied to the following technologies: PV systems, Battery storage for PV systems, wind power and other technologies such as grid-connected PV systems, which consists of inverter and PV array [42]. The array may be fixed, single or dual axis deployed. SAM requires data of the installation performance characteristics of the equipment in the system and meteorological data [40]. It is also possible to simulate the system degradation due to equipment aging. Stein et al. stated the major elements for model validation [41]:

1. The first step is to develop data sets, including weather data, system description and performance data (technologies, applications, and climates).
2. The next step is to model the system and provide results.
3. Then apply a unified statistical/mathematical approach for analyzing the modeled and measured quantities and document it.
4. Identify improvements to the model.

2.5.7 Standard one-diode model

PVsyst use Shockley's simple "one diode" model, for describing the operation of a PV module [43]. The model is illustrated in Figure 9. The model is primarily designed for one single cell, used as a module implies that all cells are identical. Usually implying 2 different diodes is proposed for very accurate modeling of a single cell, however this one-diode model is used in this thesis.

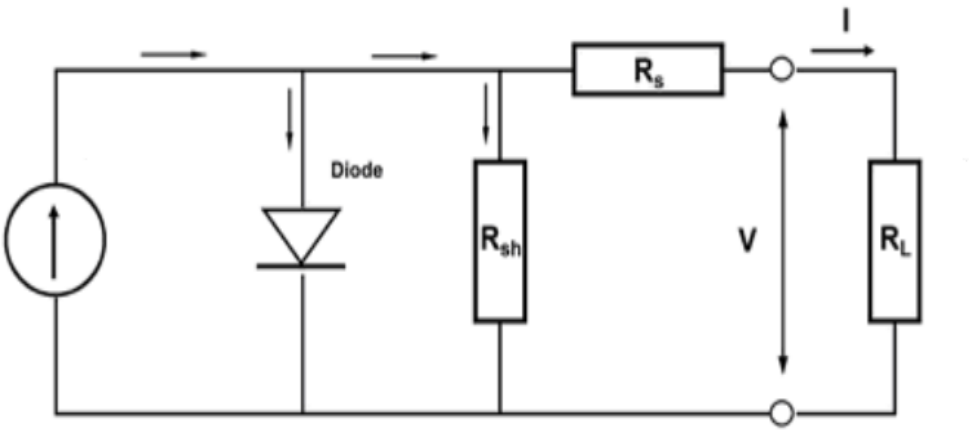

Figure 9: Illustration of the one diode model.

The one-diode model can be expressed as:

$$I = I_L - I_o(exp \cdot (\frac{q \cdot (V + IRs)}{N_{cs} \cdot \gamma \cdot kT_c}) - 1) - \frac{V + IR_s}{R_{sh}} \tag{12}$$

Where the parameters refer to:
I = Current supplied by the module [A].
V = Voltage [V]
I_L = Photocurrent [A] which is proportional to the irradiance and corrected by Tc which is explained below.
I_d = Diode current [A]. I_o = Saturation current [A]
R_s = Series resistance [ohm]
R_{sh} = Shunt resistance [ohm]
R_L = Load [ohm]
q = Charge of the electron
k = Boltzmann's constant [J/K]
γ = Diode quality factor
N_{cs} = Number of cells in series
T_c = Temperature of the cells [K]

I_L varies with the irradiance and temperature, and the model assumes it is proportional to the irradiance. Therefore I_L can be determined with respect to reference conditions:

$$I_L = \frac{G}{G_{ref}} \cdot (I_{Lref} + mu_{ISC} \cdot (T_c - T_{cref}) \tag{13}$$

Where: G = Effective irradiance $[W/m^2]$
G_{ref} = Reference irradiance $[W/m^2]$
T_c = Effective cell temperature [K]
T_{cref} = Reference temperature [K]
mu_{ISC} = temperature coefficient to the photocurrent (short-circuit current).

3 State of the art

This chapter contains a literature review of PV performance, which includes methods and metrics for analyzing a PV installation. First a few metrics will be discussed and then a few software programs, for analyzing the performance of an installation, will be presented.

3.1 PV performance modeling

Many models and software have been developed in recent times. Sandia National Laboratories has played a major part in developing these software, such as The Photovoltaic System Simulation Program (PVSS), SOLCELL, Evans and Facinelli Model, PVForm and more [1]. This thesis will focus on PVsyst, but this chapter will also take a look at two other common models, PVSOL and SAM, where examples of PV systems evaluated by using PVsyst, PVSOL and SAM.

3.1.1 PVsyst and PVSOL

A performance analysis of a 100 kWp grid-connected PV system conducted by Kumar et al. [44]. The system was simulated in PVsyst. The study was done to evaluate practicability of constructing a PV system for supplying the electric load of an educational institute. The simulation was done by using Meteonorm 7.1 weather data consisting of solar radiation and ambient temperature. The annual PR value was found to be approximately 0.8.

Malvoni et al. [45] conducted a study in Italy which explored the degradation of a grid-connected PV system. The study is composed of a comparative analysis of theoretical and actual output power, over a period of five years by using actual meteorological data. This is done by using the software PVsyst. The study concluded with the reliability of the PV system depends on operating conditions, that is not related to weather conditions. The result showed a reliability of 85% between theoretical and actual power output. A degradation of 1.12%/year can be expected according to Malvoni et al. This degradation rate is higher than the degradation rate which was found in a study conducted by Jordan et al. [46]. This study was done for 200 PV systems and found the degradation rate to be 0.8% annually.

A Stand-Alone Photovoltaic (SAPV) system has been simulated in PVsyst [30]. SAPV is a system which supplies electricity to a load without being connected to the grid. The study found the sizing system to be dependent on geographical site location.

Another study of BIPV mounted on an office building, as an alternative fuel source for fossil fuel, was carried out by Gindi et al. [47]. A feasibility analysis of the building has been done through the simulation modeling software PVSOL. Different types of mounting structures and varies type of PV modules were used to complete the analysis. The system output capacity has been calculated, annual energy output and the initial project cost for the different systems have been found. The result showed higher production for the roof and south oriented mounted PV modules, compared with other orientations. Where the PR value of 0.752 and 0.743 respectively.

The article concluded that PV modules can contribute to reducing electric energy consumption by choosing appropriate orientation, tilt angles and module types.

A study carried out by Babatunde et al. [48], compares the performance of PV systems under the influence of dust, different orientations and various tilt angles in Cyprus. PVSOL was used for this task and Meteonorm provided meteorological data. Babatunde et al. found that the mathematical models, used in this study, was more reliable than the simulation done in PVSOL. The accuracy of the simulation is strongly dependent on the quality of meteo data used. The average variance of energy output on an inclined surface, was approximately 0.3% between calculated and measured energy by implementing the mathematical method. The reason for this may be that the simulation used data consisting of an average of 20 years measuring, while the mathematical model used real-life meteorological data. The study also concluded with an average of 2.5% variance of specific yield after implementing the cleaning procedure for cleaning dust. Also, installation with same tilt yield less deviation for installations oriented closer to the south. MacAlpine et al. [36] also found deviation in PVSOL compared to an evaluation method due to partial shading, reducing energy output. Whereas Patarau et al. [28] found that simulation in PVSOL agrees strongly with the calculations.

3.1.2 System Advisor Model

A study done by Stein et al. using SAM, evaluated the use of 2 performance models for a PV system in Albuquerque [41]. The Sandia Array Performance Model (SAPM) and the CEC 5-parameter model were used to solve this task. Stein et al. found that the models could be improved by adjusting the module temperature coefficient or cell temperature model. Cameron et al. [49] used several submodels within SAM: radiation models, module performance models and an inverter model, PVWATTS and PVMod were also used. The study found disagreement between models while using non-crystalline technologies including thin-film modules. Choudhury [50] evaluated the energy performance of BIPV roof tiles in the United States. Using SAM, the net energy savings were analyzed in correlation to temperature and different climate types (location). A technical report was done to validate SAM's ability to predict performance, where 9 PV systems were analyzed [39]. Freeman et al. found annual errors to be 3% or less for all systems when comparing SAM predicted production to measured production. The report found SAM to underpredict measured production. For hourly data, SAM found 5.1% or less due to RMSE. A study conducted by Freeman et al. [25] compared SAM to PVsyst and PVSOL. The paper evaluated root mean square error (RMSEs) for all software and found all hourly RMSEs to be less than 7 % and all annual errors to be less than 8 %. The paper found that running multiple weather data sets could make a more accurate estimate of energy production.

These examples show the usefulness of PV simulation software for early design evaluation and may also be used to compare actual measured results with simulated results and to evaluate performance losses. The literature shows expected PR values which are typically around 0.8.

3.1.3 Performance of facade versus roof PV systems

The performance of PV facade installations, for a site, are influenced by geographical position [51]. Norway, located in the northern hemisphere, has low solar zenith angle at winter seasons [52]. This makes facade installation suitable for Norway and countries located at northern latitudes. In addition, facade does not face challenges due to snow cover [52]. Multiconsult [53] published a presentation regarding solar energy in Norway of specific production, on an annual basis, for facade and roof installations in Norway. The result was roof with southwards installed solar panels had a production of 1090 kWh/kWp/year, facade produced 850 kWh/kWp/year and roof with PV installation oriented East/West produced 840 kWh/kWp/year. Hence, facade and East/West produce similarly in Norway. South-facing facade produces more on an annual basis, but have a strong peak in summer, which can be difficult to utilize. The facade also has a better seasonal profile.

A 3D urban model for calculating and visualizing solar energy potential of buildings was developed by Redweik et al. [54], used a solar radiation model based on climatic observation and a digital surface model built from LiDAR data. For the case study in Lisbon, the findings were significant solar potential, of buildings in an urban area, for the facade. Shen et al. [55] conducted another case study of triple-junction amorphous silicon PV systems for tropical climate. These systems are facade mounted and the study mounted the same system to the rooftop, facing south with a tilt angle of 12°. This study was done in Singapore which has a tropical climate and is located close to the equator. Shen et al. concluded that for this location, horizontally mounted PV systems can produce the double amount of energy compared to vertically mounted PV systems. This is due to the high elevation of the sun. The results showed a facade energy yield ranging from 37% to 51% of a rooftop mounted PV system. A paper written by Frankl et al.[56], presented a study of evaluation of BIPV system over their entire lifetime. The paper did an energy pay-back time analysis of PV systems in central Italy. Frankl et al. stated that the most effective PV systems were installations on flat roofs, and facade showed worse results due to low exposure to the sun at these latitudes. As part of the photovoltaic power system program (PVPS) of the international energy agency task 2, Nordmann et al. [57] published a paper on module temperature of BIPV facade and roof-mounted PV systems. Eighteen different PV systems in Austria, Germany, Italy, Japan and Switzerland were evaluated. The results gave higher module temperature for integrated facade systems compared to roof mounted systems.

4 Method

The installations which are simulated and analyzed in this thesis are Solsmaragden, Skarpnes and Brynseng. This chapter will explain how the systems are constructed in PVsyst, given information and constraints from the actual installation. In addition, data collected and used for the simulation will be explained in this chapter.

4.1 Data

Information regarding data collection for the three instalations will be further described in Subsections 4.1.1, 4.1.2 and 4.1.3 The time series evaluated in this thesis is 2016 and 2017 for Skarpnes, Solsmaragden and Brynseng.

Location	$Latitude^{(\circ)}$	$Longitude^{(\circ)}$	$Elevation(m)$
Skarpnes	58.426	8.722	25
Solsmaragden	59.744	10.205	5
Brynseng	59.90	10.811	81

Table 3: Information regarding location of all BIPV systems included in this thesis. Latitude is north positive, longitude is east positiv and elevation is height above sea level.

The yield is strongly dependent on efficiency, which again depends on external factors such as irradiation, temperature, and device properties. Continuous monitoring and data logging of in-plane irradiation and air or PV module temperature is, therefore, necessary for the performance analysis. However, as data is unavailable for all locations, nearby weather stations are used for more accurate data.

Plane of array (POA) and ambient temperature are data which are desired in addition to longtime series for the measured data. However global horizontal irradiance and air temperature for the weather station is used instead.

4.1.1 Skarpnes data

The site of Skarpnes is the most southern installations of all three. Skarpnes is located south of Arendal and a local weather station measures irradiation, wind speed, ambient temperature and relative humidity [58]. A pyranometer, Kipp & Zonen CMP 11 model, is used to measure the global horizontal irradiation at 1-minute resolution. In addition, temperature sensors are established on the backside of the PV modules. This gives the ability to monitor the operational conditions of the BIPV system [58]. During the time series, the weather data at the site had some downtime. As a result, Kjøita station located in Kristiansand has been used to fill in the missing data for the time period. Kjøita has been used due to close proximity to Skarpnes, and Kjøita also contributed with diffuse irradiation data that was not available for Skarpnes. In the table below, number of days with data collection errors at Skarpnes can be seen.

Month	Days of error
January	No error
February	23-29
March	1,2 and 19-28
April	No error
May	No error
June	8-19
July	5-7
August	9-31
September	No error
October	No error
November	No error
December	No error

Table 4: Information regarding measuring error at Skarpnes for 2016. Kjøita data has been used to replace the missing data retrieval, which is shown in the second column.

4.1.2 Solsmaragden data

Data collection for Solsmaragden is obtained in different ways, due to irregularities in the measured data.

Synthetic data set was gathered from PVsyst library, which obtained the data from Meteronorm 7.1. The dataset is collected for the time period 1991-2010, and is an average value for each month. This data set included global horizontal irradiance, diffuse irradiance, temperature and wind velocity.

Then data were obtained from SunnyPortal [59]. The data were collected from a pyranometer on the south facade on Solsmaragden. SunnyPortal only contributed with global horizontal irradiance data, and the temperature is also needed to perform a simulation. The weather station Berskog, located in Drammen, were elected to provide temperature data. For the data given by SunnyPortal, a few months contained errors. PVsyst compensated for lost data.

Month	Days of error
January	16-31
February	1-12

Table 5: Information regarding measuring error at Solsmaragden for 2017. PVsyst synthetic data has been used to replace the missing data retrieval, which is shown in the second column.

PVsyst also generated diffuse irradiation based on the global horizontal irradiance. Wind velocity was also generated by PVsyst.

Figure 10: Solsmaragden south side.

The pyranometer is mounted vertically and parallel with the south side. Solsmaragden south side is shown in Figure 10.
Data obtained from SunnyPortal was not as expected and measured irradiation data started in

October 2016. Due to these issues, it was decided to obtain irradiation- and temperature data from the weather station at Lier, which gives values similar to what could be expected for Drammen area. The time period was 2016-2018. The data set for 2016, January lack six days irradiance data. PVsyst substituted the missing values. All measured data is measured hourly. Table 6 includes irradiance data which were obtained and used in PVsyst for the Solsmaragden simulation.

$kWh/m^2/month$	1991-2010	2016	2017	
	PVsyst	Lier	SunnyPortal	Lier
January	7.4	7.4	11.7	8.4
February	22.2	35.4	38.8	24.4
March	65.4	61.2	78.2	65.7
April	108.7	101.4	88.6	112.5
May	148.0	153.6	88.1	138.5
June	161.9	166.8	80.2	145.0
July	148.8	159.1	87.4	160.2
August	104.9	112.3	83.3	119.1
September	74.2	83.8	46.4	51.1
October	33.5	30.7	59.2	34.7
November	10.7	9.9	33.1	14.0
December	4.4	5.9	14.8	4.8
Year	890.2	927.5	709.8	878.3

Table 6: Global horizontal irradiance data used in PVsyst for Solsmaragden. PVsyst values are an average monthly value measured from 1991 to 2010. All values are given in monthly [kWh/m^2]

4.1.3 Brynseng data

Synthetic data set was gathered from PVsyst library, which obtained the data from Meteronorm 7.1. The data set is collected for the time period 1991-2010 for the Oslo area. Due to no measured irradiance data on site, Blindern and Aas have been chosen to provide measured data which will be compared to synthetic data. Blindern data was obtained through eKlima and Aas data gathered through NIBIO, [60], all data is measured hourly.

$kWh/m^2/month$	1991-2010	2016		2017	
	PVsyst	Ås	Blindern	Ås	Blindern
January	7.4	8.4	7.9	10.2	4.9
February	22.1	30.7	26.3	27.0	20.5
March	64.7	61.2	56.9	64.9	62.0
April	106.9	97.8	97.6	111.8	106.6
May	152.9	158.9	154.5	151.2	139.4
June	164.1	176.0	164.7	159.3	148.2
July	151.7	164.6	162.5	170.2	154.1
August	106.7	121.7	114.3	128.3	123.1
September	74.8	82.8	82.4	56.1	48.3
October	32.3	33.0	30.4	37.9	34.6
November	10.0	12.3	8.9	15.5	11.8
December	4.5	6.3	3.2	6.6	3.1
Year	898.3	953.9	909.5	939.1	856.4

Table 7: Global horizontal irradiance data used in PVsyst for Brynseng. All values are given in monthly $[kWh/m^2]$

Missing data for Blindern and Ås is substituted by PVsyst. Blindern lacks data for 22 days in January 2016 and Ås experienced seven days of error in May 2017. PVsyst supplied missing data and generated diffuse irradiance and wind velocity.

4.2 Skarpnes

Skarpnes is located south of Arendal and is a project for zero-emission houses. There are a total of 20 houses at Skarpnes but, as seen in Figure 11, only five of the houses are of interest to this thesis. These houses are constructed with BIPV system on the roof [58], and the installations are mounted in two different orientations as illustrated in Figure 11.

Figure 11: Overview of Skarpnes BIPV systems. The five blue rectangles ilustrates where the BIPV system is mounted. [58]

The PV system is designed with 32 panels and with a single inverter. The panel model is 230 Wp Sunpower mono-Si [61]. The inverter type is an SMA Tripower 7000TL-20. The active solar panel area is $40.5m^2$. This gives a total installed PV power per house of $32 * 230W_p = 7360W_p$. Zero emission houses at Skarpnes and the PV installation can be seen in Figure 12

Figure 12: Zero emission house at Skarpnes [3]

This case has been modeled using default albedo values, chosen due to urban situation. In PVsyst, the "Lower temperature for Absolute Voltage Limit" option has been set to -15°C, the value is based on lowest measured value for Skarpnes and is retrieved from yr.no [62]. Other limitations regarding shading representations are set to default values.

4.2.1 Orientation and system

The zero-emission houses at Skarpnes are constructed with the BIPV system installed for two different orientations, as illustrated in Figure 13. Two of the houses have the BIPV system constructed with an azimuth angle of 129°, which equals $-51°$ in PVsyst. The remaining houses have an azimuth angle of 228° which corresponds to 48° in PVsyst. 180° means the modules are facing directly southwards. The roof tilt of all houses is 32°.
The next step is to define the PV system in use at Skarpnes. Since the total installed PV power, per house, is known presizing of the planned power can be set to $7.36kWp$. PVsyst includes the PV module which is needed for this task: SPR-230NE-BLK-D manufactured by Sunpower as well as the inverter SMA Tripower 7000TL-20. After selecting PV module and inverter, PVsyst proposed an array design with two strings of 16 modules for this situation, which corresponds to the actual installation.

4.2.2 Horizon and shading

For the task of creating the horizon and far shadings of the site, PVGIS[63] was used. With the interactive map, it was possible to get the exact coordinates of the houses located at Skarpnes.

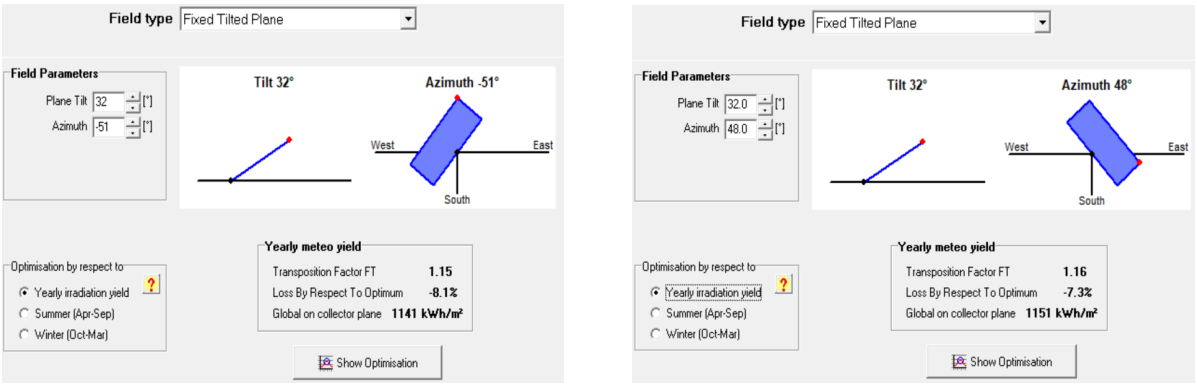

(a) Orientation 1 (b) Orientation 2

Figure 13: Illustration of BIPV system for houses at Skarpnes

Because of minor differences of the far horizon shading, the house located at the most southern position was selected with the coordinates of 58.426, 8.722. The horizon profile was then extracted from PVGIS manually as shown in Figure 14. According to PVsyst, houses with an azimuth angle of 48(∘) has a higher yield on the collector plane than the houses with an azimuth angle of −51(∘).

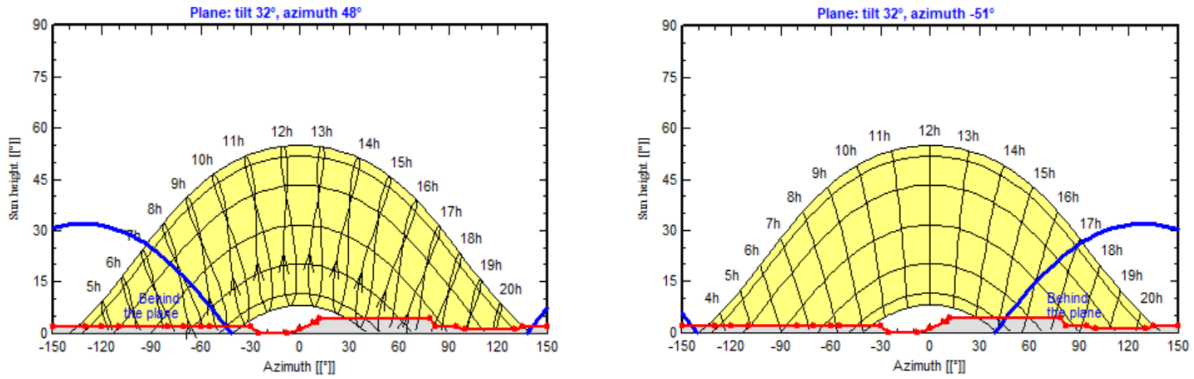

(a) Horizon for Skarpnes, orintation 48° (b) Horizon for Skarpnes, orintation -51°

Figure 14: Illustration of the Horizon surrounding Skarpnes.

In figure 14, the X-axis is the azimuth angle (∘) and the Y-axis is the height of the sun (∘). The green area is supposed to resemble the horizon while the blue line indicates when the sun is behind the PV plane at Skarpnes. For the houses with an azimuth angle of -51°, the sun is available from around 04:00 to 17:30 in the evening. For the houses with an azimuth angle of 48°, the sun is available from 07:00 to 21:00.

In Figure 15, the design of the zero-emission houses at Skarpnes. Figure 15b shows the houses with an azimuth angle of -51°.

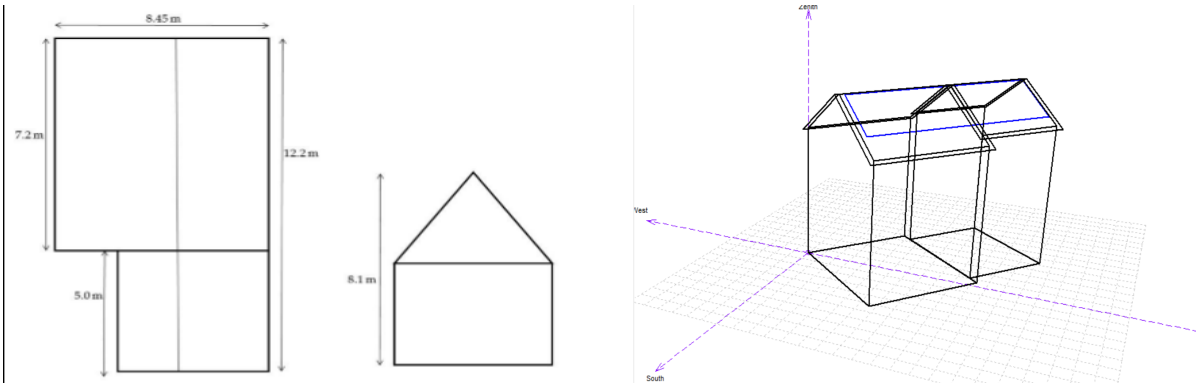

(a) Scematic layout of zero emission houses at Skarpnes[23].

(b) 3D-model of zero emission houses at skarpnes made in PVsyst.

Figure 15: Illustration of 3Dmodel of zero emission houses at Skarpnes

The blue rectangle represents the PV module with an area of 39.8 m^2.

This setup results in an integration with fully insulated back, in accordance with the mounting solution in the simulation. Soiling losses are also set to 20 % for the winter month, which deviates from the standard 3 % for the rest of the year. This soiling is higher in the winter month due to snow is not a part of the meteo data in PVsyst, and this value can be difficult to assume. Near shading impact for this simulation is created by the roof.

4.3 Solsmaragden

Solsmaragden is an office building located in Drammen. The building has seven floors and the BIPV system has green laminated glasses.

4.3.1 System

All the facades are BIPV installations but the roof has a BAPV solution, and this thesis will simulate the south facade. The whole building has a PV area of 1620 m^2 where 1220 m^2 form the facade. The facade has a nominal effect of 127 kWp, which includes 979 panels, and 22 different PV modules are used as well as 13 inverters. The only inverters relevant for this task is inverter 7 and 8, which are located on the south side of the building, with an Azimuth angle of 205°.

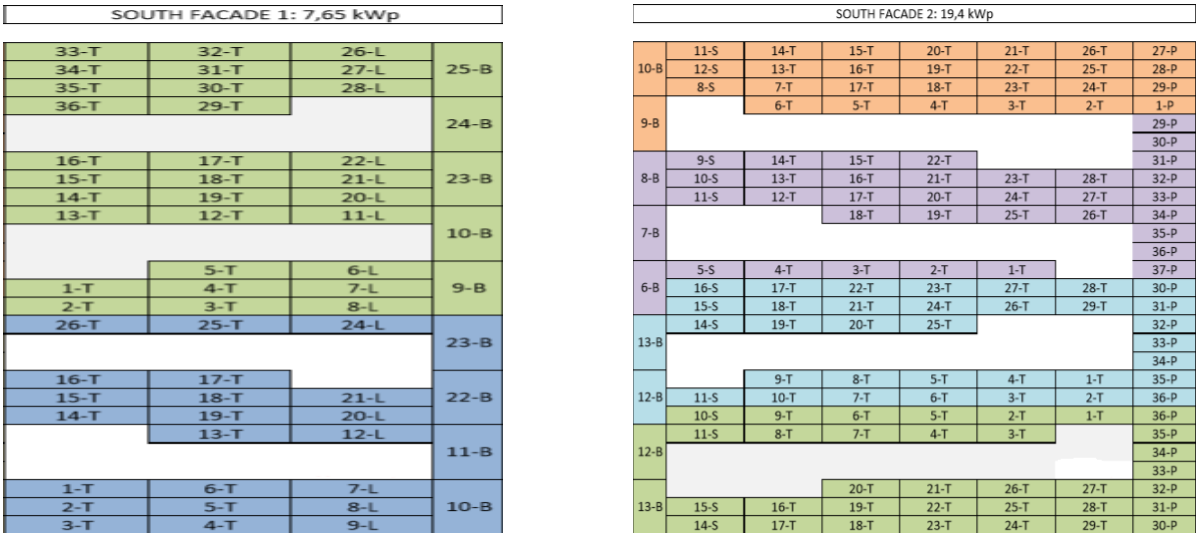

(a) Overview of PV modules connected to inverter 7. (b) Overview of PV modules connected to inverter 8.

Figure 16: Overview of the 2 inverters of interest for this thesis.

As seen in Figure 16, inverter 7 has 2 strings and inverter 8 has 4 strings, which are illustrated in different colors. The letter represents the cell type, and the number behind represent the position in the strings. This means inverter 7 contains PV module B, L and T, while inverter 8 contains modules like B, S, T and P. Modules used in the simulation is based on an average area of the actual active area of each inverter.

Inverter number	Module type	Amount of modules	Area[m^2]
Inverter 7	B	9	7.89
Inverter 7	L	17	16.75
Inverter 7	T	36	52.88
Inverter 8	B	9	7.89
Inverter 8	S	15	21.82
Inverter 8	T	87	127.81
Inverter 8	P	27	32.50

Table 8: Table of modules used at Solsmaragden for inverter 7 and 8.

Table 8 gives information regarding modules used at the south facade of Solsmaragden. The area is also listed, which gives a total area of the inverters 7 and 8 of 77.52 m^2 and 190 m^2 respectively. According to PVsyst this area yields a planned power of 8000 W_p and 19400 W_p. Using the planned power and dividing by the quantity of modules, the type of module can be selected in PVsyst to create a similar situation as the real case. Inverter 7 has 62 modules of different sorts, but the PVsyst simulation has 61 modules of 125 Wp Issol CENIT 125 model. While inverter 8 has 129 modules consisting of 4 different types in the actual case, but 129 modules of 150 W_p Issol CENIT 220 is used for the simulation. This estimation has been done due to the lack of possibility in PVsyst to select several module types for each inverter.

Due to the choice of the module in inverter 8, it resulted in a higher active area than the actual system. This choice was done in order to obtain actual installed power for the system, which has a yield production impact. Which lead to a removal of 12 modules in inverter 8 for gaining an acceptable active area. For the simulation, the modules are mounted semi integrated with air duct behind, as is the case with the actual system.

Furthermore, the simulation is done by creating 2 subarrays in order to use 2 different inverters which is the real case. Inverter 7, for sub-array 7, is an STP 6000 TL-20 inverter and for sub-array 8 an STP 15000 TL-10 inverter has been used [64, 65].

4.3.2 Shading and 3D-model

PVGIS [63] was used to create a horizon profile for Solsmaragden, which was drawn manually.

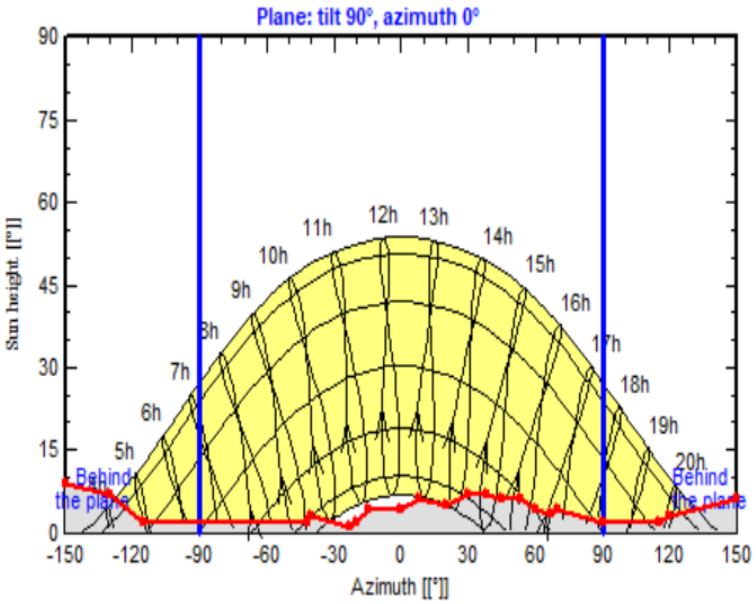

Figure 17: Illustration of the horizon surrounding Solsmaragden.

As the PV modules are integrated on the facades the tilt of the PV modules are 90°. As a result, the sun will only reach the panels between approximately 07:00 in the morning until nearly 17:00 in the afternoon. As seen in Figure 18b, a sign is covering some of the modules on inverter 8. However, the sign does not have any effect on the system, because the modules covered by it are not connected. For the simulation, the only near shading affecting the system is shading caused by the building which is illustrated in Figure 18.

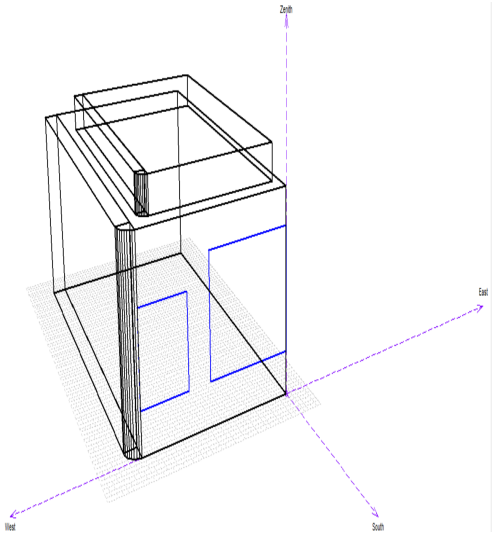

(a) Illustration of Solsmaragden made in PVsyst. The smaller blue rectangle represents inverter 7 and the larger blue rectangle represents inverter 8.

(b) Picture of the actual system, at the south side of the building.

Figure 18: On the left side is the 3D model of Solsmaragden, which is shown on the right side.

The model is a simplification of Solsmaragden. North and east side of the building has a more detailed outline, but because this does not affect the PV panels at the south side the model was done this way. In figure 18a, the 2 blue rectangles illustrates inverter 7 and 8. Inverter 7 is the smaller one. However, the modeled PV area is larger than the actual area at Solsmaragden, this is due to the module choice. There is also a sign mounted on the top right side of the south facade, however, this does not have any impact on the production. An actual representation of the PV fields was difficult due to the windows.

4.4 Brynseng

The primary school Brynseng in Oslo is located at Gamle Oslo district (59.909N, 10.811E). Brynseng is one of the largest BIPV constructions in Norway and Undervisningsbygg is constructing the project. It is a 6-level building with BIPV facade system of 1046 m^2 area which is estimated to produce 100 MWh per year. Just like the Skarpnes case, Bryseng primary school is constructed as a nearly zero-emission building. ISSOL delivers the PV-modules and the modules are installed by Staticus, a Lithuanian company, with NCCs [66] entrepreneurs doing the electrical couplings. In Figure 19, an illustration of the system is shown.

Figure 19

4.4.1 System

The BIPV system at Brynseng has some similarities to Solsmaragden, such as modules mounted with a 90° tilt and several inverters. The facade is composed of three parts: Left, Right and Central part, shown in Figure 19. Modules mounted on the facade has an azimuth angle of 185°.

Brynseng uses PV modules of the type: CENIT 220 from ISSOL. These vary in sizes to fit the facade and are glass-glass modules with monocrystalline PV cells. The active facade is composed of 1122 modules, with a total power of 163.3 kWp which means a total surface of 1598 m^2. The available area for PV field is larger than the actual area on Brynseng. Different type of PV module CENIT 220 is used with different sizes to fit the facade for the actual system, PVsyst is unable to scale the same module for the same sub-array. All modules are mounted without frames, and the mounting system allows for air circulation between the PV modules and the facade, which is the case for the actual system.

For the facade, 3 different inverters of different sizes are used in the simulation, and in Table 9 an overview of the positioning of the inverters is presented. These inverters are three-phased with two independent MPP inputs.

Position	Inverter	Inverter type	Peak power (kWh)
Left side	1	SMA STP 15000	17.5
Left side	2	SMA STP 15000	16.7
Left side	3	SMA STP 15000	16.1
Central part	4	SMA STP 15000	17.5
Central part	5	SMA STP 12000	14.57
Right side	6	SMA STP 25000	29
Right side	7	SMA STP 25000	27.9
Right side	8	SMA STP 25000	26.1

Table 9: Table of inverters and their positioning at the BIPV system of Brynseng school and the planned power for each inverter.

The system is designed with 3 sub-arrays, left side, central part and right side. Left side and center part contain inverter type SMA STP 15000 CENIT 220 and right side inverter SMA STP 25000 CENIT 220 is selected [67].

4.4.2 Shading and 3D-model

PVGIS [63] is used to get a horizon shading the site, and just like the other cases, the horizon was drawn manually in PVsyst.

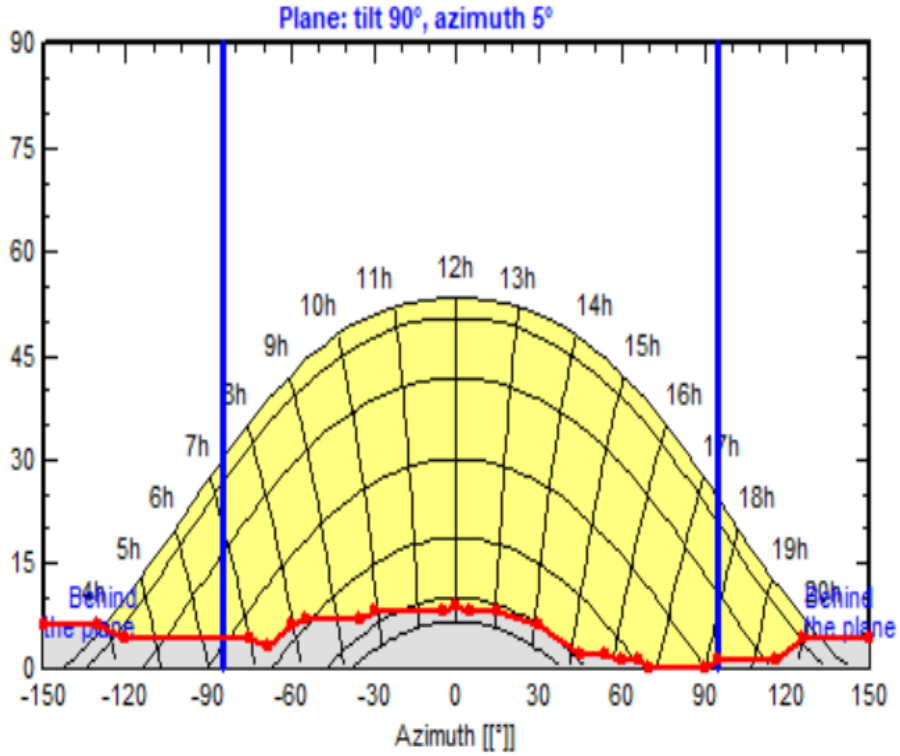

Figure 20: Brynseng horizon

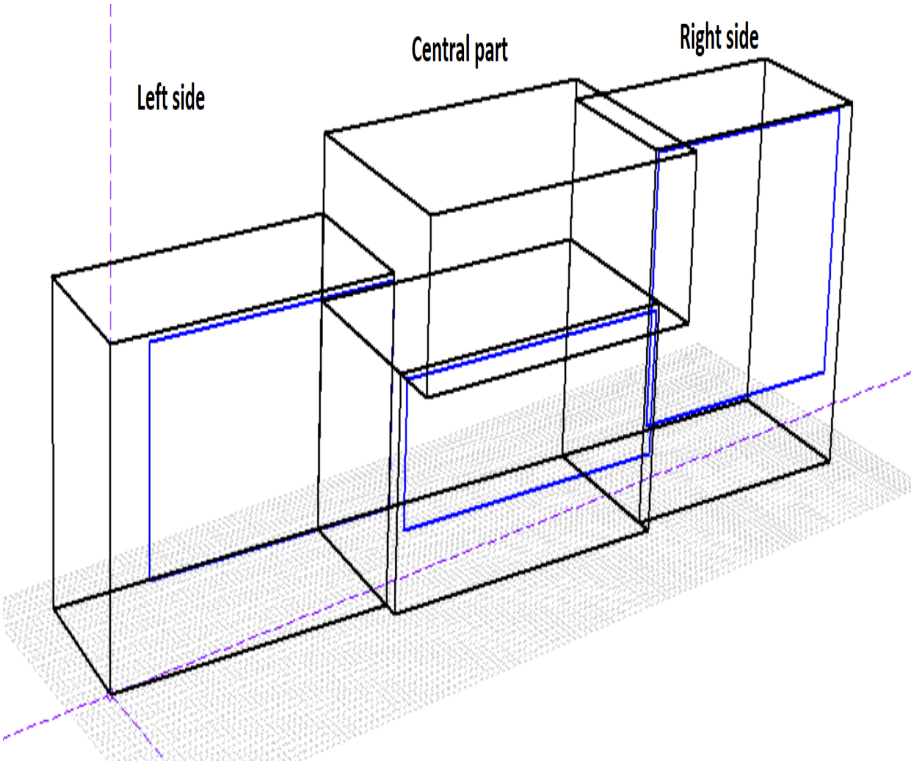

Figure 21: 3D model of Brynseng.

Figure 21 illustrate the school building and PV fields as designed in PVsyst. The blue rectangles resemble PV area and the system has an azimuth angle of 5°. Unable to include windows into the PV fields, gives another reason to larger PV area than the actual system.

4.5 Roof versus facade

Solsmaragden has been selected to be the system for which the simulation has been conducted, to test the hypothesis of facades are more advantageous for northern location. Firstly the simulation is done by using the Solsmaragden system for different locations. Then the simulation is done by mounting the PV field on the roof. The system is identical in both scenarios however, the two rectangular PV planes are now mounted on the roof instead of the south facade. The PV field has a tilt angle of 10° but the azimuth angle is identical. Synthetic data produced in PVsyst, retrieved from Meteonorm 7.1 has been used for all simulations.

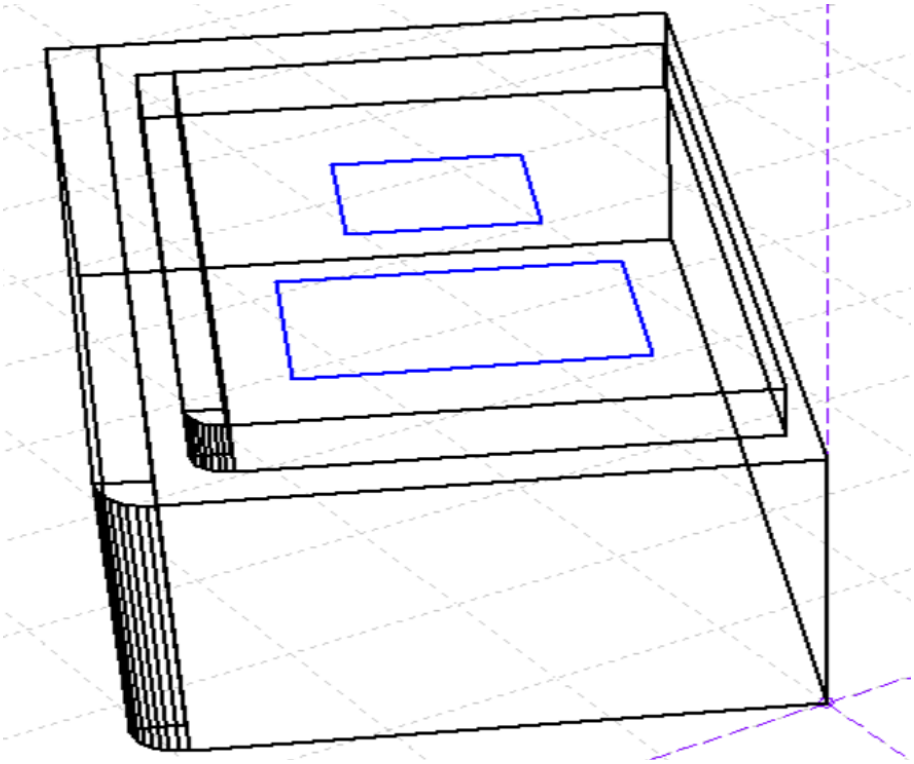

Figure 22: Solsmaragden with roof mounted PV field.

As seen in the Figure 22, the PV field is mounted on the roof instead of the south facade.

The simulation is done for a few different locations for the system. Bodø, Drammen and Roma and Cape Town has been selected in order to assess the hypothesis.
All facade production has been evaluated in comparison with the roof production, according to the following expression.

$$(\frac{FacadeProd - RoofProd}{RoofProd}) * 100 = \% \tag{14}$$

where FacadeProd is the annual energy produced from the facade and RoofProd is the energy production from the roof.

Location	$Latitude(\circ)$	$Longitude(\circ)$	$Elevation(m)$
Bodø	67.27	17.37	19
Drammen	59.744	10.205	5
Rome	41.58	12.58	107
Cape Town	-33.97	18.60	50

Table 10: All locations for the assessment of the hypothesis.

4.6 Partial shading model

A major loss parameter in PVsyst is shading, far shading and near shading. Partial shading model is used to calculate effect for PV array under shading impact. The model used in this thesis is an expansion on a partial shading model published by MathWork [68]. This thesis will use the model to create different scenarios for which modules will be exposed to shading, and inspect how this will impact I-V- and P-V curves, affect output of the PV system. Brynseng system has been chosen, and a string from inverter 8 has been recreated

The model is composed of a PV string containing 14 modules, with 72 series-connected cells in parallel with 14 bypass diodes which allows current flows when cells are damaged or shaded. The module used is Sunpower SPR-X20-250-BLK (250W) [69], due to the simulink library did not include Issol modules used at Brynseng.

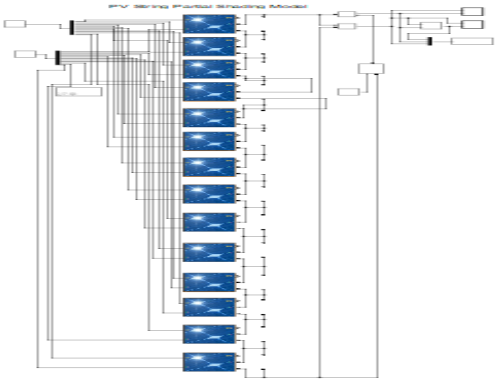

(a) Illustration of the full partial shading model used in Simulink

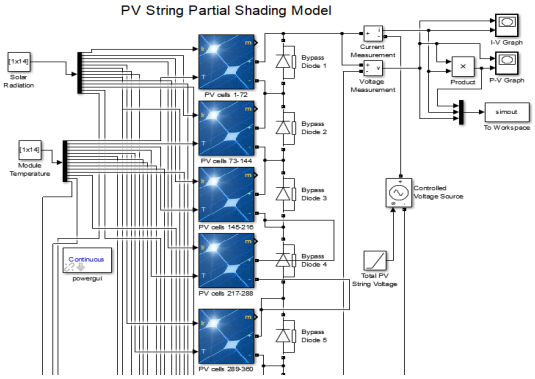

(b) Illustration of the setup for partia shading model

Figure 23: Partial shading model used for the Brynseng case.

Figure 23 a, the full model is illustrated. Figure 23 b gives a close up look at how the model is designed.
Four situations have been assessed in this thesis. Standard irradiance 1000 W/m^2 is applied to all modules for the first situation. The temperature for each module is 25°.

For situation 2, the string is 25 % shaded where module 1-3 is completely shaded and partial

shading is applied on module 4, resulting in irradiance of 500 W/m^2. Standard irradiance 1000 W/m^2 is applied to the rest of the modules. The temperature for each module is 25°.

For situation 3, the string is 50% shaded, which means only seven modules experience irradiance of $1000W/m^2$. The temperature for each module is 25°.

For the last situation, various irradiance will be applied in the modules.

5 Results

Simulation results of the three different systems are analyzed in this section. The chapter is divided into three parts, one section for each system. The results obtained were analyzed for assessing the performance of the chosen installations. Results regarding partial shading model are also addressed, in addition to results of roof compared to facade production for different location.

5.1 Skarpnes

Skarpnes has two different scenarios for its case, which are two different orientations. The results were obtained from the simulation model of 7.36 kWp Si-mono PV system simulated in PVsyst.

5.1.1 Main simulation results

From the results, three main parameters were assessed. The first parameter is the total amount of energy produced on an annual basis. The total production, for 48° and −51° orientation, was 6.88 MWh/year and 6.85 MWh/year respectively. The second parameter is specific yield on an annual basis per installed kWp, and this value is 935 kWh/kWp/year and 931 kWh/kWp/year for the orientation 48° and −51° respectively. The third parameter is the average annual performance ratio which is 79.5% and 79.8%.

Month	GHI kWh/m^2	T_{amb} $°C$	GII kWh/m^2	G_{Eff} kWh/m^2	E_{array} MWh	E_{grid} MWh	AAE %	AAE_s %
January	12.8	-2.60	20.3	15.0	0.108	0.099	13.38	12.28
February	38.8	2.00	63.0	47.5	0.338	0.327	13.48	13.03
March	62.9	4.00	79.6	73.0	0.508	0.491	16.02	15.48
April	116.1	5.80	130.0	120.9	0.823	0.799	15.90	15.44
May	173.5	11.80	183.6	171.0	1.120	1.090	15.32	14.92
June	166.2	15.70	164.7	152.7	0.996	0.967	15.18	14.75
July	173.0	16.20	179.9	167.3	1.079	1.050	15.07	14.66
August	134.0	15.70	146.4	136.2	0.885	0.860	15.18	14.75
September	95.3	15.10	115.2	106.8	0.700	0.681	15.27	14.85
October	35.1	6.70	47.2	43.3	0.299	0.285	15.94	15.18
November	16.8	3.20	22.6	17.0	0.120	0.111	13.35	12.35
December	13.0	4.70	24.6	18.3	0.130	0.124	13.25	12.63
Year	1037.5	8.22	1177.1	1069.1	7.106	6.885	15.16	14.69

Table 11: Balance and main result

In Table 11 GHI is global horizontal irradiation, T_{amb} is ambient temperature, GII is global incident irradiation on collector plane, G_{Eff} is global irradiance considering soiling losses and shading losses, E_{array} is effective energy at the output of the array, E_{grid} is energy injected into

the grid, AAE is annual average efficiency of a PV array and AAE_s is the annual average efficiency of the system.

For this study annual global irradiance on the horizontal plane is 1037.5 kWh/m^2, for measured Skarpnes irradiance- and temperature data, and on the collector on annual basis is 1177.1 kWh/m^2. Annual DC energy produced is 7.106 MWh and the annual AC energy ejected into the grid is 6.885 MWh. The annual average efficiency of the PV array is simulated to be 15.16% and the system found to have an efficiency of 14.69%.

5.1.2 Normalized production

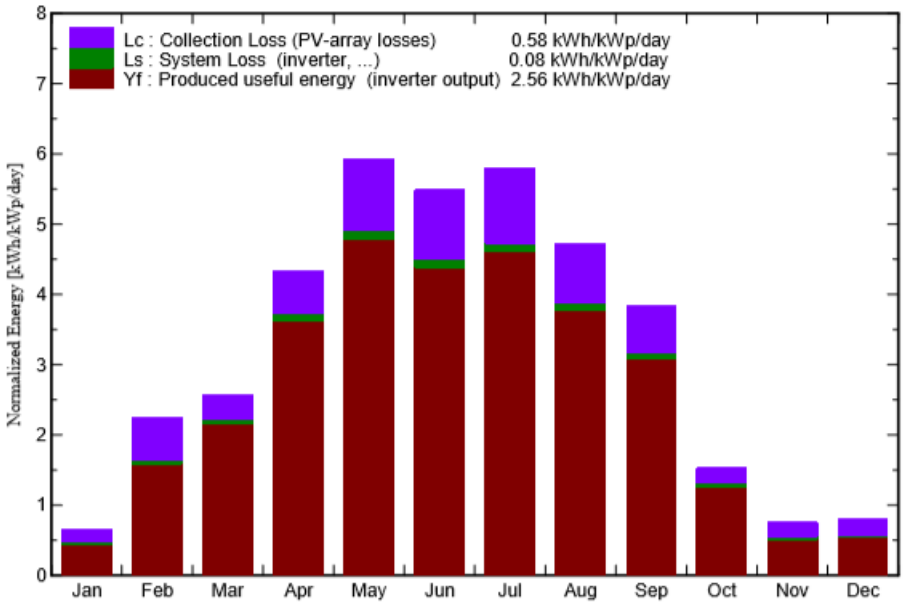

Figure 24: Normalized energy production for orientation for orientation 48°.

Normalized productions, which is illustrated in Figure 24, were evaluated in the study. This is collection losses, system losses and produced useful energy. These normalized productions are defined by IEC norms [70]. Lc is collection losses (PV-array losses) and has a value of 0.58 kWh/kWp/day. System losses, Ls (such as losses due to inverters), has a value of 0.08 kWh/kWp/day and the system has a useful energy production of 2.56 kWh/kWp/day.

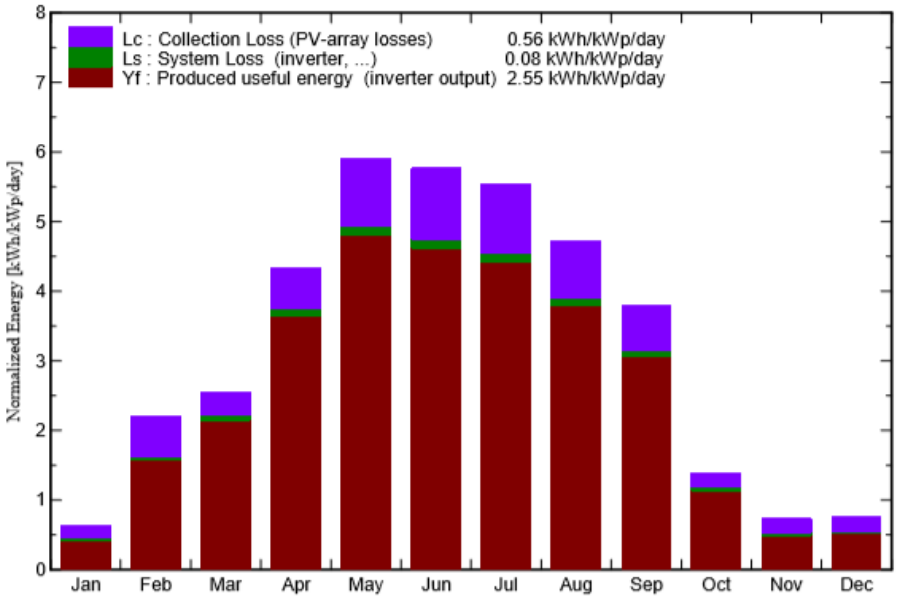

Figure 25: Normalized energy production for orientation $-51°$

Figure 25 illustrates normalized production for the house with orientation $-51°$. Collection losses, Lc, has a value of 0.56 kWh/kWp/day and system losses are identical for both situations. The system has a useful energy production of 2.55 kWh/kWp/day.

5.1.3 Performance ratio

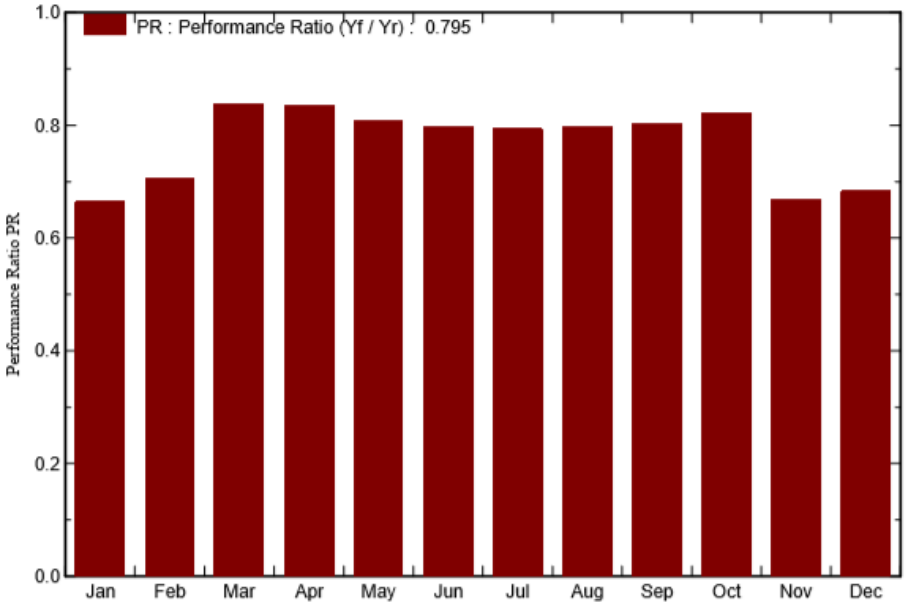

Figure 26: PR value

PR value, for the zero emission house oriented with an azimuth angle of 48°, is given in figure 26. The PR is significantly lower for the time period November-February, and have an average value of 79.5%.

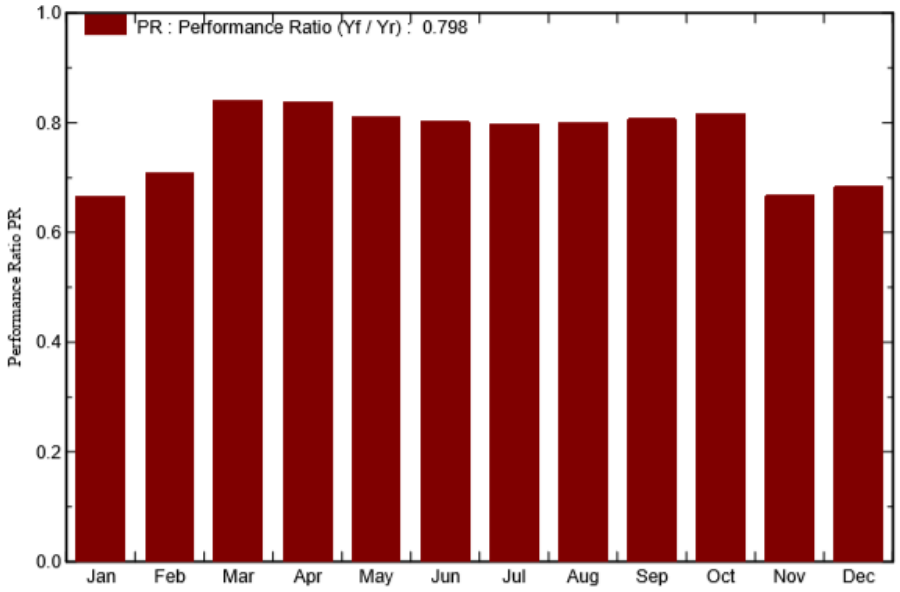

Figure 27: PR value

PR value, for the zero emission house oriented with an azimuth angle of −51°, is given in figure 26. The PR is significantly lower for the time period November-February, and have an average value of 79.8 %.

Lower PR value in the time period November-February is due to simulated soiling. Soling losses represent 1.7% decrease in PR value, and by using standard values for the system would increase the performance ratio to 81.3% and 81.5% for the two scenarios.

5.1.4 Arrow loss diagram

The arrow loss diagram, as shown in Figure 28, illustrates various losses for the simulated system. Global irradiance on the horizontal plane is 1038 kWh/m^2, however, the effective irradiance on collectors is 1069 kWh/m^2 which gives a 1.5% loss due to irradiance level. When the effective irradiance hits cover a module or array, electric energy or electricity is produced. This gives an efficiency for the PV array at STC of 18.52%. Annual array virtual energy at MPP is 7.11 MWh. The losses at this stage are 4.9% due to temperature, 1% due to degradation, 2% due to array mismatch and 0.8% due to ohmic wiring losses. The available energy on an annual basis at inverter output is 6.88 MWh, and this is injected into the grid. Here two losses occur: 3% due to inverter operation and 0.1% inverter loss due to the power threshold.

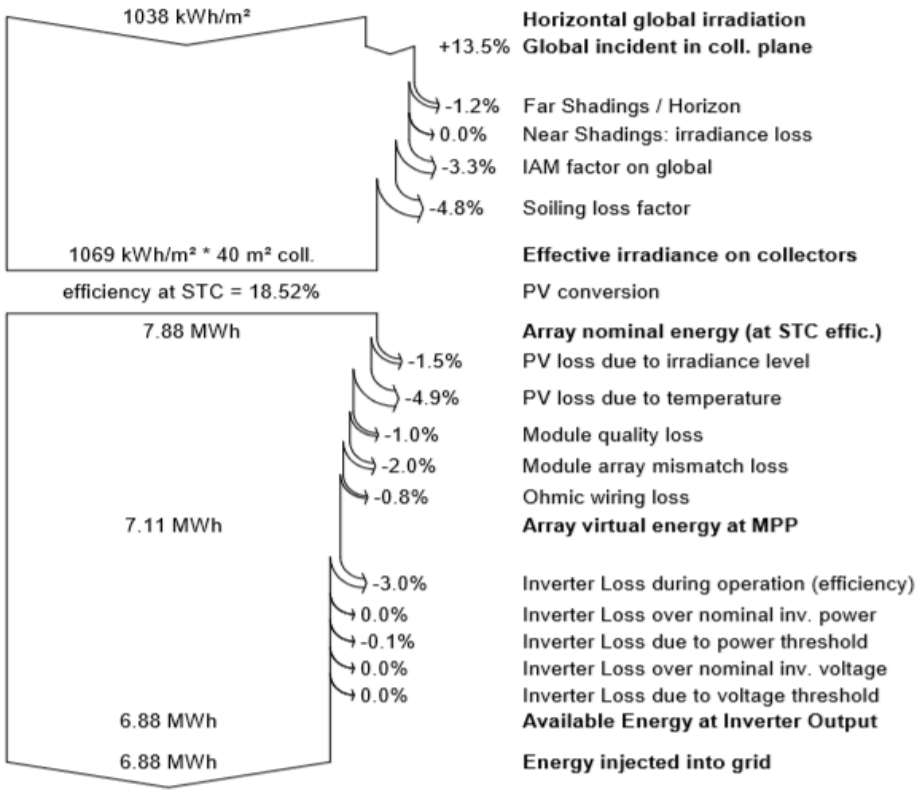

Figure 28: Arrow loss diagram for system oriented 48 degrees.

Figure 29 gives losses for the system rotated to the azimuth angle of $-51°$.

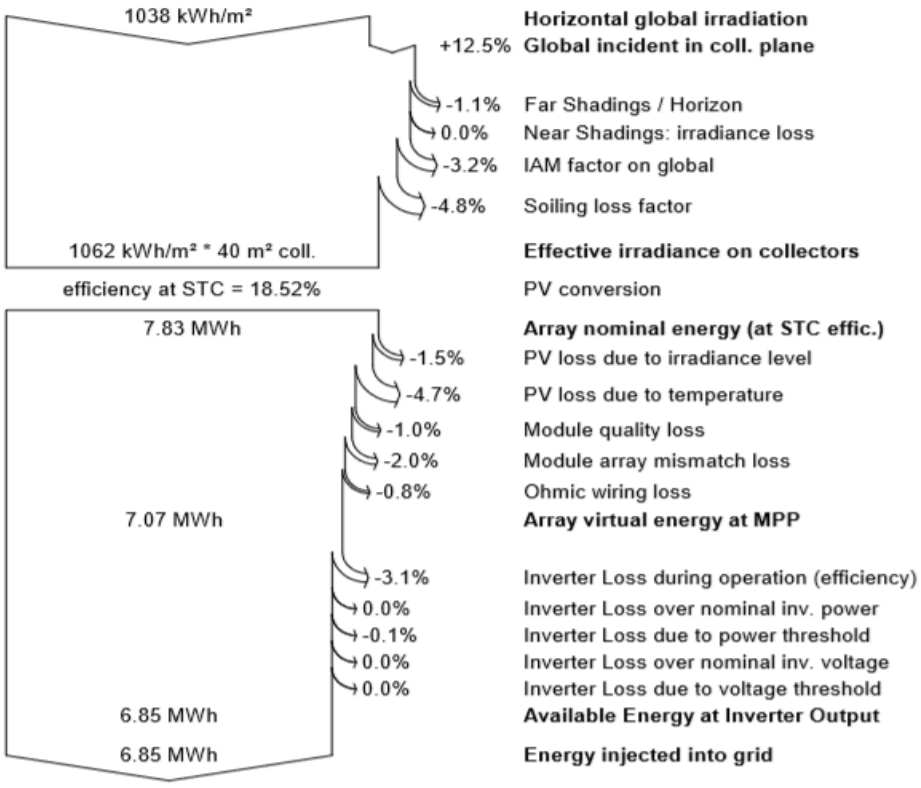

Figure 29: Arrow loss diagram for system oriented -51 degrees.

The similarities for these results are minor and the energy ejected into the grid is slightly higher for the system with the azimuth angle of 48°. Temperature is the biggest loss contributor followed by soiling losses. Temperature losses are based on mounting choice and, by using semi integrated mounting with air duct behind will increase production of 0.16 MWh and 0.155 MWh on an annual basis. By mitigating soiling losses to standard values, the production will increase with 0.123 MWh and 0.116 MWh on an annual basis. By using synthetic data generated by PVsyst through Meteonorm 7.1, the system production is 3.93% inferior compared to real measured data. Inverter losses during operation is also a major loss contributor.

Uncertainty in measured data was 52 days in 2016, and made a major impact on the production and performance of the simulated system. The simulated system production decreased with 1412 MWh annually when taking irradiation data uncertainty into account. As a result, the performance ratio decreased to 64.0%.

5.2 Solsmaragden

Solsmaragden was simulated with different data sets, and this section will evaluate the most relevant results for each simulation.

5.2.1 Main results

Three main parameters were assessed for Solsmaragden. Simulation of the south side of Solsmaragden gave an annual energy production of 17.01 MWh/year for synthetic data. The specific yield on an annual basis resulted in 637 kWh/kWp/year. The annual performance ratio was 79.7% for synthetic data.

Month	GHI kWh/m^2	T_{amb} $^{\circ}C$	GII kWh/m^2	G_{Eff} kWh/m^2	E_{array} MWh	E_{grid} MWh	AAE %	AAE_s %
January	7.4	1.05	16.5	13.34	0.342	0.328	7.86	7.54
February	22.2	0.55	35.7	32.09	0.841	0.811	8.90	8.59
March	65.4	2.41	92.1	84.61	2.163	2.105	8.87	8.64
April	108.7	6.48	102.9	93.28	2.335	2.269	8.57	8.33
May	148.0	10.86	102.5	90.47	2.234	2.163	8.24	7.98
June	161.9	13.89	96.2	83.57	2.052	1.983	8.06	7.79
July	148.8	16.46	94.2	82.09	1.991	1.923	7.98	7.71
August	104.9	16.11	83.7	74.22	1.791	1.732	8.09	7.82
September	74.2	12.42	84.6	77.21	1.872	1.816	8.36	8.11
October	33.5	8.06	52.9	48.31	1.201	1.161	8.59	8.30
November	10.7	4.62	26.3	21.28	0.542	0.518	7.79	7.45
December	4.4	1.60	11.5	8.33	0.213	0.204	7.03	6.72
Year	890.2	7.92	799.1	708.80	17.577	17.013	8.31	8.05

Table 12: Balance and main result for Solsmaragden synthetic data

For this study annual global irradiance on the horizontal plane is 890.2 kWh/m^2, and on the collector on annual basis is 799.1 kWh/m^2. Annual DC energy produced is 17.577 MWh and the annual AC energy ejected into the grid is 17.013 MWh. The annual average efficiency of the PV array is simulated to be 8.31% and the system has an efficiency of 8.05%.

Including days of error into synthetic data, for January and February, the annual production declines to 15.456 MWh with a PR value of 72.4%. This yield a 9.2% loss due to system unavailability. Changing mounting possibility to integration with fully insulated back, the production decreases to 15.073 MWh on an annual basis with a PR value of 70.6%. This loss is due to temperature on array level.

5.2.2 Normalized production and PR value

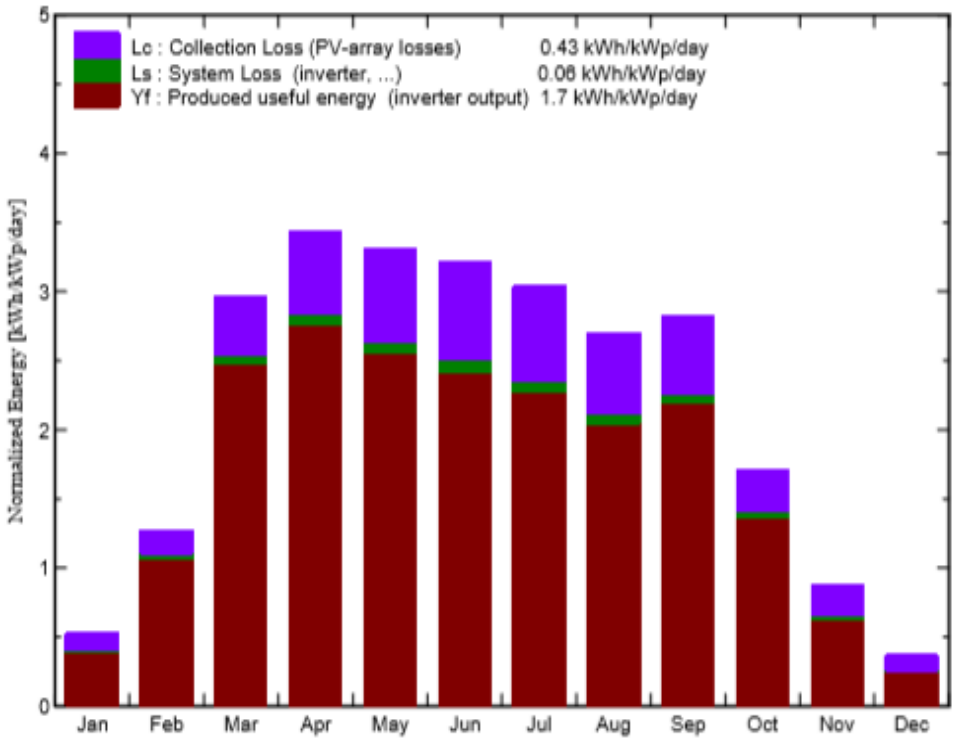

Figure 30: Results for synthetic data.

In Figure 30 normalized production is presented in the left graph. Usefull energy for Solsmaragden is 1.75 kWh/kWp/day. Collection loss is 0.39 kWh/kWp/day and system losses are calculated to 0.06 kWh/kWp/day.

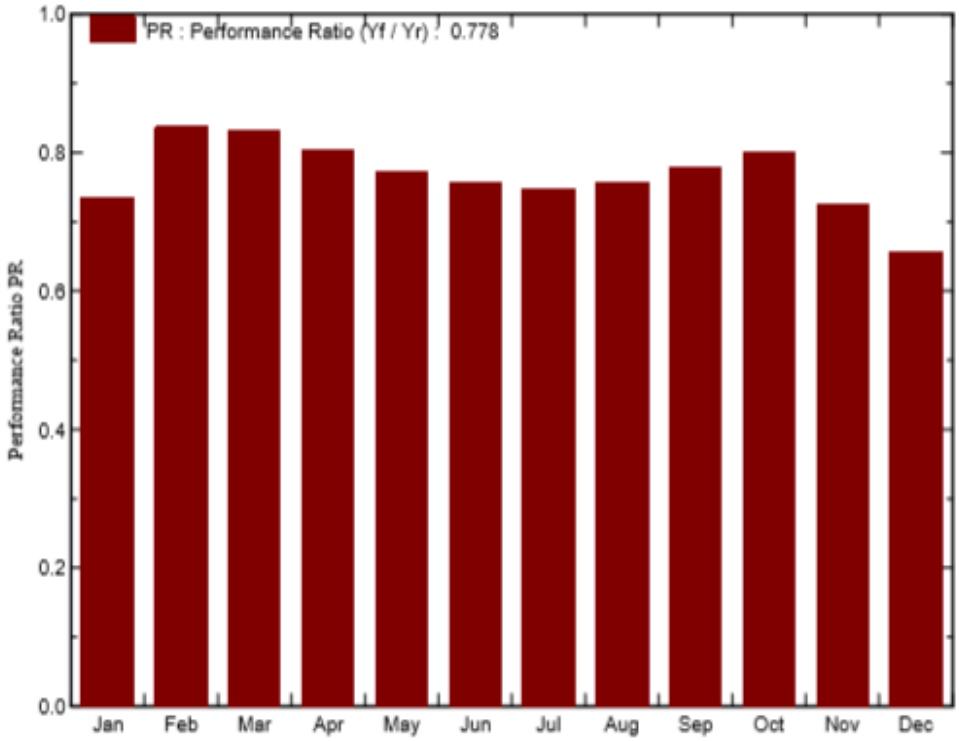

Figure 31: PR results for synthetic data.

Figure 31 gives the performance ratio result for Solsmaragden by using synthetic data, which is an average value of 77.8% on an annual basis. There are slightly monthly variations in PR value, and February, March and October are the months with highest PR value.

5.2.3 Losses

Figure 32 illustrates a loss diagram for various losses of the simulated system.

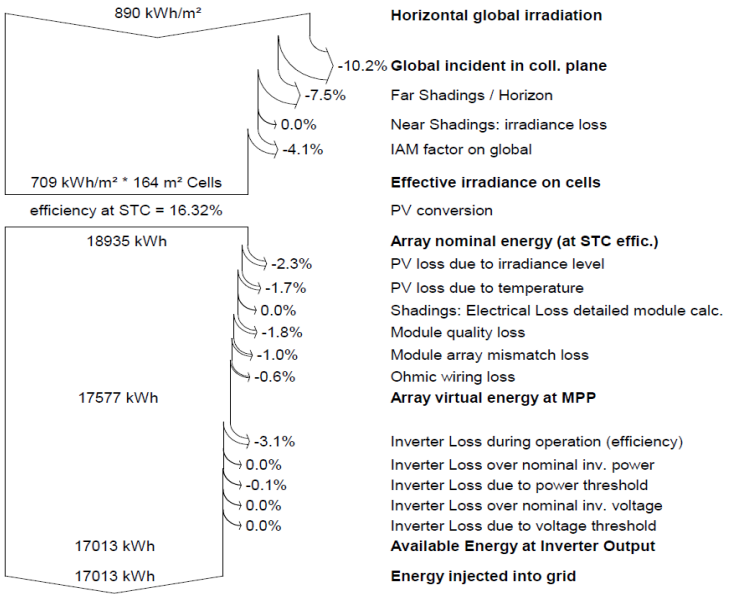

Figure 32: Losses for Solamaragden given synthetic data.

Global irradiance on the plane is 890 kWh/m^2 while only 709 kWh/m^2 effective irradiance reaches the cells which give a 2.3% loss due to irradiance. Within these losses, horizon shading and global incident irradiation on collector plane is the main reason for irradiance losses. This means 18.94 MWh energy is produced and the system has an efficiency of 16.32% at STC. Annual array virtual energy at MPP is 17.577 MWh. The losses at this stage are 1.7% due to temperature, 1.8% due to degradation, 1.0% due to array mismatch and 0.6% due to ohmic wiring losses. The available energy (annual basis) at inverter output is 17.013 MWh, and this is injected into the grid. Here two losses occur: 3.1% due to inverter operation and 0.1% inverter loss due to the power threshold.

5.2.4 Measured data

Data measured from SunnyPortal were implemented in the simulation, for the exact same system. The total amount of energy produced was 20.02 MWh/year, with a specific yield of 750 kWh/kWp/year and an average annual performance ratio of 74.7%.

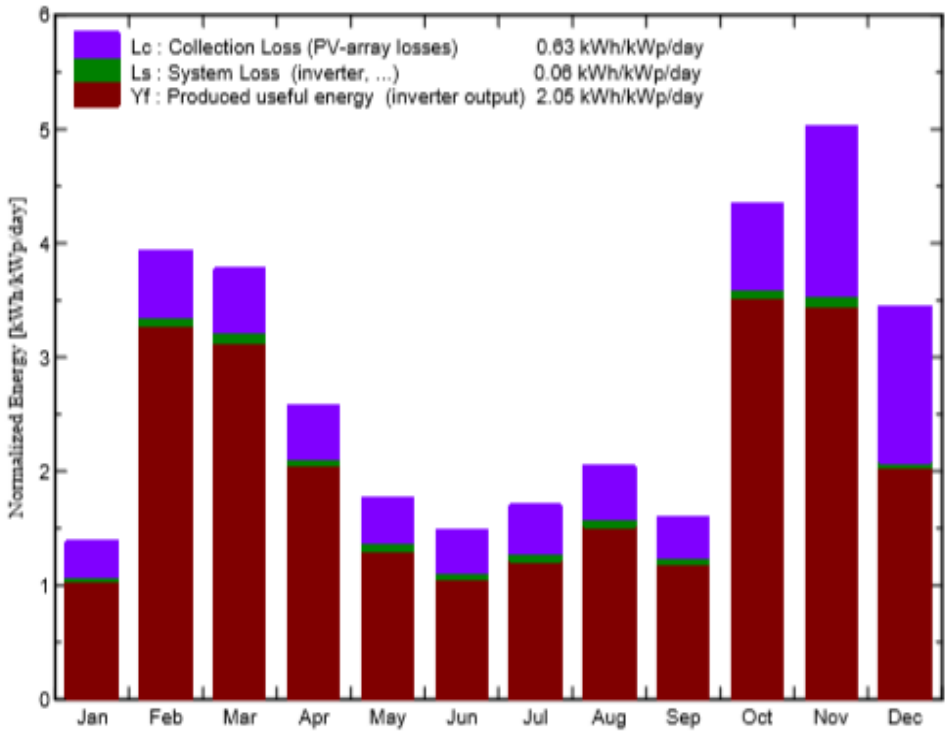

Figure 33: Normalized production results for Solsmaragden, given measured data.

Normalized production, which is illustrated in the left graph in Figure 33, includes 3 parameters. Lc, collection losses, has a value of 0.63 kWh/kWp/day, which is large and extensive for November and December. Ls, system losses, resulted in 0.06 kWh/kWp/day, which gives no changes compared to synthetic data. The last parameter is useful energy production which is 2.05 kWh/kWp/day.

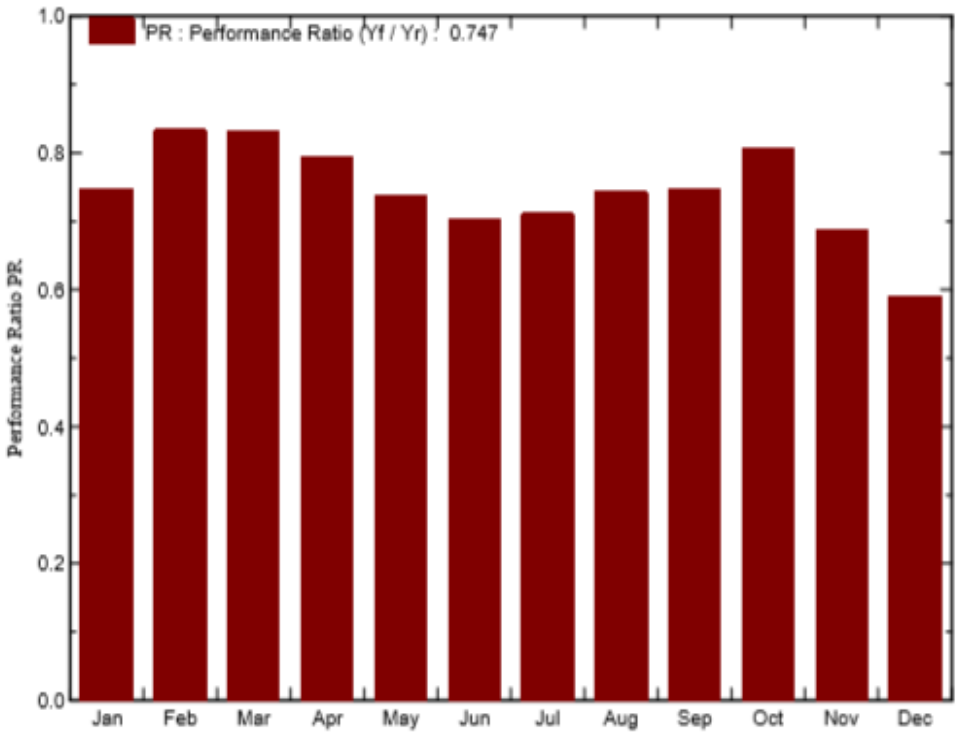

Figure 34: Results for Solsmaragden given measured data.

The performance ratio, shown in Figure 34, has an average annual value of 74.7%. November, December and January contribute to low PR value, due to irradiance data set issue which is explained below.

Using measured data for GHI gave an annual irradiance of 709.84 kWh/m^2 which is inferior to the annual irradiance for synthetic data, which was 890.2 kWh/m^2. Due to PVsyst issues with processing the irradiance data, incident irradiance on collector plane receives an enormous gain which should not occur in this system. This facade system should experience losses due to incident irradiance on collector plane. As GHI is 709.84 kWh/m^2, increased global incident irradiance on collector plane is simulated to be 1003.4 kWh/m^2 on an annual basis. Ambient temperature also decreased for real measured data, which has an average value of 6.78° annually, compared to the synthetic data which is simulated to have an average value of 7.92° annually. Using measured data increases the energy injected into the grid with 3.006 MWh compared to using synthetic data. The efficiency of the array and system decreased from 8.31% to 7.78% and 8.05 to 7.54% respectively.

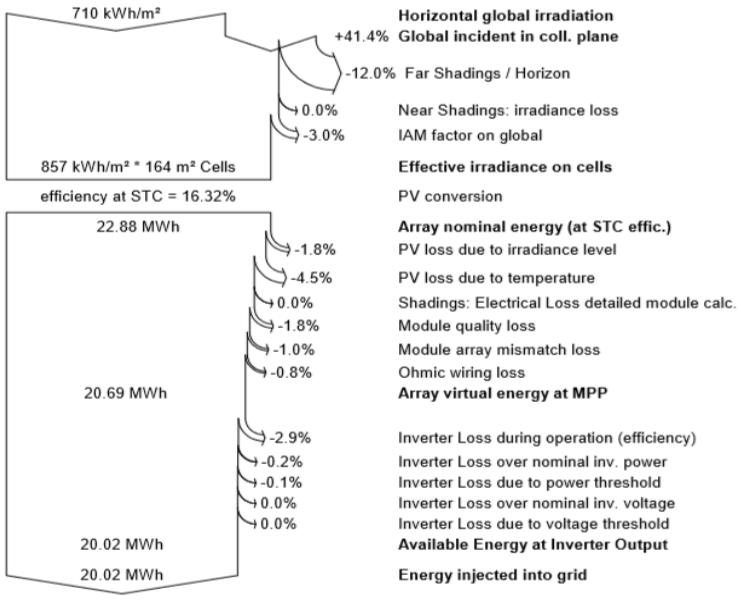

Figure 35: Losses for Solamaragden given measured data.

As seen in Figure 35, the major differences for real measured data simulation and synthetic data is the global incident in collector plane. A huge gain of 41.4% is added to the production.

5.2.5 Measured data from Lier

Simulation is done by using Lier data for 2016 and 2017 resulted in the annual production of 17.014 MWh and 16.983 MWh respectively. Specific yield is 637 kWh/kWp in 2016 on an annual basis, specific yield of 2017 annually is 636 kWh/kWp. Performance ratio is 79.7% and 79.9% for 2016 and 2017 respectively.

Applying days of unavailability to Lier meteo for 2016 give a production of 15.343 MWh annually and 15.810 MWh for 2017. PR value is 74.6% and 74.4%.

5.3 Brynseng

Brynseng data started logging April 2017, and measurement of real production of Brynseng obtained for the time period April 2017 - April 2018. The production on an annual basis was 91.233 MWh, where 61.097 MWh were generated in 2017 and 30.136 MWh in 2018. April 2018 contained 8 days of error in production logging. Brynseng was simulated by using irradiance data from PVsyyst, Blindern and Aas weather station.

5.3.1 Main results

Synthetic data gave a production of 90.653 MWh on an annual basis, which resulted in a specific yield of 539 kWh/kWp annually. Performance ratio value for Brynseng is 65.2%.

Month	GHI kWh/m^2	T_{amb} $°C$	GII kWh/m^2	G_{Eff} kWh/m^2	E_{array} MWh	E_{grid} MWh	AAE %	AAE_s %
January	7.4	-1.66	20.6	14.15	2.275	2.204	6.70	6.49
February	22.1	-2.08	46.8	36.49	6.047	5.900	7.84	7.64
March	64.7	0.79	91.4	72.09	11.748	11.500	7.79	6.85
April	106.9	6.31	99.9	72.64	11.559	11.285	7.02	6.85
May	152.9	11.82	105.7	72.67	11.364	11.079	6.52	6.36
June	164.1	15.17	97.5	65.82	10.107	9.828	6.29	6.11
July	151.7	17.80	97.1	66.32	10.073	9.800	6.30	6.12
August	106.7	16.83	83.3	58.53	8.884	8.641	6.47	6.29
September	74.8	12.17	90.1	68.95	10.647	10.409	7.17	7.01
October	32.3	6.52	55.9	45.70	7.131	6.955	7.74	7.55
November	10.0	2.66	22.1	15.22	2.451	2.376	6.74	6.53
December	4.5	-1.27	16.3	4.52	0.712	0.677	2.66	2.53
Year	898.3	7.14	826.8	593.08	92.999	90.653	6.82	6.65

Table 13: Balance and main result for Brynseng synthetic data

For this study annual global irradiance on the horizontal plane is 890.2 kWh/m^2 while the incident on the collector is 826.8 kWh/m^2 on an annual basis. DC energy produced on an annual basis is 92.999 MWh and AC energy injected into the grid is 90.653 MWh annually. The annual average efficiency of the PV array is simulated to be 6.82% and the system has an efficiency of 6.65%.

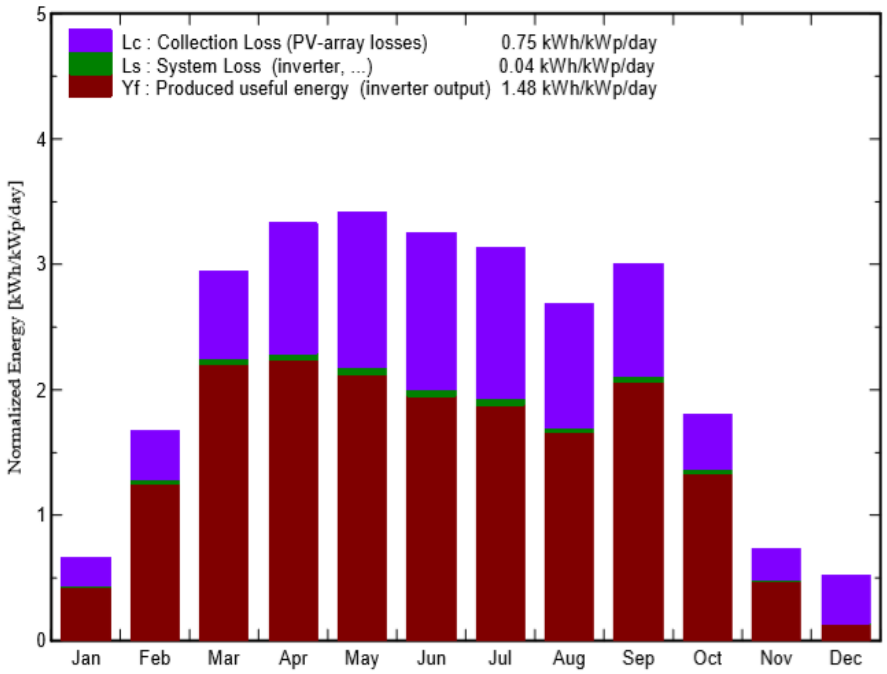

Figure 36: Production and losses for Brynseng.

Figure 36 illustrates normalized production, where collection losses has an enormous value of 0.75 kWh/kWp/day. The months March-September increase these losses, due to the design of the school the shading for the entire system is significant. Ls, system losses, resulted in 0.04 kWh/kWp/day, and useful energy production is 1.48 kWh/kWp/day.

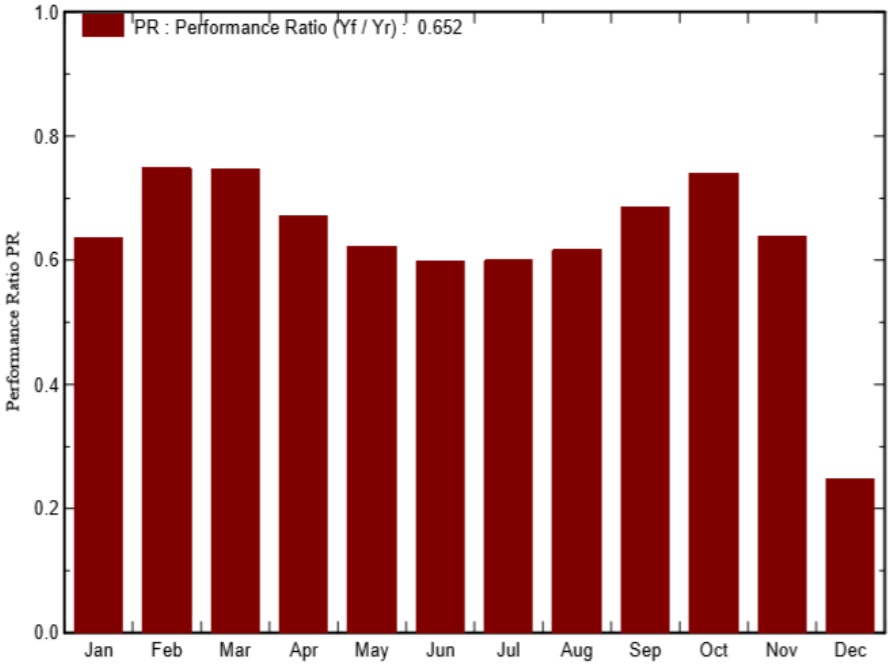

Figure 37: Performance ratio for Brynseng.

The performance ratio, shown in the right graph, has an average annual value of 65.2%. PR values for every month are below what could be expected of such a system, however due to shading losses the performance is low. In Section 5.3.3, a simulation is done without shading from the schools superstructure to illustrate the differences.

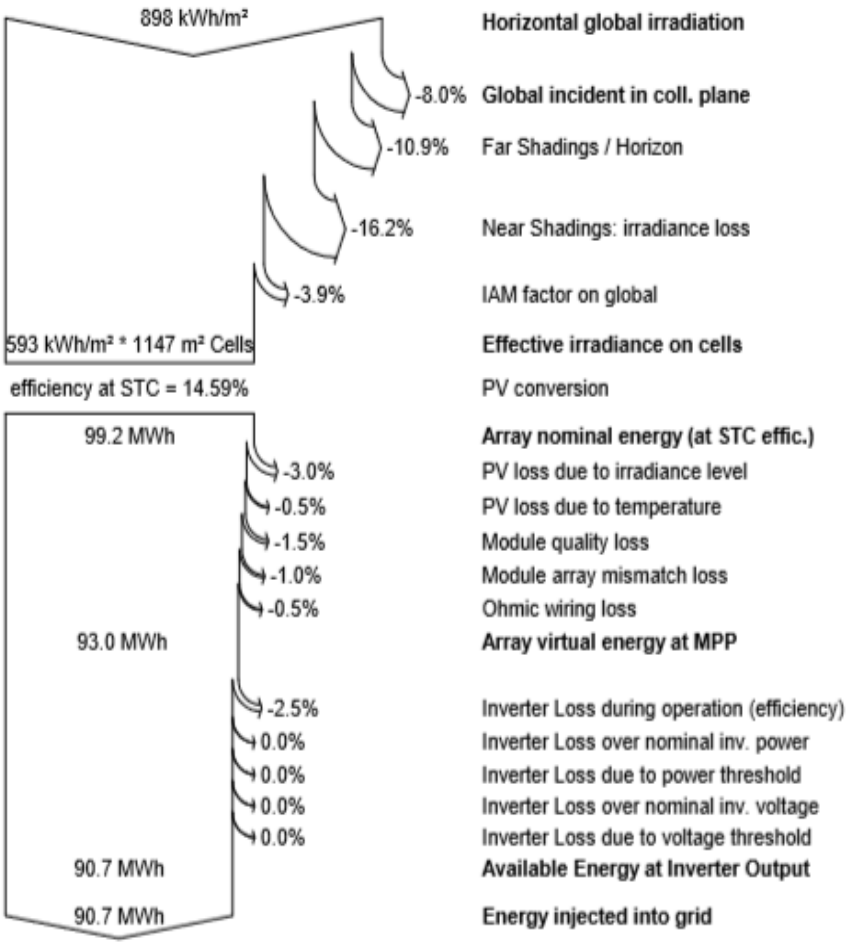

Figure 38: Arrow loss diagram for Brynseng.

Figure 38 gives an overview of losses for the Brynseng system.
Global irradiance on the plane is 898 kWh/m^2 while only 593 kWh/m^2 effective irradiance reaches the cells. Near and far shading are major losses in addition to global incident on collector plane and IAM. This means 99.2 MWh energy is produced and the system has an efficiency of 14.59% at STC. Annual array virtual energy at MPP is 93.0 MWh. The losses at this stage are 3.0% due to irradiance level, 0.5% due to temperature, 1.5% due to degradation, 1.0% due to array mismatch and 0.5% due to ohmic wiring losses. The available energy (annual basis) at inverter output is 90.7 MWh, and this is injected into the grid. At this stage the system experience loss during inverter operation which is 2.5%.

5.3.2 Measured data from Ås and Blindern

Using same parameters and conditions, weather data from Ås and Blindern were used to compare the performance of the system.

By using weather data obtained from Ås in 2016 and 2017 gave an energy production of 103.3 MWh and 102.9 MWh annually. With a specific yield of 614 kWh/kWp and 611 kWh/kWp on an annual basis. Performance ratios of 65.2% and 65.7% were simulated.

Weather data obtained from Blindern in 2016 and 2017 gave an energy production of 91.456 MWh and 83.18 MWh annually. With a specific yield of 543 kWh/kWp and 494 kWh/kWp on an annual basis. Performance ratio of 65.3% and 65.4% was found.

5.3.3 Shading impact

Because of the huge losses due to near shading, a simulation has been done by removing the superstructure for the central part of the building. Using synthetic data and keeping the rest of the system identical as in the previous situation. Without the superstructure Brynseng would increase the production by 15.347 MWh annually, according to the PVsyst simulation. Performance ratio would reach an average value of 76.1%, which is an increase of 10.9% compared to simulation with the superstructure included in the 3D-model. Collector losses are mitigated to 0.50 kWh/kWp/day and useful energy increased to 1.72 kWh/kWp/day.

5.4 Facade versus roof

As part of the hypothesis, Solsmaragden were used as an experiment in the performance of the same system for a facade and a roof system installation. The same modules and inverters were attached to the roof for different locations. Synthetic data obtained from Meteronorm 7.1 through PVsyst is used for facade and roof systems. Albedo has been set to 0.8 for December-February for Bodø and Drammen but is set to standard value for Rome and Cape Town. This is to simulate more realistic situations for each location.

Location	South facade			Roof		
	E	S_{pr}	PR	E_{pr}	S_{pr}	PR
Bodø	18.29	685	0.805	18.42	690	0.857
Drammen	17.01	637	0.797	20.29	780	0.854
Rome	21.49	805	0.777	30.92	1158	0.825
Cape Town	27.99	1048	0.776	42.97	1609	0.814

Table 14: South facade compared with roof for differnt locations.

Here E is energy produced [kWh/kWp/year], S_{pr} is the specific production [kWh/kWp/year] and PR is the performance value. Table 14 gives production and PR differences for roof and facade systems for different locations. The facade is facing south. For Bodø the difference in energy produced between roof and facade is minor. Bodø has a production loss of 0.65% for using the south facade in substitution to the roof.
The other installations reach losses of 16.17%, 30.5% and 34.86% for Drammen, Rome and Cape Town respectively. Production and performance ratio is superior for the roof installations. The

difference in PR value is slightly larger for facade installations compared to the roof, with 0.05 to 0.04.
The simulation was also executed for facade facing North, West and East, see Table 15.

Location	North fasade			West facade			East fasade		
	E	S_{pr}	PR	E	S_{pr}	PR	E	S_{pr}	PR
Bodø	6.88	257	0.751	19.81	742	0.760	16.58	621	0.829
Drammen	6.68	250	0.751	10.37	389	0.775	15.26	571	0.816
Rome	8.76	328	0.755	14.85	556	0.771	19.96	747	0.798
Cape Town	9.58	359	0.730	19.59	734	0.775	27.22	1019	0.804

Table 15: North, West and East facade.

The North facade experience loss in energy production compared to the roof by 62.76%, 67.08%, 71.67% and 77.70% for Bodø, Drammen, Rome and Cape Town respectively. For the West facade, the losses for the identical locations are 44.46%, 48.89%, 51.97% and 54.40%. The East facade experienced losses in comparison to the roof of 9.98%, 24.80%, 35.45% and 36.65%. The difference in PR value of the roof exceeds the difference in PR value of the facades by 0.18, 0.028 and 0.012 for the North, West and East facade respectively.

5.5 Partial shading model

The effect of various shading conditions on the PV string has been simulated as described in section 4.6. First situation with no shading effects for the string can be seen figure 39. The Figure gives 3500 W produced at P_{mpp}.

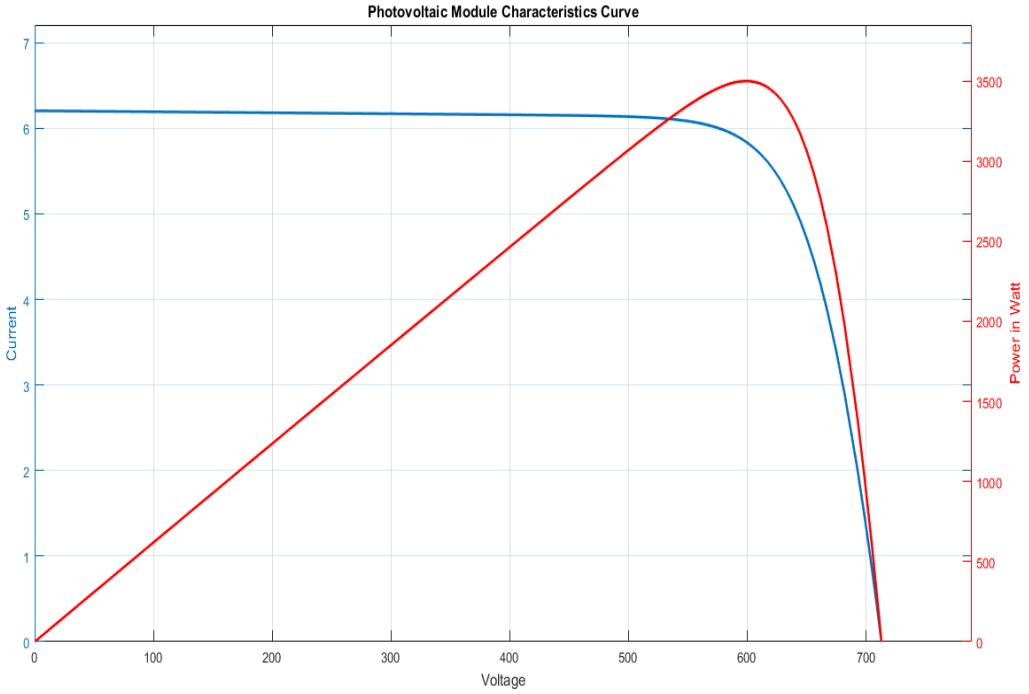

Figure 39: Standard irradiance.

By applying 25% shading on the string, results can be seen in Figure 40. 2481 W is produced at P_{mpp} corresponding to 425 V.

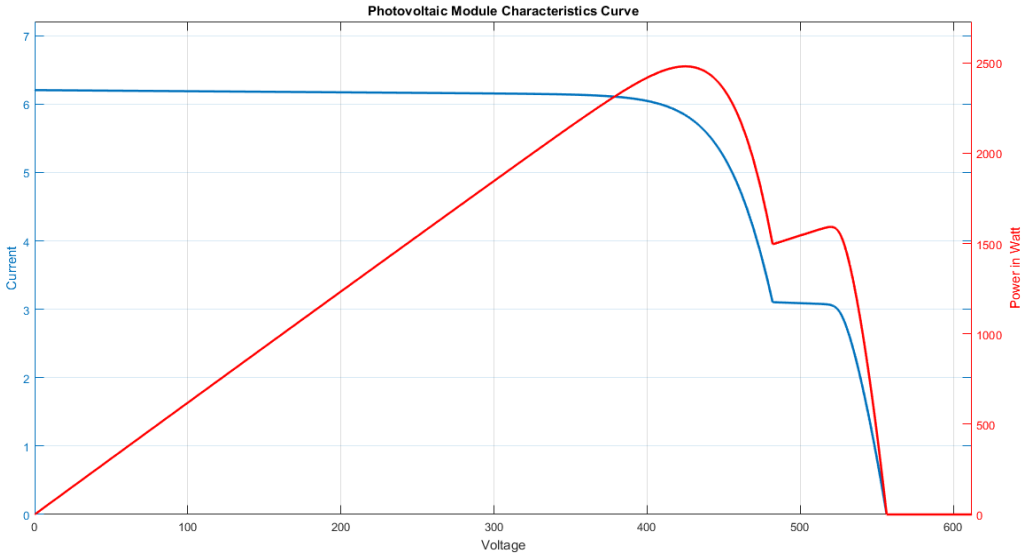

Figure 40: 25% shading of the string.

By applying 50% shading on the string, results can be seen in Figure 41. 1717 W is produced at

P_{mpp} corresponding to 295 V.

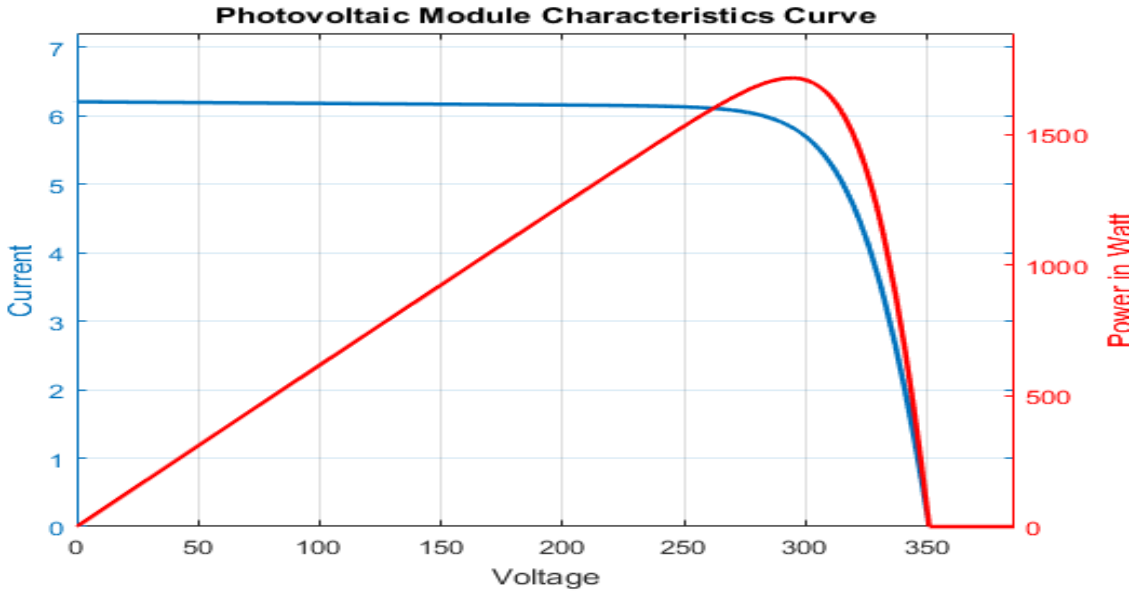

Figure 41: 50% shading on string.

Various irradiance has been applied to several modules and can be seen in Figure 42. 1717 W is produced at P_{mpp} corresponding to 295 V, same as the previous situation.

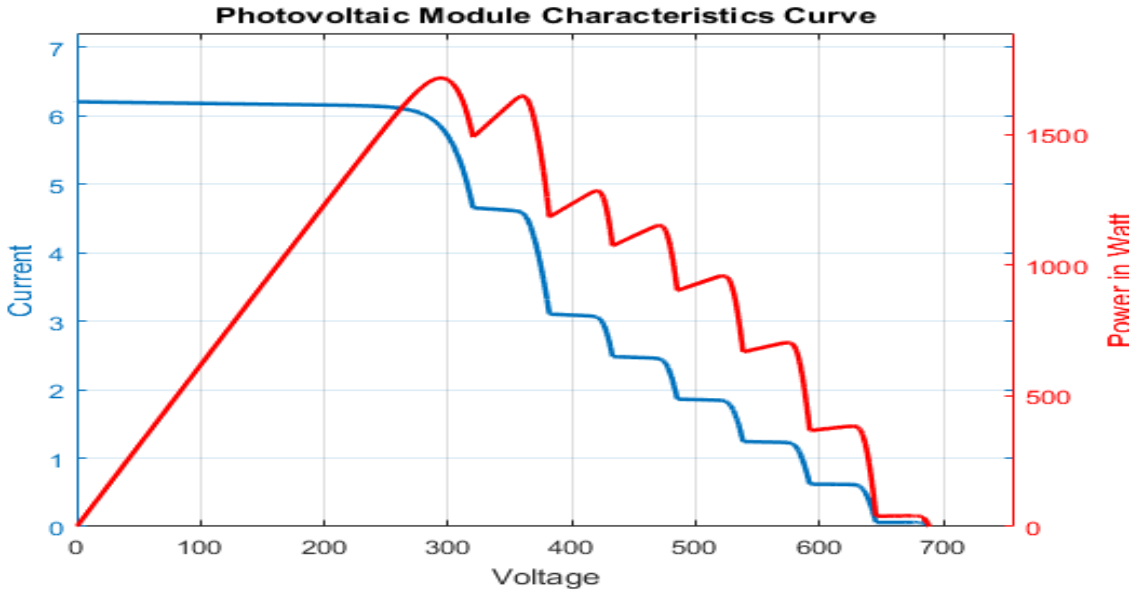

Figure 42: Various shading has been applied on the modules

Multiple steps in current correspond to multiple peaks of power, as is illustrated in Figures 40 and 42. The results can be related to conduction of bypass diodes under partially shaded conditions. At low voltages the shaded cells do not affect the system current due to the bypass

diodes. At higher voltages, the diodes become reverse-biased and the current is limited to that of a shaded module. The larger differences in peak power relate to increase or decrease in shading conditions for the module. Temperature also has a major impact on the I-V and P-V curves, by affecting the voltage. Increase in temperature reduces voltage which leads to a decrease in power. A reduction in temperature increases voltage and power.

6 Discussion and Conclusion

PVsyst proved to be a reliable software for simulating actual situations and cases for different PV installation. PVsyst gave results as expected and discovered losses, which had a major impact on the performance of the installations. While this thesis has used manual plotting of horizontal shading, PVGIS could be used to import horizon profile for the sites. This will have an impact on shading losses and overall production. However, the Skarpnes results proved that the impact is minimal. Perez model for global incident in collector plane is used in the simulation due to higher accuracy according to PVsyst [33], which proved to be right for the Skarpnes case. This study found measured weather data at Solsmaragden to be unreliable while implemented in PVsyst, which lead to an unrealistic gain in production for Solsmaragden. However, weather data from PVsyst and Lier gave results approximate actual production. For facade installations, shading is a major loss factor. Brynseng is an installation which proves this, and therefore the partial shading model was used to show the power loss.

For Skarpnes case, a simulation of the site has been done in PVsyst in another study [71]. Sorensen et al. scaled the simulation to fit the actual installed system and the simulation predicted an annual production of 6.82 MWh for the South-East facing system. With a predicted production of 7 MWh on an annual basis [58], this thesis simulated an annual production of 6.88 MWh and 6.85 MWh on an annual basis. The rotation of the 2 houses simulated yielded similar production results. Performance value was found to be 79.5% and 79.8% which is within range of what can be expected from new PV installations in moderate climate [58]. The uncertainty of measuring the error in regards to irradiation data resulted in a 20.5% drop in production. However Kjøita data filled in the missing values excellent, even though the distance between the site and the weather station is 58 km.

Using synthetic values obtained from Meteonorm 7.1 through PVsyst gave an annual production of 6.61 MWh which gives noticeable changes in energy production. Performance ratio increased to 81% and the overall efficiency of the system increased slightly by using synthetic values.

The case used albedo of 0.8 for January until March, for simulating snow. Using standard PVsyst albedo values of 0.2 for all months gave production of 6.86 MWh and 6.83 MWh, which gave a difference of 20 kWh in annual production. For this tilt of the PV panels, albedo influence of the system is minor.

Due to the tilt of the PV field, soiling is one of the major losses for the Skarpnes system. Temperature leads to the largest loss due to the mounting choice. Incidence Angle Modifier losses also play a part on the radiation level, this is due to the transmission and reflection of the sun's ray at each PV material surface. The system simulated in PVsyst gives reliable and comparable results of the actual installation.

Solsmaragden had a total production of 95.5 MWh in 2016, which is approximately 10% inferior to what was estimated. Results for inverter 7 and 8 obtained calculation from an unpublished article

by Christian Hals Frivold, gave the production of 4685.3 kWh and 11759.1 kWh respectively. This gives a total production for the south facade of 16444.4 kWh and 15480.125 kWh for 2016 and 2017 respectively. Real measured data obtained from Sunnyportal through pyranometer at the south facade yielded a production of 20.019 MWh. Synthetic data gave a production of 17.01 MWh annually. While including days of error in measuring into synthetic data set, the production for 2017 is 15.456 MWh which is approximately similar to actual production. Lier data set generated higher production for both years. The difference between actual produced energy and simulation including real measured data is enormous. The main reason for this is the major gain in global incident in collector plane which is a result of the data used. This parameter should be a loss applied to the overall loss diagram, due to the tilt of the PV field. This can be seen in simulation in Section 5.4, where the same system is simulated with other data set for different locations. PVsyst had trouble with the data set, and using SunnyPortal data for this case gave unrealistic results. Simulating with SunnyPortal data set gave a production of 21.75% and 29.33% higher than actual production for 2016 and 2017 respectively. Lier measured data, including system unavailability, gave a production of 6.69% inferior to actual production for 2016 and 2% more production for 2017. PVsyst synthetic values, including system unavailability, gave a production of 6% increase compared to actual production in 2016, and produced -0.16% less for 2017. PVsyst and Lier give an indication of what this system can produce, and with no errors in data measuring, the south facade may be able to produce 16-17 MWh annually.

Average PR value of the south facade was 0.79 for 2017, PR data was only available from October 2016. For synthetic data, the PR value was 0.78 and for real measured data the PR value was 0.75, which is an inferior to the actual system. Including days of system unavailability decreased the PR value further. The simulated PR values are also below what could be expected of a new BIPV system. Shading may be the main reason to PR values lower than expected, as shading has a major part in PR values for a system [72].

Due to many different PV modules used in both inverters, a replica of the actual system was challenging. PVsyst did not allow various modules attached to the same inverter. As a result the active PV area is larger than the actual system. Distribution of the modules was done within the PV field in the 3D model, however the actual system has modules surrounding windows and covers a major part of the south facade. The simulation did not resemble the module distribution design of the actual system. Using Perez's transposition model gave more accurate results than Hay's model.

The Brynseng installation was supposed to produce 100 MWh, the installation however did not perform as expected. Due to no weather data measured on the site, synthetic data and data retrieved from the weather stations Ås and Blindern gave similar production results of what was expected. Performance ratio of 65.2% illustrated a system under-performing, however the system has great potential. Near shading from the superstructure was the main issue for the system performance. By removing the superstructure an increase of 15 MWh annually could be expected according to the simulation as well as a major increase in performance ratio. The partial shading

model of the string implemented in inverter 8 gave an insight of the enormous losses due to shading.

1122 modules were used in the simulation, which is 466 modules more than what is actually used. This was in order to obtain real planned power of 166 kWp. In addition to being unable to scale the modules as desired, this will impact the system performance compared to actual system performance.

Use of different weather data gave various results regarding production and performance ratio for Brynseng. PVsyst and Blindern were the most accurate data set used.

For simulation and recreation of installed systems, PVsyst is a reliable software in order to evaluate performance, losses and find problems related to production. Irradiation data especially had a major impact on the systems and gave various results. This thesis found Skarpnes and Solsmaragden to be efficient and well-performing systems. Brynseng however is limited by the design of the building in regards to major shading losses throughout the year. As for facade installations in Norway and northern latitudes, facades make a great solution compared to southern locations due to low solar angle and cold climate. South facade- and roof installations had similar production as this thesis found. Performance value was higher for roof installations, compared to the facade, regardless of location.

6.1 Further work

For further work, an exact replica of the systems Brynseng and Solsmaragden should be simulated by placing the modules where they should be. Longer time series for measured weather data applied to the simulation for all systems for a better comparison of the installations. Since the partial shading model was done by using other modules than the modules installed at Brynseng, a study should be done for the same model, using the same modules.

References

[1] G. T. Klise and J. S. Stein, "Models used to assess the performance of photovoltaic systems," Sandia National Laboratories, Tech. Rep., 2009.

[2] T. I. Westgaard, "Pvps annual report 2016 norway photovoltaic technology status and prospect," International Energy Agency, techreport, 2016. [Online]. Available: http://iea-pvps.org/

[3] "Bipv for norway," http://bipvno.no/, (Accessed on 05/13/2018).

[4] S. R. Wenham, M. A. Green, and M. E. Watt, *Applied Photovoltaics*. Centre for Photovoltaic Devices and Systems, 2005. [Online]. Available: https://www.amazon.com

[5] C. Honsberg and S. Bowden, "Standard solar spectra," pveducation visited 26.11.2017. [Online]. Available: http://www.pveducation.org/pvcdrom/appendices/standard-solar-spectra

[6] "A powerful software for your photovoltaic systems," pVsyst visited 06.04.2018. [Online]. Available: http://www.pvsyst.com/en/

[7] "Iea annual trend report of 2016," 2016. [Online]. Available: http://www.iea-pvps.org/?id=256

[8] G. Stapleton, S. Neill, and G. Miline, "Photovoltaic systems," 2013. [Online]. Available: http://www.yourhome.gov.au/energy/photovoltaic-systems

[9] D. Sera, R. Teodorescu, and P. Rodriguez, "Pv panel model based on datasheet values," in *2007 IEEE International Symposium on Industrial Electronics*, June 2007, pp. 2392–2396.

[10] C. Honsberg and S. Bowden, "Solar cell efficiency," pveducation visited 26.02.2018. [Online]. Available: http://www.pveducation.org/pvcdrom/solar-cell-efficiency

[11] "Today in energy," u.S. Energy Information Administration visited 20.03.2018. [Online]. Available: https://www.eia.gov/todayinenergy/detail.php?id=30912

[12] S. Kurtz, E. Riley, J. Newmiller, T. Dierauf, A. Kimber, J. McKee, R. Flottemesch, and P. Krishnani, "Analysis of photovoltaic system energy performance evaluation method," National Renewable Energy Laboratory (NREL), techreport, 11 2013. [Online]. Available: https://www.nrel.gov/docs/fy14osti/60628.pdf

[13] A. G. Imenes, "Performance of bipv and bapv installations in norway," in *Photovoltaic Specialists Conference (PVSC), 2016 IEEE 43rd.* IEEE, 2016, pp. 3147–3152.

[14] B. Marion, J. Adelstein, K. Boyle, H. Hayden, B. Hammond, T. Fletcher, B. Canada, D. Narang, A. Kimber, L. Mitchell *et al.*, "Performance parameters for grid-connected pv systems," in *Photovoltaic Specialists Conference, 2005. Conference Record of the Thirty-first IEEE.* IEEE, 2005, pp. 1601–1606.

[15] C. Jardine and G. Conibeer, "Pv-compare: Direct comparison of eleven pv technologies at two locations in northern and southern europe," 11 2017.

[16] T. James, A. Goodrich, M. Woodhouse, R. Margolis, and S. Ong, "Building-integrated photovoltaics (bipv) in the residential sector: An analysis of installed rooftop system prices," Nationa Renewable Energy Laboratory, Tech. Rep., 11 2011. [Online]. Available: https://www.nrel.gov/docs/fy12osti/53103.pdf

[17] L. Maturi, G. Belluardo, D. Moser, and M. D. Buono, "Bipv system performance and efficiency drops: Overview on pv module temperature conditions of different module types," *Energy Procedia*, vol. 48, no. Supplement C, pp. 1311 – 1319, 2014, proceedings of the 2nd International Conference on Solar Heating and Cooling for Buildings and Industry (SHC 2013). [Online]. Available: http://www.sciencedirect.com/science/article/pii/S187661021400410X

[18] U. Jahn and B. Grimmig, "Operational performance of pv systems and subsystems," IEA Photovoltaic Systems Programme, Tech. Rep., 2000, report IEA-PVPS T2-01:2000.

[19] L. Ayompe, A. Duffy, S. McCormack, and M. Conlon, "Measured performance of a 1.72kw rooftop grid connected photovoltaic system in ireland," *Energy Conversion and Management*, vol. 52, no. 2, pp. 816 – 825, 2011. [Online]. Available: http://www.sciencedirect.com/science/article/pii/S0196890410003730

[20] U. Jahn and W. Nasse, *Operational Performance ofGrid-connected PV Systemson Buildings in Germany*. John Wiley & Sons, Ltd, 2004.

[21] J. Leloux, L. Narvarte, and D. Trebosc, "Review of the performance of residential pv systems in france," *Renewable and Sustainable Energy Reviews*, vol. 16, no. 2, pp. 1369 – 1376, 2012. [Online]. Available: http://www.sciencedirect.com/science/article/pii/S136403211100517X

[22] B. Marion, J. Adelstein, K. Boyle, H. Hayden, B. Hammond, T. Fletcher, B. Canada, D. Narang, A. Kimber, L. Mitchell, G. Rich, and T. Townsend, "Performance parameters for grid-connected pv systems," in *Conference Record of the Thirty-first IEEE Photovoltaic Specialists Conference, 2005.*, Jan 2005, pp. 1601–1606.

[23] *PVsyst user manual*, Univerity of Agder.

[24] P. Karki, B. Adhikary, and K. Sherpa, "Comparative study of grid-tied photovoltaic (pv) system in kathmandu and berlin using pvsyst," in *2012 IEEE Third International Conference on Sustainable Energy Technologies (ICSET)*, Sept 2012, pp. 196–199.

[25] J. Freeman, J. Whitmore, N. Blair, and A. P. Dobos, "Validation of multiple tools for flat plate photovoltaic modeling against measured data," in *2014 IEEE 40th Photovoltaic Specialist Conference (PVSC)*, June 2014, pp. 1932–1937.

[26] K. J. Sauer, T. Roessler, and C. W. Hansen, "Modeling the irradiance and temperature dependence of photovoltaic modules in pvsyst," *IEEE Journal of Photovoltaics*, vol. 5, no. 1, pp. 152–158, Jan 2015.

[27] "photovoltaic planning software pv*sol — valentin software," https://www.valentin-software.com/en/products/photovoltaics/55/pvsol, (Accessed on 05/02/2018).

[28] T. Patarau, D. Petreus, and R. Etz, "Analysis and optimization of a geothermal, biomass, solar hybrid system: An application of pv*sol software," in *2015 38th International Spring Seminar on Electronics Technology (ISSE)*, May 2015, pp. 370–375.

[29] B. Wittmer, A. Mermoud, and T. Schott, "European photovoltaic solar energy conference," in *ANALYSIS OF PV GRID INSTALLATIONS PERFORMANCE, COMPARING MEASURED DATA TO SIMULATION RESULTS TO IDENTIFY PROBLEMS IN OPERATION AND MONITORING*, 2015.

[30] Y. Irwan, A. Amelia, M. Irwanto, Fareq.M, W. Leow, N. Gomesh, and I. Safwati, "Stand-alone photovoltaic (sapv) system assessment using pvsyst software," *Energy Procedia*, vol. 79, pp. 596 – 603, 2015, 2015 International Conference on Alternative Energy in Developing Countries and Emerging Economies. [Online]. Available: http://www.sciencedirect.com/science/article/pii/S1876610215022717

[31] A. M. B. Wittmer, "29th european photovoltaic solar energy conference," in *A TOOL TO OPTIMIZE THE LAYOUT OF GROUND-BASED PV INSTALLATIONS TAKING INTO ACCOUNT THE ECONOMIC BOUNDARY CONDITIONS*, 2014.

[32] A. Mermoud and T. Lejeune, "Performance assessment of a simulation model for pv modules of any available technology," 2010, iD: unige:38547. [Online]. Available: https://archive-ouverte.unige.ch/unige:38547

[33] "Physical models used for incident irradiation models transposition model," *http* : $//files.pvsyst.com/help/meteo_transposition.htm$, (Accessed on 05/15/2018).

[34] "Pv performance modeling collaborative — perez sky diffuse model," https://pvpmc.sandia.gov/modeling-steps/1-weather-design-inputs/plane-of-array-poa-irradiance/calculating-poa-irradiance/poa-sky-diffuse/perez-sky-diffuse-model/, (Accessed on 05/15/2018).

[35] "Pv*sol expert 6.0 - manual," https://www.valentin-software.com/sites/default/files/downloads/handbuecher pvsol-en.pdf, (Accessed on 05/02/2018).

[36] S. M. MacAlpine, R. W. Erickson, and M. J. Brandemuehl, "Characterization of power optimizer potential to increase energy capture in photovoltaic systems operating under nonuniform conditions," *IEEE Transactions on Power Electronics*, vol. 28, no. 6, pp. 2936–2945, June 2013.

[37] S. MacAlpine, M. Brandemuehl, and R. Erickson, "Beyond the module model and into the array: Mismatch in series strings," in *2012 38th IEEE Photovoltaic Specialists Conference*, June 2012, pp. 003 392–003 396.

[38] "System advisor model (sam) —," https://sam.nrel.gov/, (Accessed on 05/02/2018).

[39] J. Freeman, J. Whitmore, L. Kaffine, N. Blair, and A. P. Dobos, "System advisor model: Flat plate photovoltaic performance modeling validation report," NREL, Tech. Rep., 12 2013.

[40] N. Blair, A. P. Dobos, J. Freeman, T. Neises, and M. Wagner, "System advisor model, sam 2014.1.14: General description," National Renewable Energy Laboratory, Tech. Rep., 2014.

[41] J. S. Stein, C. P. Cameron, B. Bourne, A. Kimber, J. Posbic, and T. Jester, "A standardized approach to pv system performance model validation," in *2010 35th IEEE Photovoltaic Specialists Conference*, June 2010, pp. 001 079–001 084.

[42] P. Gilman, N. Blair, M. Mehos, C. Christensen, S. Janzou, and C. Cameron, "Solar advisor model user guide for version 2.0," National Renewable Energy Laboratory, Tech. Rep., 08 2008.

[43] "Physical models used for pv module standard one-diode-model," *http* : $//files.pvsyst.com/help/pvmodule_model.htm$, (Accessed on 05/19/2018).

[44] P. R. R. M. M. Nallapaneni Manoj Kumar, M. Rohit Kumar, "Performance analysis of 100 kwp grid connected si-poly photovoltaic system using pvsyst simulation tool," *Energy Procedia*, vol. Volume 117, pp. 180–189, 2017. [Online]. Available: http://www.sciencedirect.com/science/article/pii/S1876610217323287

[45] M. Malvoni, M. G. D. Giorgi, and P. M. Congedo, "Study of degradation of a grid connected photovoltaic system," *Energy Procedia*, vol. 126, pp. 644 – 650, 2017, aTI 2017 - 72nd Conference of the Italian Thermal Machines Engineering Association. [Online]. Available: http://www.sciencedirect.com/science/article/pii/S1876610217337694

[46] D. C. Jordan and S. R. Kurtz, "Photovoltaic degradation rates – an analytical review: Preprint," *NREL/JA-5200-51664*, 2012, (Accessed on 05/07/2018).

[47] S. E. Gindi, A. R. Abdin, and A. Hassan, "Building integrated photovoltaic retrofitting in office buildings," *Energy Procedia*, vol. 115, pp. 239 – 252, 2017, international Conference – Alternative and Renewable Energy Quest, AREQ 2017, 1-3 February 2017, Spain. [Online]. Available: http://www.sciencedirect.com/science/article/pii/S187661021732221X

[48] A. Babatunde, S. Abbasoglu, and M. Senol, "Analysis of the impact of dust, tilt angle and orientation on performance of pv plants," *Renewable and Sustainable Energy Reviews*, vol. 90, pp. 1017 – 1026, 2018. [Online]. Available: http://www.sciencedirect.com/science/article/pii/S1364032118302028

[49] C. P. Cameron, W. E. Boyson, and D. M. Riley, "Comparison of pv system performance-model predictions with measured pv system performance," in *2008 33rd IEEE Photovoltaic Specialists Conference*, May 2008, pp. 1–6.

[50] D. I. Choudhury, "Bipv roof tiles: Effect of locations on energy cost savings," in *121st ASEE Conference and Exposition, Indianapolis USA*, 2014.

[51] T. D. Atmaja, "Façade and rooftop pv installation strategy for building integrated photo voltaic application," *Energy Procedia*, vol. 32, pp. 105 – 114, 2013, international Conference on Sustainable Energy Engineering and Application (ICSEEA) 2012. [Online]. Available: http://www.sciencedirect.com/science/article/pii/S1876610213000167

[52] "Bygningsintegrerte solcelle- og solvarmeanlegg," https://www.irenewables.no/bipv, (Accessed on 05/13/2018).

[53] B. Thorud, "Det store bildet – en solenergirevolusjon," https://n-e-f.no, 10 2017, (Accessed on 05/13/2018). [Online]. Available: https://n-e-f.no

[54] P. Redweik, C. Catita, and M. Brito, "Solar energy potential on roofs and facades in an urban landscape," *Solar Energy*, vol. 97, pp. 332 – 341, 2013. [Online]. Available: http://www.sciencedirect.com/science/article/pii/S0038092X13003460

[55] J. F. Lin Tong Shen, "Study on the performance of vertical solar pv systems in tropical region," *School of Electrical and Electronic Engineering, Singapore Polytechnic 500 Dover Road, Singapore 139651*, vol. Volume 3, 1015. [Online]. Available: www.seipub.org/aee

[56] M. G. P. FRANKL, A. MASINI and D. TOCCACELI, "Simplified life-cycle analysis of pv systems in buildings: Present situation and future trends," *Printed at INSEAD, Fontainebleau, France.*, 1997.

[57] T. Nordmann and L. Clavadetscher, "Understanding temperature effects on pv system performance," in *3rd World Conference onPhotovoltaic Energy Conversion, 2003. Proceedings of*, vol. 3, May 2003, pp. 2243–2246 Vol.3.

[58] A. G. Imenes, "Performance of zero energy homes in smart village skarpnes," 2016.

[59] "Sensors - 3045 drammen - solsmaragden - sunny portal," https://www.sunnyportal.com/FixedPages/Sensors.aspx, (Accessed on 04/06/2018).

[60] "Hent klimadata agrometbase," http://lmt.bioforsk.no/agrometbase/getweatherdata.php, (Accessed on 05/15/2018).

[61] "230wp sunpower solar panel," $https://us.sunpower.com/sites/sunpower/files/media-library/data-sheets/ds-e18-series-230-solar-panel-datasheet.pdf$, (Accessed on 05/29/2018).

[62] "Yr – været som var skarpnes, arendal (aust-agder)," https://www.yr.no/sted/Norge/Aust-Agder/Arendal/Skarpnes/statistikk.html, (Accessed on 03/15/2018).

[63] "Pv potential estimation utility," http://re.jrc.ec.europa.eu/pvgis/apps4/pvest.php?lang=en&map=europe, (Accessed on 03/15/2018).

[64] "Operating manual - sunny tripower 5000tl/6000tl/7000tl/8000tl/9000tl/10000tl/12000tl," http://files.sma.de/dl/17781/STP5-12TL-20-BE-en-15.pdf, (Accessed on 04/04/2018).

[65] "Sunny tripower 15000tl," http://files.sma.de/dl/8552/STP15000TL-DEN1602-V10web.pdf, (Accessed on 04/04/2018).

[66] "Sintef - forskning, teknologi og innovasjon," https://www.sintef.no/, (Accessed on 04/20/2018).

[67] "Operating manual - sunny tripower 15000tl / 20000tl / 25000tl," http://files.sma.de/dl/24336/STP15-25TL-30-BE-en-13.pdf, (Accessed on 04/04/2018).

[68] "Mathworks - makers of matlab and simulink - matlab & simulink," https://se.mathworks.com/, (Accessed on 05/01/2018).

[69] "Sunpower spr-x20-250-blk (250w) solar panel," http://www.solardesigntool.com/components/module-panel-solar/Sunpower/2798/SPR-X20-250-BLK/specification-data-sheet.html, (Accessed on 05/01/2018).

[70] *Photovoltaic system performance monitoring — Guidelines for measurement, data exchange and analysis*, En 61724 ed., The European Standard, 12 1998.

[71] Åse Lekang Sørensen, A. G. Imenes, S. Grynning, and T. H. Dokka, "Energy measurements at skarpnes zero energy homes in southern norway: Do the loads match up with the on-site energy production?" *Energy Procedia*, vol. 132, pp. 567 – 573, 2017, 11th Nordic Symposium on Building Physics, NSB2017, 11-14 June 2017, Trondheim, Norway. [Online]. Available: http://www.sciencedirect.com/science/article/pii/S1876610217348944

[72] B. Decker and U. Jahn, "Performance of 170 grid connected pv plants in northern germany—analysis of yields and optimization potentials," *Solar Energy*, vol. 59, no. 4, pp. 127 – 133, 1997, selected Proceeding of ISES 1995: Solar World Congress. Part IV. [Online]. Available: http://www.sciencedirect.com/science/article/pii/S0038092X96001326

7 Appenix

PVSYST V6.39		07/05/18	Page 1/5

Grid-Connected System: Simulation parameters

Project : **Grid-Connected Project at Skarpnes**

Geographical Site		**Skarpnes**		Country	**Norway**
Situation		Latitude	58.4°N	Longitude	8.7°E
Time defined as		Legal Time	Time zone UT+1	Altitude	46 m

Monthly albedo values

	Jan.	Feb.	Mar.	Apr.	May	June	July	Aug.	Sep.	Oct.	Nov.	Dec.
Albedo	0.80	0.80	0.80	0.20	0.20	0.20	0.20	0.20	0.20	0.20	0.20	0.20

Meteo data: **Skarpnes Real** Synthetic - Skarpnes weather data

Simulation variant : **Skarpnes_Meteo(Synthetic)**

Simulation date 07/05/18 10h28

Simulation parameters

Collector Plane Orientation	Tilt	32°	Azimuth	48°	
Models used	Transposition	Perez	Diffuse	Erbs, Meteonorm	
Horizon	Average Height	2.2°			
Near Shadings	Linear shadings				

PV Array Characteristics

PV module	Si-mono	Model	**SPR-230NE-BLK-D**		
Custom parameters definition		Manufacturer	SunPower		
Number of PV modules		In series	16 modules	In parallel	2 strings
Total number of PV modules		Nb. modules	32	Unit Nom. Power	230 Wp
Array global power		Nominal (STC)	**7.36 kWp**	At operating cond.	6.67 kWp (50°C)
Array operating characteristics (50°C)		U mpp	576 V	I mpp	12 A
Total area		Module area	**39.8 m²**	Cell area	35.7 m²

Inverter		Model	**Sunny Tripower 7000TL-20**		
		Manufacturer	SMA		
Characteristics		Operating Voltage	290-800 V	Unit Nom. Power	7.00 kWac
Inverter pack		Nb. of inverters	1 * MPPT 0.60	Total Power	7.0 kWac

PV Array loss factors

Array Soiling Losses

Jan.	Feb.	Mar.	Apr.	May	June	July	Aug.	Sep.	Oct.	Nov.	Dec.
20.0%	20.0%	3.0%	3.0%	3.0%	3.0%	3.0%	3.0%	3.0%	3.0%	20.0%	20.0%

Thermal Loss factor		Uc (const)	15.0 W/m²K	Uv (wind)	0.0 W/m²K / m/s
Wiring Ohmic Loss		Global array res.	851 mOhm	Loss Fraction	1.5 % at STC
Module Quality Loss				Loss Fraction	1.0 %
Module Mismatch Losses				Loss Fraction	2.0 % at MPP
Incidence effect, ASHRAE parametrization		IAM =	1 - bo (1/cos i - 1)	bo Param.	0.05

User's needs : Unlimited load (grid)

PVsyst Education License, University of Agder (Norway)

PVSYST V6.39		07/05/18	Page 2/5

Grid-Connected System: Horizon definition

Project : **Grid-Connected Project at Skarpnes**

Simulation variant : **Skarpnes_Meteo(Synthetic)**

Main system parameters	System type	**Grid-Connected**		
Horizon	Average Height	2.2°		
Near Shadings	Linear shadings			
PV Field Orientation	tilt	32°	azimuth	48°
PV modules	Model	SPR-230NE-BLK-D	Pnom	230 Wp
PV Array	Nb. of modules	32	Pnom total	**7.36 kWp**
Inverter	Model	Sunny Tripower 7000TL-20	Pnom	7.00 kW ac
User's needs	Unlimited load (grid)			

Horizon

Average Height	2.2°	Diffuse Factor	0.98
Albedo Factor	100 %	Albedo Fraction	0.84

Height [°]	2.0	2.0	2.0	2.0	2.0	2.0	2.0	2.0	2.0	0.0	0.0
Azimuth [°]	-150	-130	-120	-110	-80	-71	-60	-55	-30	-25	-8
Height [°]	1.0	3.0	3.0	4.0	4.0	2.0	2.0	1.0	1.0	2.0	2.0
Azimuth [°]	0	8	10	12	79	82	95	100	130	135	150

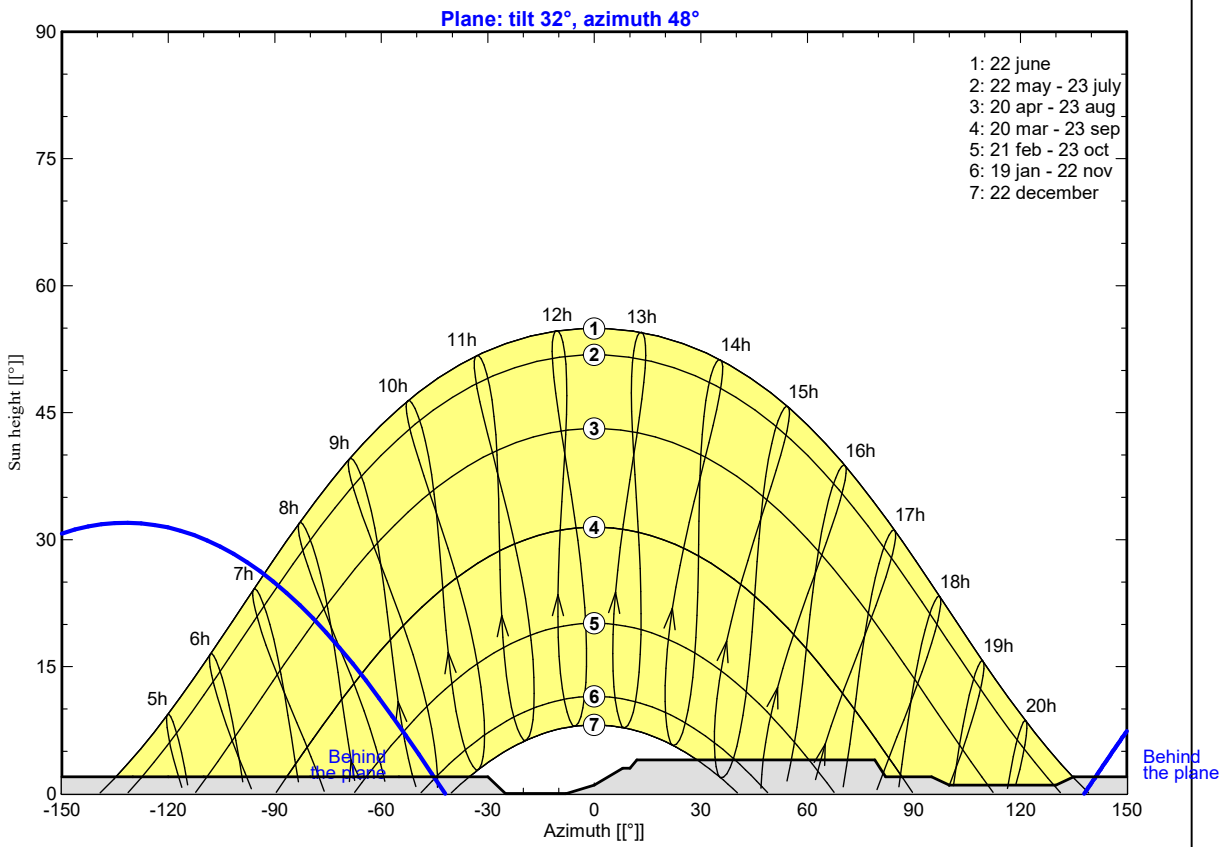

PVSYST V6.39		07/05/18	Page 3/5

Grid-Connected System: Near shading definition

Project : **Grid-Connected Project at Skarpnes**

Simulation variant : **Skarpnes_Meteo(Synthetic)**

Main system parameters	System type	**Grid-Connected**		
Horizon	Average Height	2.2°		
Near Shadings	Linear shadings			
PV Field Orientation	tilt	32°	azimuth	48°
PV modules	Model	SPR-230NE-BLK-D	Pnom	230 Wp
PV Array	Nb. of modules	32	Pnom total	**7.36 kWp**
Inverter	Model	Sunny Tripower 7000TL-20	Pnom	7.00 kW ac
User's needs	Unlimited load (grid)			

Perspective of the PV-field and surrounding shading scene

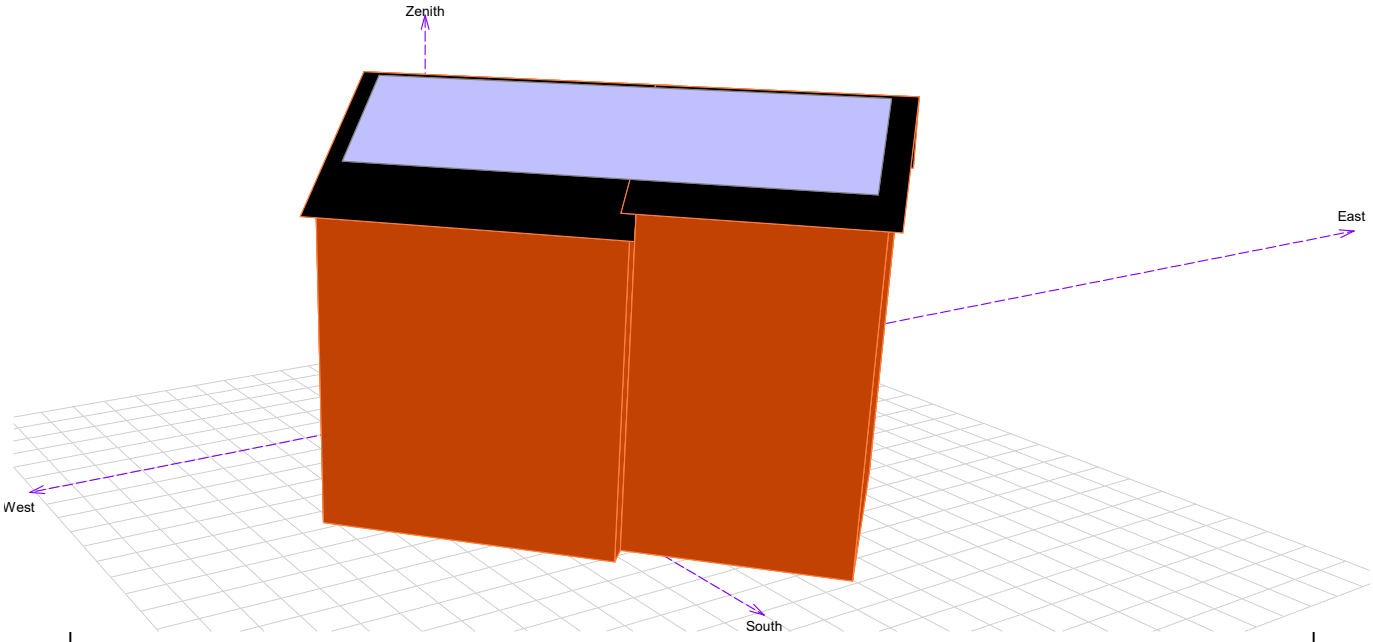

Iso-shadings diagram

Grid-Connected Project at Skarpnes

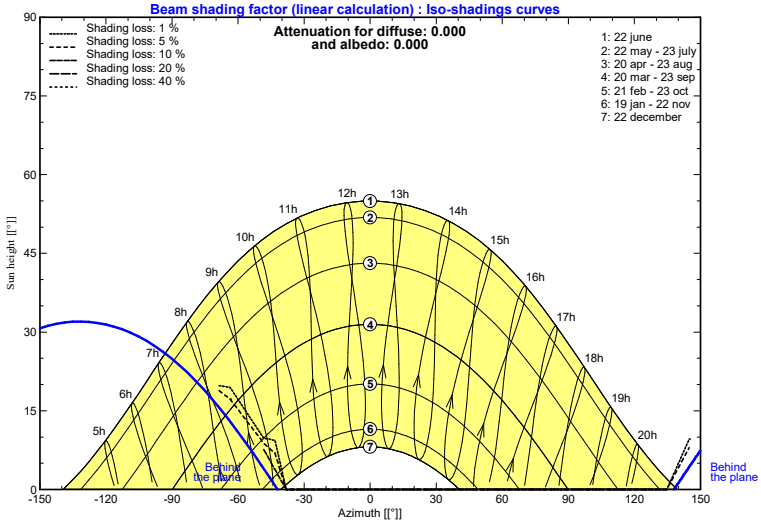

PVSYST V6.39		07/05/18	Page 4/5

Grid-Connected System: Main results

Project : **Grid-Connected Project at Skarpnes**

Simulation variant : **Skarpnes_Meteo(Synthetic)**

Main system parameters	System type	**Grid-Connected**		
Horizon	Average Height	2.2°		
Near Shadings	Linear shadings			
PV Field Orientation	tilt	32°	azimuth	48°
PV modules	Model	SPR-230NE-BLK-D	Pnom	230 Wp
PV Array	Nb. of modules	32	Pnom total	**7.36 kWp**
Inverter	Model	Sunny Tripower 7000TL-20	Pnom	7.00 kW ac
User's needs	Unlimited load (grid)			

Main simulation results

System Production	**Produced Energy**	**6.88 MWh/year**	Specific prod.	935 kWh/kWp/year
	Performance Ratio PR	79.5 %		

Normalized productions (per installed kWp): Nominal power 7.36 kWp

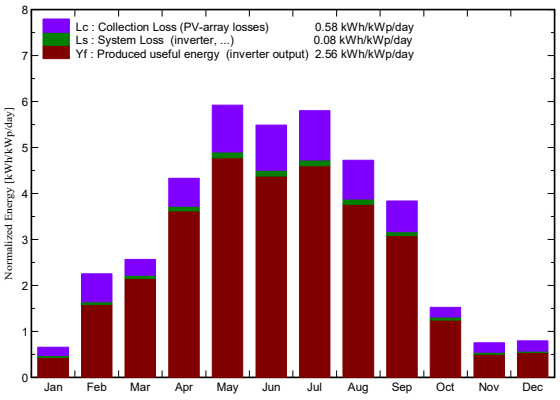

Performance Ratio PR

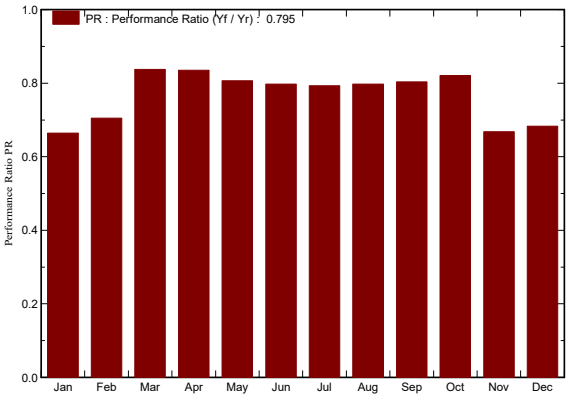

Skarpnes_Meteo(Synthetic)

Balances and main results

	GlobHor kWh/m²	T Amb °C	GlobInc kWh/m²	GlobEff kWh/m²	EArray MWh	E_Grid MWh	EffArrR %	EffSysR %
January	12.8	-2.60	20.3	15.0	0.108	0.099	13.38	12.28
February	38.8	2.00	63.0	47.5	0.338	0.327	13.48	13.03
March	62.9	4.00	79.6	73.0	0.508	0.491	16.02	15.48
April	116.1	5.80	130.0	120.9	0.823	0.799	15.90	15.44
May	173.5	11.80	183.6	171.0	1.120	1.090	15.32	14.92
June	166.2	15.70	164.7	152.7	0.996	0.967	15.18	14.75
July	173.0	16.20	179.9	167.3	1.079	1.050	15.07	14.66
August	134.0	15.70	146.4	136.2	0.885	0.860	15.18	14.75
September	95.3	15.10	115.2	106.8	0.700	0.681	15.27	14.85
October	35.1	6.70	47.2	43.3	0.299	0.285	15.94	15.18
November	16.8	3.20	22.6	17.0	0.120	0.111	13.35	12.35
December	13.0	4.70	24.6	18.3	0.130	0.124	13.25	12.63
Year	1037.5	8.22	1177.1	1069.1	7.106	6.885	15.16	14.69

Legends:

GlobHor	Horizontal global irradiation	EArray	Effective energy at the output of the array
T Amb	Ambient Temperature	E_Grid	Energy injected into grid
GlobInc	Global incident in coll. plane	EffArrR	Effic. Eout array / rough area
GlobEff	Effective Global, corr. for IAM and shadings	EffSysR	Effic. Eout system / rough area

PVSYST V6.39		07/05/18	Page 5/5

Grid-Connected System: Loss diagram

Project : **Grid-Connected Project at Skarpnes**

Simulation variant : **Skarpnes_Meteo(Synthetic)**

Main system parameters	System type	**Grid-Connected**		
Horizon	Average Height	2.2°		
Near Shadings	Linear shadings			
PV Field Orientation	tilt	32°	azimuth	48°
PV modules	Model	SPR-230NE-BLK-D	Pnom	230 Wp
PV Array	Nb. of modules	32	Pnom total	**7.36 kWp**
Inverter	Model	Sunny Tripower 7000TL-20	Pnom	7.00 kW ac
User's needs	Unlimited load (grid)			

Loss diagram over the whole year

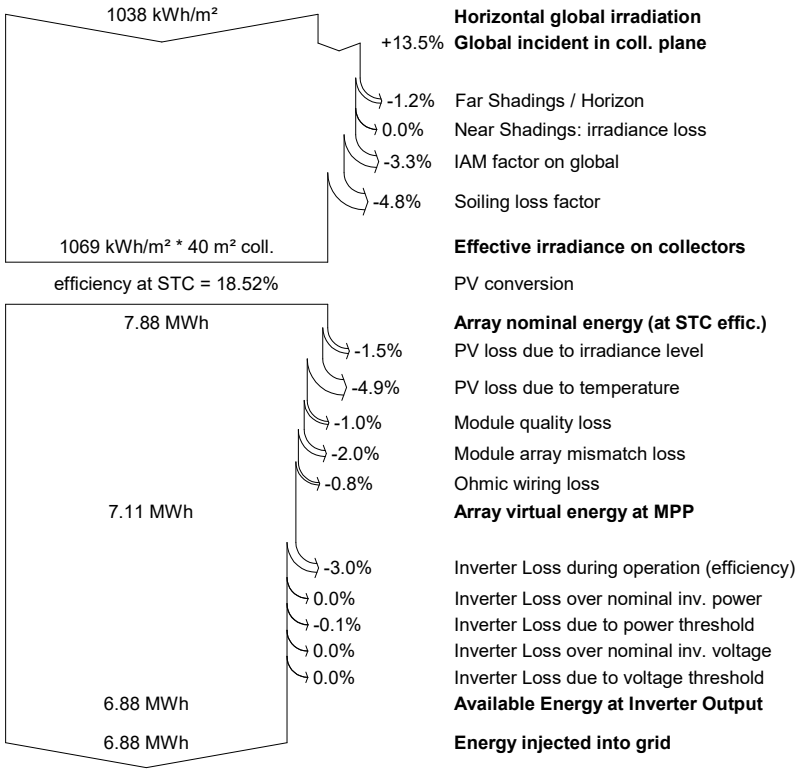

Appendix A

PVSYST V6.39		07/05/18	Page 1/5

Grid-Connected System: Simulation parameters

Project : **Grid-Connected Project at Skarpnes**

Geographical Site **Skarpnes** Country **Norway**

Situation Latitude 58.4°N Longitude 8.7°E
Time defined as Legal Time Time zone UT+1 Altitude 46 m
Monthly albedo values

	Jan.	Feb.	Mar.	Apr.	May	June	July	Aug.	Sep.	Oct.	Nov.	Dec.
Albedo	0.80	0.80	0.80	0.20	0.20	0.20	0.20	0.20	0.20	0.20	0.20	0.20

Meteo data: **Skarpnes Real** Synthetic - Skarpnes weather data

Simulation variant : **Skarpnes_Meteo(Synthetic)**

Simulation date 07/05/18 10h33

Simulation parameters

Collector Plane Orientation Tilt 32° Azimuth -51°

Models used Transposition Perez Diffuse Erbs, Meteonorm

Horizon Average Height 2.2°

Near Shadings Linear shadings

PV Array Characteristics

PV module Si-mono Model **SPR-230NE-BLK-D**
Custom parameters definition Manufacturer SunPower

Number of PV modules	In series	16 modules	In parallel	2 strings
Total number of PV modules	Nb. modules	32	Unit Nom. Power	230 Wp
Array global power	Nominal (STC)	**7.36 kWp**	At operating cond.	6.67 kWp (50°C)
Array operating characteristics (50°C)	U mpp	576 V	I mpp	12 A
Total area	Module area	**39.8 m²**	Cell area	35.7 m²

Inverter Model **Sunny Tripower 7000TL-20**
Manufacturer SMA

Characteristics	Operating Voltage	290-800 V	Unit Nom. Power	7.00 kWac
Inverter pack	Nb. of inverters	1 * MPPT 0.60	Total Power	7.0 kWac

PV Array loss factors

Array Soiling Losses

Jan.	Feb.	Mar.	Apr.	May	June	July	Aug.	Sep.	Oct.	Nov.	Dec.
20.0%	20.0%	3.0%	3.0%	3.0%	3.0%	3.0%	3.0%	3.0%	3.0%	20.0%	20.0%

Thermal Loss factor	Uc (const)	15.0 W/m²K	Uv (wind)	0.0 W/m²K / m/s
Wiring Ohmic Loss	Global array res.	851 mOhm	Loss Fraction	1.5 % at STC
Module Quality Loss			Loss Fraction	1.0 %
Module Mismatch Losses			Loss Fraction	2.0 % at MPP
Incidence effect, ASHRAE parametrization	IAM =	1 - bo (1/cos i - 1)	bo Param.	0.05

User's needs : Unlimited load (grid)

PVSYST V6.39		07/05/18	Page 2/5

Grid-Connected System: Horizon definition

Project : **Grid-Connected Project at Skarpnes**

Simulation variant : **Skarpnes_Meteo(Synthetic)**

Main system parameters	System type	**Grid-Connected**		
Horizon	Average Height	2.2°		
Near Shadings	Linear shadings			
PV Field Orientation	tilt	32°	azimuth	-51°
PV modules	Model	SPR-230NE-BLK-D	Pnom	230 Wp
PV Array	Nb. of modules	32	Pnom total	**7.36 kWp**
Inverter	Model	Sunny Tripower 7000TL-20	Pnom	7.00 kW ac
User's needs	Unlimited load (grid)			

Horizon

Average Height	2.2°	Diffuse Factor	0.98
Albedo Factor	100 %	Albedo Fraction	0.91

Height [°]	2.0	2.0	2.0	2.0	2.0	2.0	2.0	2.0	2.0	0.0	0.0
Azimuth [°]	-150	-130	-120	-110	-80	-71	-60	-55	-30	-25	-8
Height [°]	1.0	3.0	3.0	4.0	4.0	2.0	2.0	1.0	1.0	2.0	2.0
Azimuth [°]	0	8	10	12	79	82	95	100	130	135	150

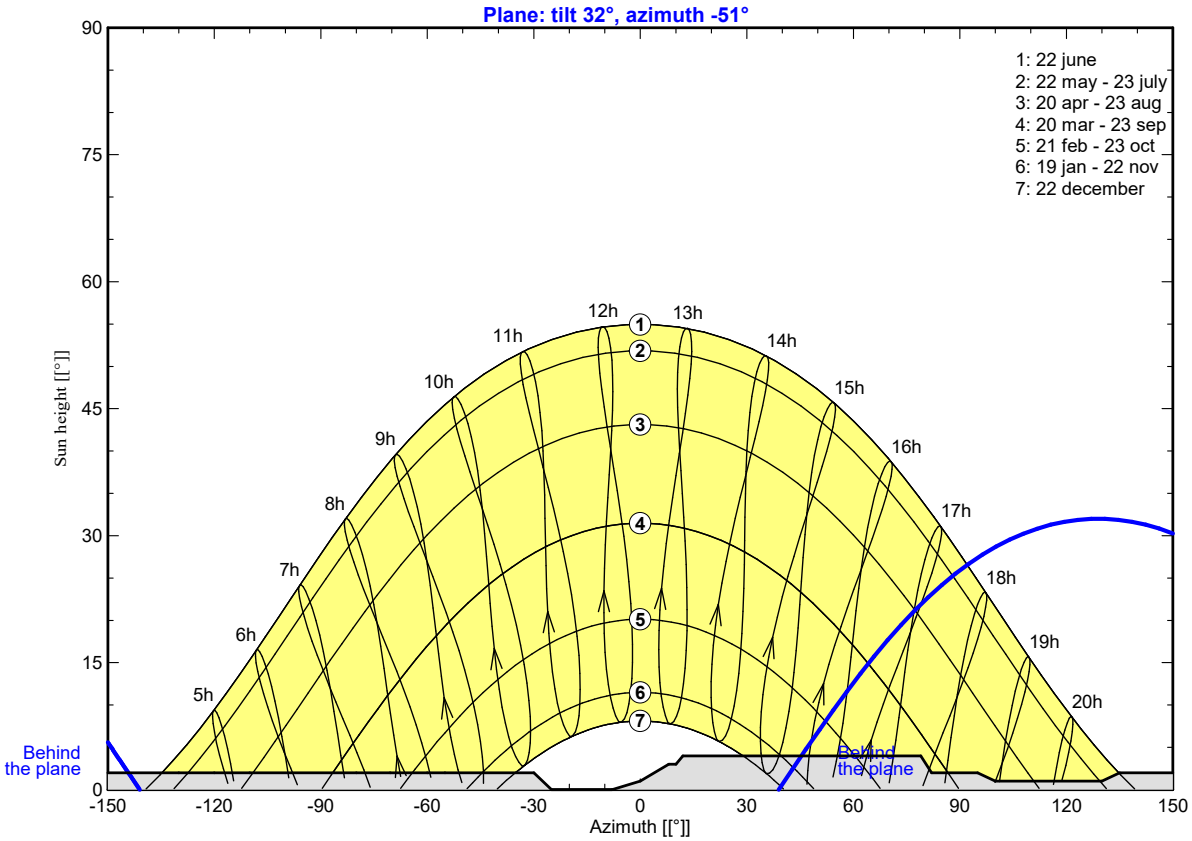

PVSYST V6.39		07/05/18	Page 3/5

Grid-Connected System: Near shading definition

Project : **Grid-Connected Project at Skarpnes**

Simulation variant : **Skarpnes_Meteo(Synthetic)**

Main system parameters	System type	**Grid-Connected**		
Horizon	Average Height	2.2°		
Near Shadings	Linear shadings			
PV Field Orientation	tilt	32°	azimuth	-51°
PV modules	Model	SPR-230NE-BLK-D	Pnom	230 Wp
PV Array	Nb. of modules	32	Pnom total	**7.36 kWp**
Inverter	Model	Sunny Tripower 7000TL-20	Pnom	7.00 kW ac
User's needs	Unlimited load (grid)			

Perspective of the PV-field and surrounding shading scene

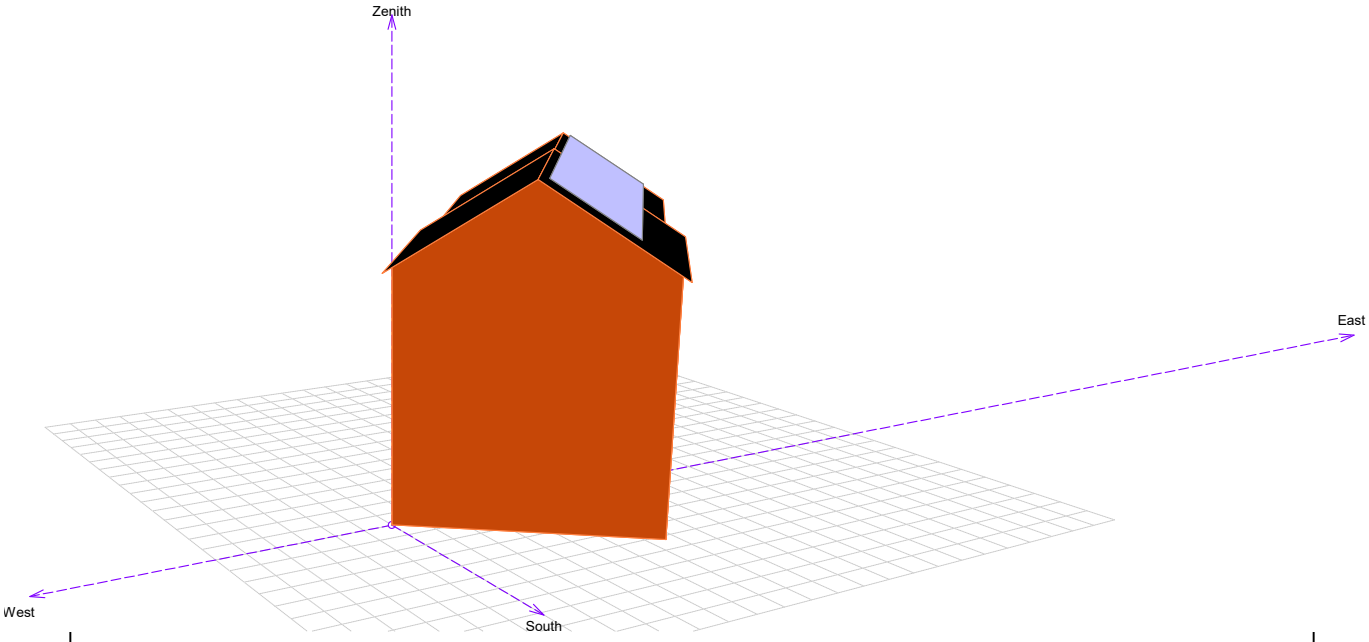

Iso-shadings diagram

Grid-Connected Project at Skarpnes

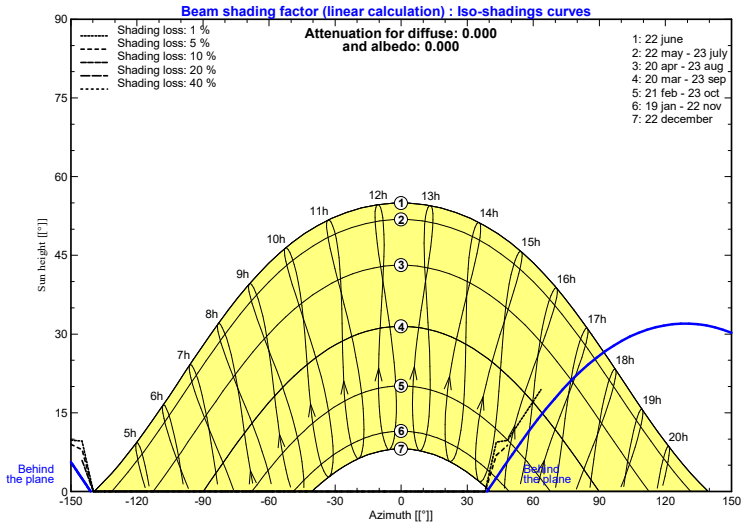

Grid-Connected System: Main results

Project : **Grid-Connected Project at Skarpnes**

Simulation variant : **Skarpnes_Meteo(Synthetic)**

Main system parameters	System type	**Grid-Connected**		
Horizon	Average Height	2.2°		
Near Shadings	Linear shadings			
PV Field Orientation	tilt	32°	azimuth	-51°
PV modules	Model	SPR-230NE-BLK-D	Pnom	230 Wp
PV Array	Nb. of modules	32	Pnom total	**7.36 kWp**
Inverter	Model	Sunny Tripower 7000TL-20	Pnom	7.00 kW ac
User's needs	Unlimited load (grid)			

Main simulation results

System Production	**Produced Energy**	**6.85 MWh/year**	Specific prod.	931 kWh/kWp/year
	Performance Ratio PR	79.8 %		

Normalized productions (per installed kWp): Nominal power 7.36 kWp

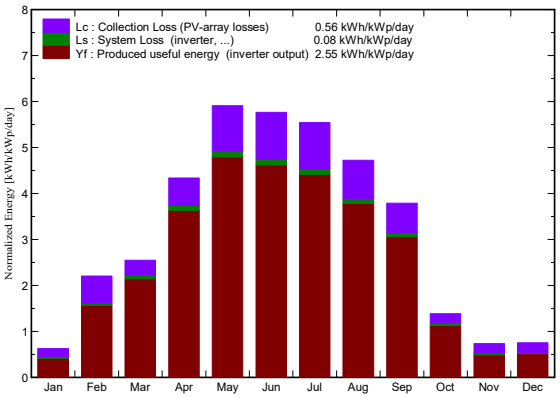

Performance Ratio PR

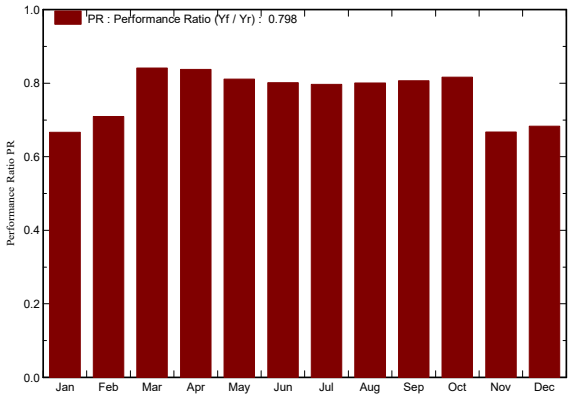

Skarpnes_Meteo(Synthetic)

Balances and main results

	GlobHor kWh/m²	T Amb °C	GlobInc kWh/m²	GlobEff kWh/m²	EArray MWh	E_Grid MWh	EffArrR %	EffSysR %
January	12.8	-2.60	19.4	14.4	0.104	0.095	13.45	12.33
February	38.8	2.00	61.7	46.7	0.333	0.322	13.58	13.12
March	62.9	4.00	79.0	72.9	0.507	0.489	16.10	15.56
April	116.1	5.80	130.2	121.1	0.826	0.802	15.94	15.49
May	173.5	11.80	183.3	171.1	1.124	1.095	15.40	15.00
June	166.2	15.70	172.9	161.3	1.049	1.020	15.24	14.81
July	173.0	16.20	171.8	159.8	1.037	1.008	15.16	14.73
August	134.0	15.70	146.4	136.3	0.888	0.863	15.24	14.81
September	95.3	15.10	113.8	105.7	0.695	0.675	15.34	14.91
October	35.1	6.70	42.9	39.3	0.271	0.258	15.89	15.09
November	16.8	3.20	22.0	16.5	0.117	0.108	13.36	12.34
December	13.0	4.70	23.4	17.5	0.124	0.118	13.32	12.63
Year	1037.5	8.22	1166.7	1062.4	7.075	6.853	15.23	14.75

Legends:

GlobHor	Horizontal global irradiation	EArray	Effective energy at the output of the array
T Amb	Ambient Temperature	E_Grid	Energy injected into grid
GlobInc	Global incident in coll. plane	EffArrR	Effic. Eout array / rough area
GlobEff	Effective Global, corr. for IAM and shadings	EffSysR	Effic. Eout system / rough area

PVSYST V6.39		07/05/18	Page 5/5

Grid-Connected System: Loss diagram

Project : **Grid-Connected Project at Skarpnes**

Simulation variant : **Skarpnes_Meteo(Synthetic)**

Main system parameters	System type	**Grid-Connected**		
Horizon	Average Height	2.2°		
Near Shadings	Linear shadings			
PV Field Orientation	tilt	32°	azimuth	-51°
PV modules	Model	SPR-230NE-BLK-D	Pnom	230 Wp
PV Array	Nb. of modules	32	Pnom total	**7.36 kWp**
Inverter	Model	Sunny Tripower 7000TL-20	Pnom	7.00 kW ac
User's needs	Unlimited load (grid)			

Loss diagram over the whole year

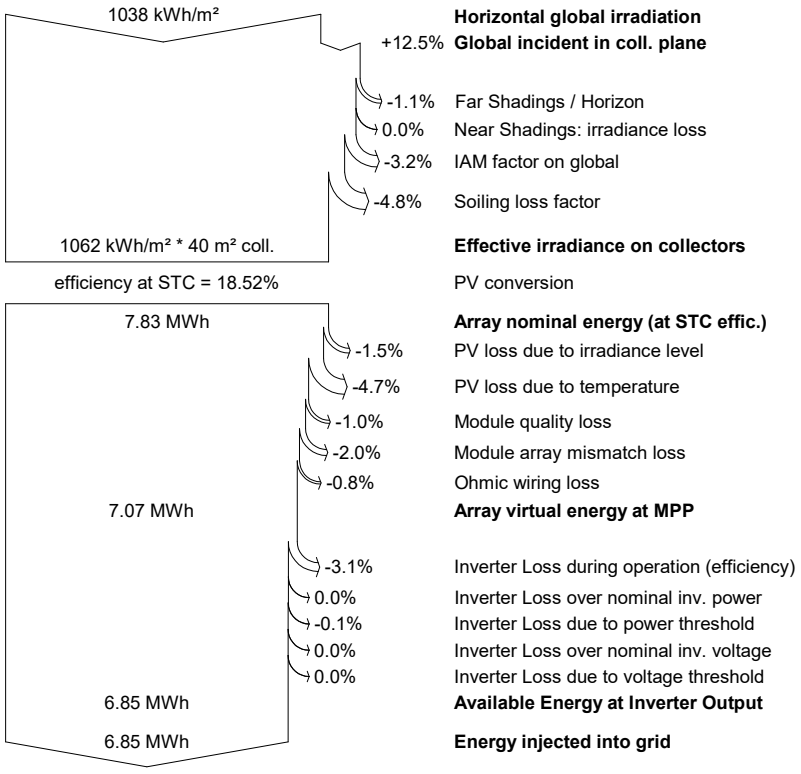

Appendix C

PVSYST V6.39		22/05/18	Page 1/6

Grid-Connected System: Simulation parameters

Project : **Grid-Connected Project at Solsmaragden**

Geographical Site	**SolsmaragdenReal**		Country	**Norway**
Situation	Latitude	59.7°N	Longitude	10.2°E
Time defined as	Legal Time	Time zone UT+1	Altitude	5 m
	Albedo	0.20		
Meteo data:	**Solsmaragden**	Synthetic - Meteonorm 7.1 (1991-2010), Sat=100%		

Simulation variant : **Solsmaragden**

Simulation date 22/05/18 13h28

Simulation parameters

Collector Plane Orientation	Tilt	90°	Azimuth	25°
Models used	Transposition	Perez	Diffuse	Erbs, Meteonorm
Horizon	Average Height	3.8°		
Near Shadings	Detailed electrical calculations	(acc. to module layout)		

PV Arrays Characteristics (2 kinds of array defined)

Sub-array "Inv7"	Si-poly	Model	**CENIT-125**		
Original PVsyst database		Manufacturer	Issol		
Number of PV modules		In series	30 modules	In parallel	2 strings
Total number of PV modules		Nb. modules	60	Unit Nom. Power	125 Wp
Array global power		Nominal (STC)	**7.50 kWp**	At operating cond.	6.81 kWp (50°C)
Array operating characteristics (50°C)		U mpp	450 V	I mpp	15 A
Sub-array "Inv 8"	Si-mono	Model	**CENIT-220**		
Custom parameters definition		Manufacturer	Issol		
Number of PV modules		In series	32 modules	In parallel	4 strings
Total number of PV modules		Nb. modules	128	Unit Nom. Power	150 Wp
Array global power		Nominal (STC)	**19.20 kWp**	At operating cond.	17.03 kWp (50°C)
Array operating characteristics (50°C)		U mpp	647 V	I mpp	26 A
Total Arrays global power		Nominal (STC)	**27 kWp**	Total	188 modules
		Module area	**265 m²**	Cell area	164 m²

Sub-array "Inv7" : Inverter	Model	**Sunny Tripower 6000TL-20**		
	Manufacturer	SMA		
Characteristics	Operating Voltage	295-800 V	Unit Nom. Power	6.00 kWac
Inverter pack	Nb. of inverters	2 * MPPT 50 %	Total Power	6.0 kWac
Sub-array "Inv 8" : Inverter	Model	**Sunny Tripower 15000TL-10**		
	Manufacturer	SMA		
Characteristics	Operating Voltage	150-800 V	Unit Nom. Power	15.0 kWac
Inverter pack	Nb. of inverters	2 * MPPT 50 %	Total Power	15.0 kWac
Total	Nb. of inverters	2	Total Power	21 kWac

PV Array loss factors

Thermal Loss factor	Uc (const)	20.0 W/m²K	Uv (wind)	0.0 W/m²K / m/s
Wiring Ohmic Loss	Array#1	497 mOhm	Loss Fraction	1.5 % at STC
	Array#2	415 mOhm	Loss Fraction	1.5 % at STC
	Global		Loss Fraction	1.5 % at STC
Module Quality Loss		Array#1,	Loss Fraction	2.5 %
		Array#2,	Loss Fraction	1.5 %
Module Mismatch Losses			Loss Fraction	1.0 % at MPP

PVsyst Education License, University of Agder (Norway)

PVSYST V6.39		22/05/18	Page 2/6

Grid-Connected System: Simulation parameters (continued)

Incidence effect, ASHRAE parametrization IAM = 1 - bo (1/cos i - 1) bo Param. 0.05

User's needs : Unlimited load (grid)

PVSYST V6.39		22/05/18	Page 3/6

Grid-Connected System: Horizon definition

Project : **Grid-Connected Project at Solsmaragden**

Simulation variant : **Solsmaragden**

Main system parameters	System type	**Grid-Connected**		
Horizon	Average Height	3.8°		
Near Shadings	Detailed electrical calculations	(acc. to module layout)		
PV Field Orientation	tilt	90°	azimuth	25°
PV modules	Model	CENIT-125	Pnom	125 Wp
PV modules	Model	CENIT-220	Pnom	150 Wp
PV Array	Nb. of modules	188	Pnom total	**26.70 kWp**
Inverter	Model	Sunny Tripower 6000TL-20	Pnom	6.00 kW ac
Inverter	Model	Sunny Tripower 15000TL-10	Pnom	15.00 kW ac
Inverter pack	Nb. of units	2.0	Pnom total	**21.00 kW ac**
User's needs	Unlimited load (grid)			

Horizon

Average Height	3.8°	Diffuse Factor	0.90
Albedo Factor	100 %	Albedo Fraction	0.78

Height [°]	9.0	7.0	2.0	2.0	3.0	1.0	2.0	4.0	4.0	6.0	5.0
Azimuth [°]	-150	-130	-115	-42	-40	-23	-20	-15	0	8	20
Height [°]	7.0	7.0	6.0	6.0	4.0	3.5	4.0	2.0	2.0	3.0	6.0
Azimuth [°]	30	38	45	53	60	67	70	90	115	120	150

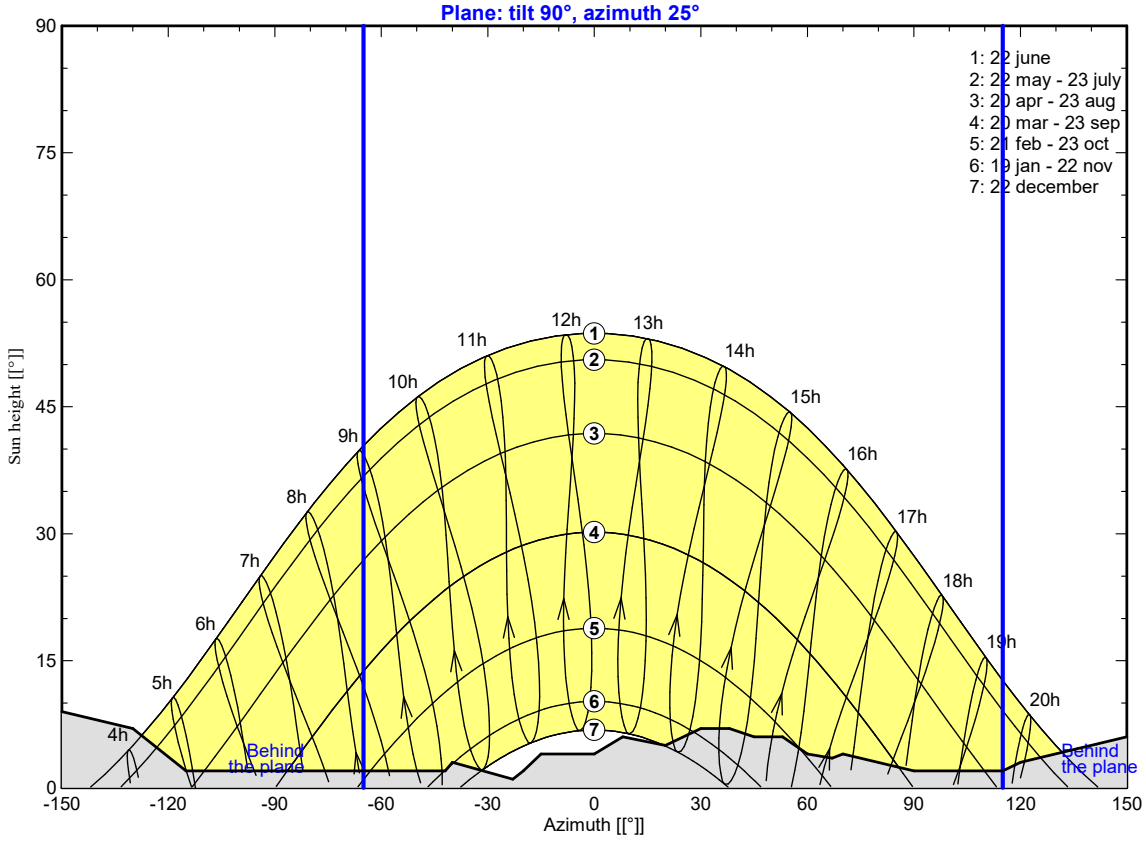

PVSYST V6.39		22/05/18	Page 4/6

Grid-Connected System: Near shading definition

Project : **Grid-Connected Project at Solsmaragden**

Simulation variant : **Solsmaragden**

Main system parameters	System type	**Grid-Connected**		
Horizon	Average Height	3.8°		
Near Shadings	Detailed electrical calculations	(acc. to module layout)		
PV Field Orientation	tilt	90°	azimuth	25°
PV modules	Model	CENIT-125	Pnom	125 Wp
PV modules	Model	CENIT-220	Pnom	150 Wp
PV Array	Nb. of modules	188	Pnom total	**26.70 kWp**
Inverter	Model	Sunny Tripower 6000TL-20	Pnom	6.00 kW ac
Inverter	Model	Sunny Tripower 15000TL-10	Pnom	15.00 kW ac
Inverter pack	Nb. of units	2.0	Pnom total	**21.00 kW ac**
User's needs	Unlimited load (grid)			

Perspective of the PV-field and surrounding shading scene

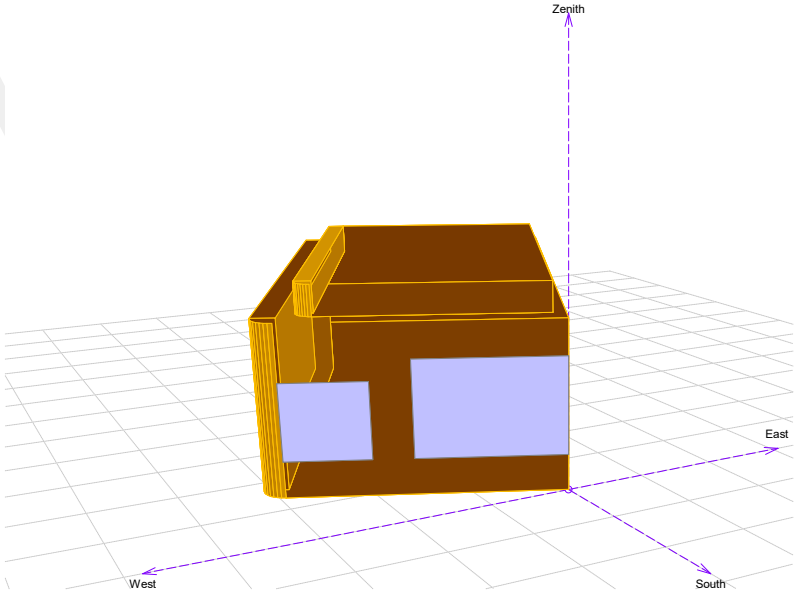

Iso-shadings diagram

Grid-Connected Project at Solsmaragden

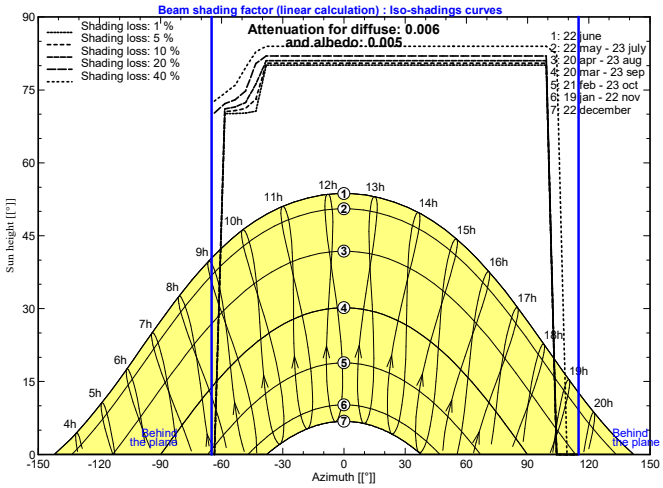

PVSYST V6.39		22/05/18	Page 5/6

Grid-Connected System: Main results

Project : **Grid-Connected Project at Solsmaragden**

Simulation variant : **Solsmaragden**

Main system parameters	System type	**Grid-Connected**		
Horizon	Average Height	3.8°		
Near Shadings	Detailed electrical calculations	(acc. to module layout)		
PV Field Orientation	tilt	90°	azimuth	25°
PV modules	Model	CENIT-125	Pnom	125 Wp
PV modules	Model	CENIT-220	Pnom	150 Wp
PV Array	Nb. of modules	188	Pnom total	**26.70 kWp**
Inverter	Model	Sunny Tripower 6000TL-20	Pnom	6.00 kW ac
Inverter	Model	Sunny Tripower 15000TL-10	Pnom	15.00 kW ac
Inverter pack	Nb. of units	2.0	Pnom total	**21.00 kW ac**
User's needs	Unlimited load (grid)			

Main simulation results

System Production	**Produced Energy**	**17.01 MWh/year**	Specific prod.	637 kWh/kWp/year
	Performance Ratio PR	79.7 %		

Normalized productions (per installed kWp): Nominal power 26.70 kWp

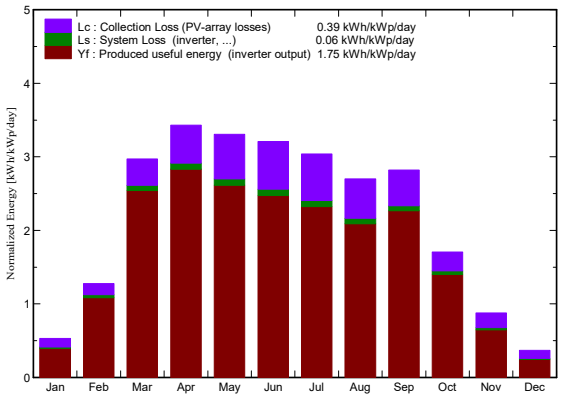

Performance Ratio PR

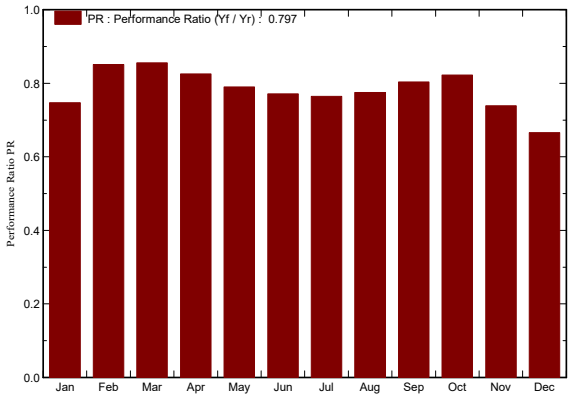

Solsmaragden

Balances and main results

	GlobHor kWh/m²	T Amb °C	GlobInc kWh/m²	GlobEff kWh/m²	EArray MWh	E_Grid MWh	EffArrR %	EffSysR %
January	7.4	1.05	16.5	13.34	0.342	0.328	7.86	7.54
February	22.2	0.55	35.7	32.09	0.841	0.811	8.90	8.59
March	65.4	2.41	92.1	84.61	2.163	2.105	8.87	8.64
April	108.7	6.48	102.9	93.28	2.335	2.269	8.57	8.33
May	148.0	10.86	102.5	90.47	2.234	2.163	8.24	7.98
June	161.9	13.89	96.2	83.57	2.052	1.983	8.06	7.79
July	148.8	16.46	94.2	82.09	1.991	1.923	7.98	7.71
August	104.9	16.11	83.7	74.22	1.791	1.732	8.09	7.82
September	74.2	12.42	84.6	77.21	1.872	1.816	8.36	8.11
October	33.5	8.06	52.9	48.31	1.201	1.161	8.59	8.30
November	10.7	4.62	26.3	21.28	0.542	0.518	7.79	7.45
December	4.4	1.60	11.5	8.33	0.213	0.204	7.03	6.72
Year	890.2	7.92	799.1	708.80	17.577	17.013	8.31	8.05

Legends:

GlobHor	Horizontal global irradiation	EArray	Effective energy at the output of the array
T Amb	Ambient Temperature	E_Grid	Energy injected into grid
GlobInc	Global incident in coll. plane	EffArrR	Effic. Eout array / rough area
GlobEff	Effective Global, corr. for IAM and shadings	EffSysR	Effic. Eout system / rough area

PVSYST V6.39		22/05/18	Page 6/6

Grid-Connected System: Loss diagram

Project : **Grid-Connected Project at Solsmaragden**

Simulation variant : **Solsmaragden**

Main system parameters	System type	**Grid-Connected**		
Horizon	Average Height	3.8°		
Near Shadings	Detailed electrical calculations	(acc. to module layout)		
PV Field Orientation	tilt	90°	azimuth	25°
PV modules	Model	CENIT-125	Pnom	125 Wp
PV modules	Model	CENIT-220	Pnom	150 Wp
PV Array	Nb. of modules	188	Pnom total	**26.70 kWp**
Inverter	Model	Sunny Tripower 6000TL-20	Pnom	6.00 kW ac
Inverter	Model	Sunny Tripower 15000TL-10	Pnom	15.00 kW ac
Inverter pack	Nb. of units	2.0	Pnom total	**21.00 kW ac**
User's needs	Unlimited load (grid)			

Loss diagram over the whole year

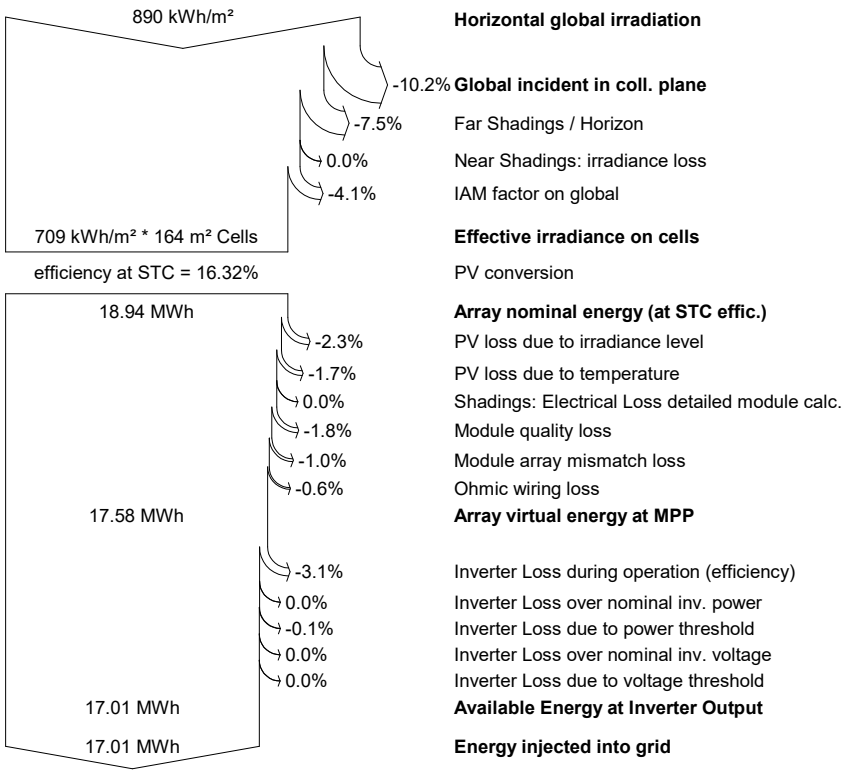

Appendix D

PVSYST V6.39		23/05/18	Page 1/6

Grid-Connected System: Simulation parameters

Project : **Brynseng SkoleAlternativtOslo**

Geographical Site **Oslo** Country **Norway**

Situation Latitude 59.9°N Longitude 10.8°E
Time defined as Legal Time Time zone UT+1 Altitude 81 m
Monthly albedo values

	Jan.	Feb.	Mar.	Apr.	May	June	July	Aug.	Sep.	Oct.	Nov.	Dec.
Albedo	0.80	0.80	0.20	0.20	0.20	0.20	0.20	0.20	0.20	0.20	0.20	0.80

Meteo data: **Oslo** Synthetic - Meteonorm 7.1 (1991-2010), Sat=100%

Simulation variant : **BrynsengSkole.**
Simulation date 23/05/18 13h20

Simulation parameters

Collector Plane Orientation Tilt 90° Azimuth 5°
Models used Transposition Perez Diffuse Erbs, Meteonorm
Horizon Average Height 4.4°
Near Shadings Linear shadings

PV Arrays Characteristics (3 kinds of array defined)
PV module Si-mono Model **CENIT-220**
Custom parameters definition Manufacturer Issol

Sub-array "Inverter 1"
Number of PV modules In series 30 modules In parallel 12 strings
Total number of PV modules Nb. modules 360 Unit Nom. Power 150 Wp
Array global power Nominal (STC) **54.0 kWp** At operating cond. 47.9 kWp (50°C)
Array operating characteristics (50°C) U mpp 606 V I mpp 79 A

Sub-array "Inverter 2"
Number of PV modules In series 30 modules In parallel 8 strings
Total number of PV modules Nb. modules 240 Unit Nom. Power 150 Wp
Array global power Nominal (STC) **36.0 kWp** At operating cond. 31.9 kWp (50°C)
Array operating characteristics (50°C) U mpp 606 V I mpp 53 A

Sub-array "Inverter 3"
Number of PV modules In series 29 modules In parallel 18 strings
Total number of PV modules Nb. modules 522 Unit Nom. Power 150 Wp
Array global power Nominal (STC) **78.3 kWp** At operating cond. 69.4 kWp (50°C)
Array operating characteristics (50°C) U mpp 586 V I mpp 118 A

Total Arrays global power Nominal (STC) **168 kWp** Total 1122 modules
Module area **1648 m²** Cell area 1147 m²

Sub-array "Inverter 1" : Inverter Model **Sunny Tripower 15000TL-10**
Manufacturer SMA
Characteristics Operating Voltage 150-800 V Unit Nom. Power 15.0 kWac
Inverter pack Nb. of inverters 6 * MPPT 50 % Total Power 45 kWac

Sub-array "Inverter 2" : Inverter Model **Sunny Tripower 15000TL-10**
Manufacturer SMA
Characteristics Operating Voltage 150-800 V Unit Nom. Power 15.0 kWac
Inverter pack Nb. of inverters 4 * MPPT 50 % Total Power 30 kWac

Sub-array "Inverter 3" : Inverter Model **Sunny Tripower 25000TL-JP-30**
Manufacturer SMA
Characteristics Operating Voltage 390-800 V Unit Nom. Power 25.0 kWac
Inverter pack Nb. of inverters 6 * MPPT 50 % Total Power 75 kWac

Total Nb. of inverters 8 Total Power 150 kWac

Grid-Connected System: Simulation parameters (continued)

PV Array loss factors

Thermal Loss factor	Uc (const)	20.0 W/m²K	Uv (wind)	0.0 W/m²K / m/s
Wiring Ohmic Loss	Array#1	130 mOhm	Loss Fraction	1.5 % at STC
	Array#2	195 mOhm	Loss Fraction	1.5 % at STC
	Array#3	84 mOhm	Loss Fraction	1.5 % at STC
	Global		Loss Fraction	1.5 % at STC
Module Quality Loss			Loss Fraction	1.5 %
Module Mismatch Losses			Loss Fraction	1.0 % at MPP
Incidence effect, ASHRAE parametrization	IAM =	1 - bo (1/cos i - 1)	bo Param.	0.05

User's needs : Unlimited load (grid)

PVSYST V6.39		23/05/18	Page 3/6

Grid-Connected System: Horizon definition

Project : **Brynseng SkoleAlternativtOslo**

Simulation variant : **BrynsengSkole.**

Main system parameters	System type	**Grid-Connected**		
Horizon	Average Height	4.4°		
Near Shadings	Linear shadings			
PV Field Orientation	tilt	90°	azimuth	5°
PV modules	Model	CENIT-220	Pnom	150 Wp
PV Array	Nb. of modules	1122	Pnom total	**168 kWp**
Inverter	Model	Sunny Tripower 15000TL-10		15.00 kW ac
Inverter	Model	Sunny Tripower 25000TL-JP-30		25.00 kW ac
Inverter pack	Nb. of units	8.0	Pnom total	**150 kW ac**
User's needs	Unlimited load (grid)			

Horizon	Average Height	4.4°	Diffuse Factor	0.86
	Albedo Factor	100 %	Albedo Fraction	0.70

Height [°]	6.0	6.0	4.0	4.0	3.0	6.0	7.0	7.0	8.0	8.0	9.0	8.0
Azimuth [°]	-150	-130	-120	-75	-68	-60	-55	-35	-30	-5	0	5
Height [°]	8.0	6.0	2.0	2.0	1.0	1.0	0.0	0.0	1.0	1.0	4.0	4.0
Azimuth [°]	15	30	45	54	60	66	70	90	95	116	126	150

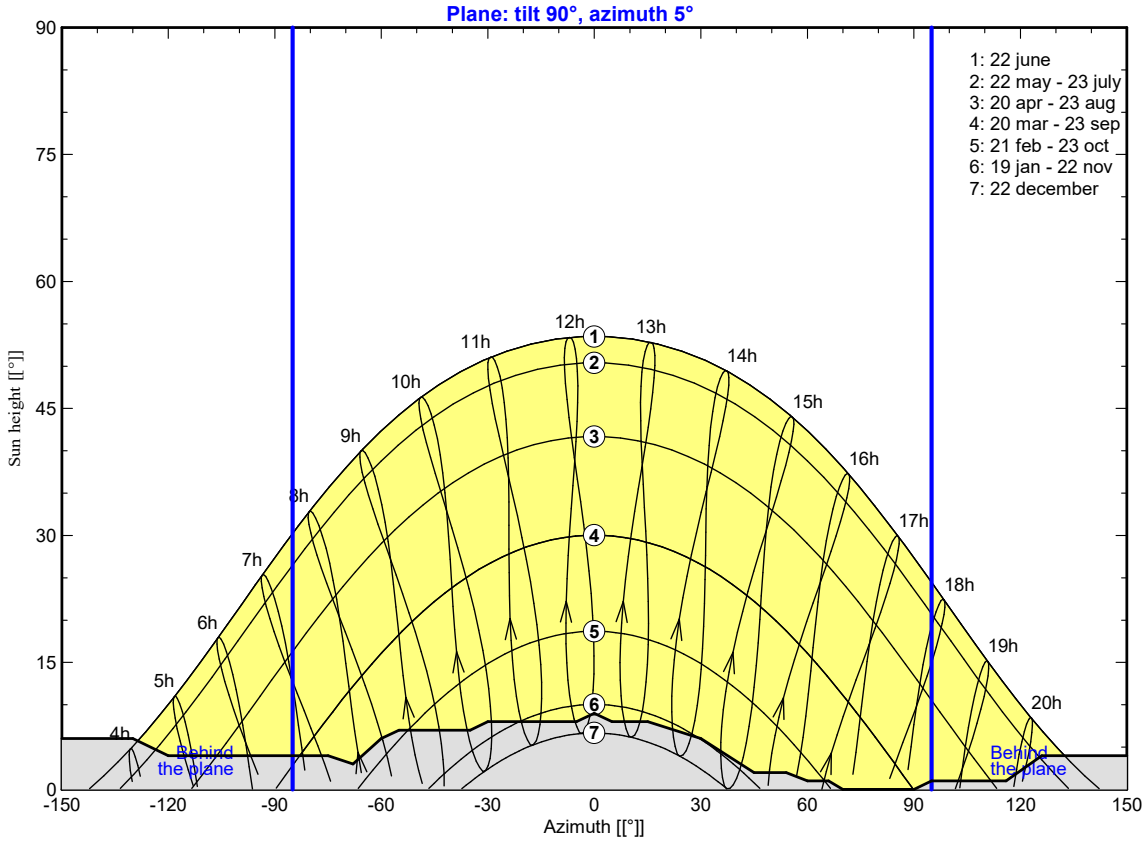

PVSYST V6.39		23/05/18	Page 4/6

Grid-Connected System: Near shading definition

Project : **Brynseng SkoleAlternativtOslo**

Simulation variant : **BrynsengSkole.**

Main system parameters	System type	**Grid-Connected**		
Horizon	Average Height	4.4°		
Near Shadings	Linear shadings			
PV Field Orientation	tilt	90°	azimuth	5°
PV modules	Model	CENIT-220	Pnom	150 Wp
PV Array	Nb. of modules	1122	Pnom total	**168 kWp**
Inverter	Model	Sunny Tripower 15000TL-10		15.00 kW ac
Inverter	Model	Sunny Tripower 25000TL-JP-30		25.00 kW ac
Inverter pack	Nb. of units	8.0	Pnom total	**150 kW ac**
User's needs	Unlimited load (grid)			

Perspective of the PV-field and surrounding shading scene

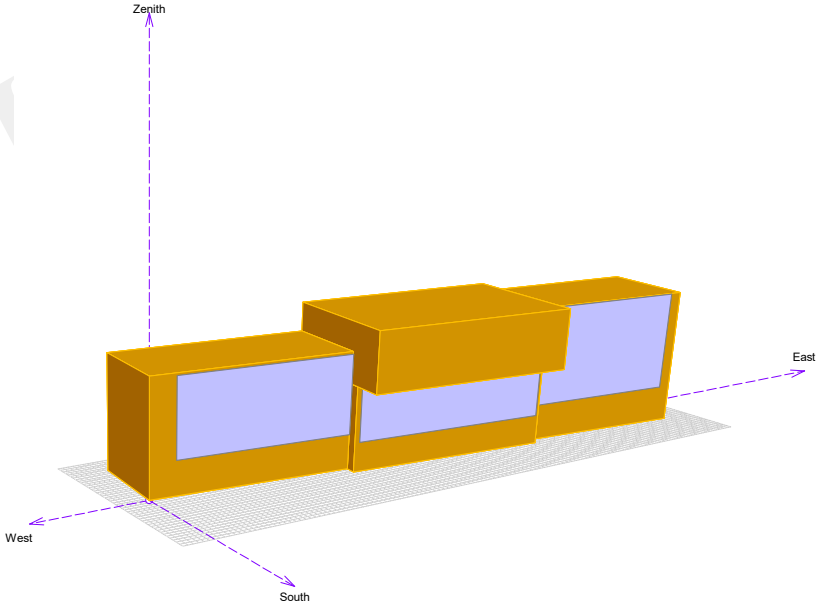

Iso-shadings diagram

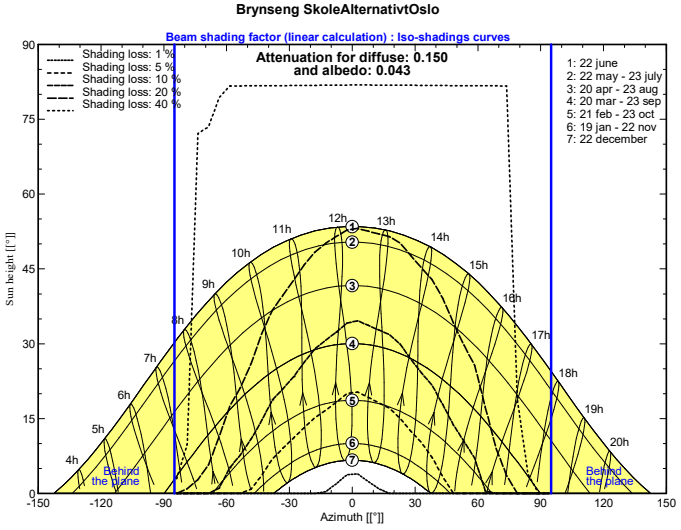

PVSYST V6.39		23/05/18	Page 5/6

Grid-Connected System: Main results

Project : **Brynseng SkoleAlternativtOslo**

Simulation variant : **BrynsengSkole.**

Main system parameters	System type	**Grid-Connected**		
Horizon	Average Height	4.4°		
Near Shadings	Linear shadings			
PV Field Orientation	tilt	90°	azimuth	5°
PV modules	Model	CENIT-220	Pnom	150 Wp
PV Array	Nb. of modules	1122	Pnom total	**168 kWp**
Inverter	Model	Sunny Tripower 15000TL-10		15.00 kW ac
Inverter	Model	Sunny Tripower 25000TL-JP-30		25.00 kW ac
Inverter pack	Nb. of units	8.0	Pnom total	**150 kW ac**
User's needs	Unlimited load (grid)			

Main simulation results

System Production

Produced Energy	**90652826 W/year**	Specific prod.	539 kWh/kWp/year
Performance Ratio PR	65.2 %		

Normalized productions (per installed kWp): Nominal power 168 kWp

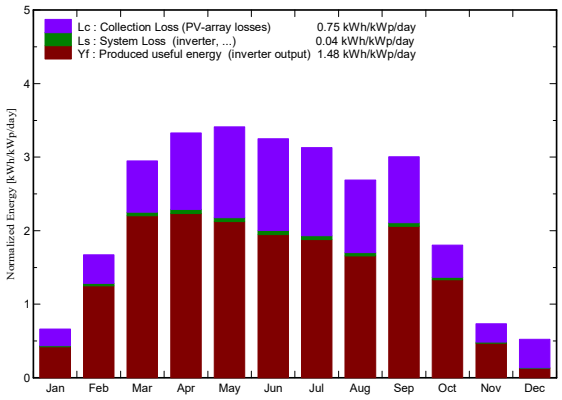

Performance Ratio PR

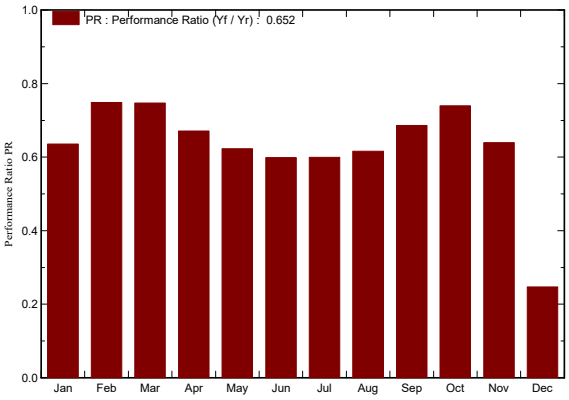

BrynsengSkole.

Balances and main results

	GlobHor kWh/m²	T Amb °C	GlobInc kWh/m²	GlobEff kWh/m²	EArray kWh	E_Grid kWh	EffArrR %	EffSysR %
January	7.4	-1.66	20.6	14.15	2275	2204	6.70	6.49
February	22.1	-2.08	46.8	36.49	6047	5900	7.84	7.64
March	64.7	0.79	91.4	72.09	11748	11500	7.79	7.63
April	106.9	6.31	99.9	72.64	11559	11285	7.02	6.85
May	152.9	11.82	105.7	72.67	11364	11079	6.52	6.36
June	164.1	15.17	97.5	65.82	10107	9828	6.29	6.11
July	151.7	17.80	97.1	66.32	10073	9800	6.30	6.12
August	106.7	16.83	83.3	58.53	8884	8641	6.47	6.29
September	74.8	12.17	90.1	68.95	10647	10409	7.17	7.01
October	32.3	6.52	55.9	45.70	7131	6955	7.74	7.55
November	10.0	2.66	22.1	15.22	2451	2376	6.74	6.53
December	4.5	-1.27	16.3	4.52	712	677	2.66	2.53
Year	898.3	7.14	826.8	593.08	92999	90653	6.82	6.65

Legends:

GlobHor	Horizontal global irradiation	EArray	Effective energy at the output of the array
T Amb	Ambient Temperature	E_Grid	Energy injected into grid
GlobInc	Global incident in coll. plane	EffArrR	Effic. Eout array / rough area
GlobEff	Effective Global, corr. for IAM and shadings	EffSysR	Effic. Eout system / rough area

PVSYST V6.39		23/05/18	Page 6/6

Grid-Connected System: Loss diagram

Project : **Brynseng SkoleAlternativtOslo**

Simulation variant : **BrynsengSkole.**

Main system parameters	System type	**Grid-Connected**		
Horizon	Average Height	4.4°		
Near Shadings	Linear shadings			
PV Field Orientation	tilt	90°	azimuth	5°
PV modules	Model	CENIT-220	Pnom	150 Wp
PV Array	Nb. of modules	1122	Pnom total	**168 kWp**
Inverter	Model	Sunny Tripower 15000TL-10		15.00 kW ac
Inverter	Model	Sunny Tripower 25000TL-JP-30		25.00 kW ac
Inverter pack	Nb. of units	8.0	Pnom total	**150 kW ac**
User's needs	Unlimited load (grid)			

Loss diagram over the whole year

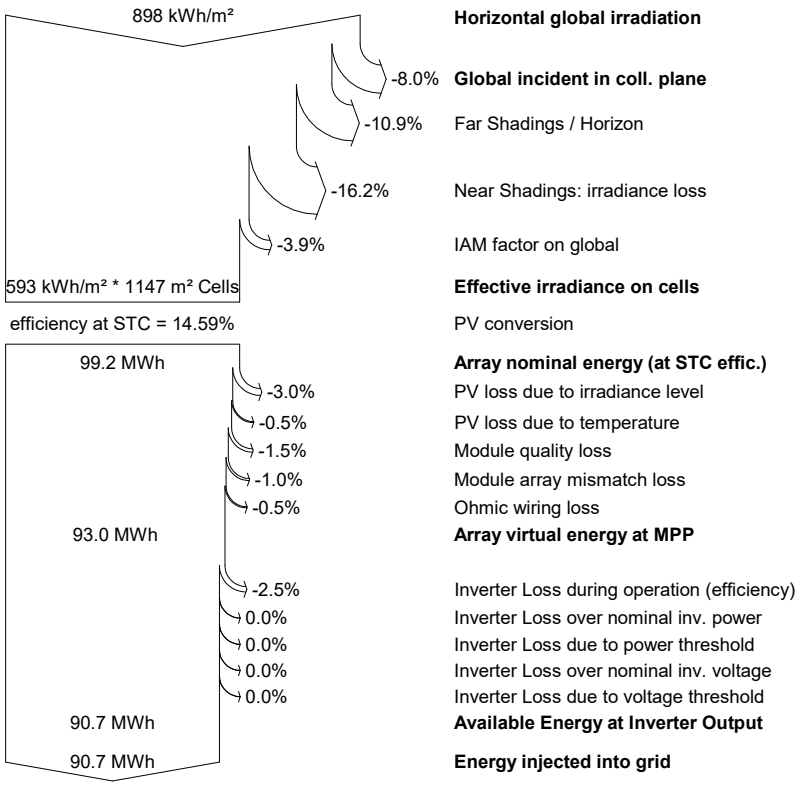

Appendix E

Coefficients and functions can be calculated:

$$a = max(0, cos(AOI) \tag{15}$$

$$b = max(cos(85^\circ, cos(\theta_z)) \tag{16}$$

$$F_1 = max \cdot [0, (f_{11} + f_{12}\Delta + \frac{\Pi \cdot \theta_z}{180^\circ} \cdot f_{13})] \tag{17}$$

$$F_2 = (f_{21} + f_{22}\Delta + \frac{\Pi \cdot \theta_z}{180^\circ} \cdot f_{23}) \tag{18}$$

$$\Delta = \frac{DHI \cdot AM_a}{E_a} \tag{19}$$

AM_a is absolute air mass and E_a is extraterrestrial radiation.

$$AM_a = AM \cdot \frac{P}{P_0} \tag{20}$$

Here P is the given pressure and P_0 is the standard pressure of 1 atm. Extraterrestrial radiation is found by include variations around the solar constant.

$$E_a = 1366.1 \cdot (\frac{R_{av}}{R})^2 W/m^2 \tag{21}$$

Here R_{av} is the average Earth-Sun distance while R is the actual distance. This correlation can be expressed:

$$(\frac{R_{av}}{R})^2 = 1.00011 + (0.034221 \cdot cos(c)) + (0.00128 \cdot sin(c)) + (0.000719) \cdot cos(2c)) + (0.000077 \cdot sin(2c)) \tag{22}$$

$$c = 2\Pi \cdot \frac{N}{365} radians \tag{23}$$

N is the number of days. The complex empirically fitted functions F_1 and F_2 are determined by implementing clearness bin ϵ, which is given by:

$$\epsilon = \frac{DHI + DNI/DHI + k \cdot \theta_z^3}{1 + k \cdot \theta_z^3} \tag{24}$$

k is a constant 1.041 for angles given in radians and $5.535 \cdot 10^-6$ for angles in degrees. The coefficients can be fund by using the ϵ values given in table:

ϵ bin	Lower bound	Upper bound
1	1	1.065
2	1.065	1.230
3	1230	1.500
4	1.500	1.950
5	1.950	2.800
6	2.800	4.500
7	4.500	6.200
8	6.200	-

Table 16: ϵ bins intervals

ϵ bin	f_{11}	f_{12}	f_{13}	f_{21}	f_{22}	f_{23}
1	-0.008	0.588	-0.062	-0.06	0.072	-0.022
2	0.13	0.683	-0.151	-0.019	0.066	-0.029
3	0.33	0.487	-0.221	0.055	-0.064	-0.026
4	0.568	0.187	-0.295	0.109	-0.152	-0.014
5	0.873	-0.392	-0.362	0.226	-0.462	0.001
6	1.132	-1.237	-0.412	0.288	-0.823	0.131
7	1.06	-1.6	-0.359	0.264	-1.127	0.131
8	0.678	-0.327	-0.25	0.156	-1.377	0.25

Table 17: ϵ bins coefficients